Science of the Total Environment 886 (2023) 163920

Contents lists available at ScienceDirect

Science of the Total Environment

journal homepage: www.elsevier.com/locate/scitotenv

Hydrothermal conversion of biomass to fuels, chemicals and materials: A review holistically connecting product properties and marketable applications

Yingdong Zhou [a,b], Javier Remón [c,*], Xiaoyan Pang [b], Zhicheng Jiang [d], Haiteng Liu [b], Wei Ding [b,*]

[a] College of Materials and Chemistry & Chemical Engineering, Chengdu University of Technology, Chengdu 610059, PR China
[b] China Leather and Footwear Research Institute Co. Ltd., Beijing 100015, PR China
[c] Thermochemical Processes Group, Aragón Institute for Engineering Research (I3A), University of Zaragoza, C/Mariano Esquillor s/n, 50.018, Zaragoza, Spain
[d] College of Biomass Science and Engineering, Sichuan University, Chengdu 610065, PR China

HIGHLIGHTS

- Holistic present and future applications for the reaction products from biomass HC.
- In-depth review of separation, upgrading and activation technologies for HC products.
- Marketable fuels (>46 MJ/kg), chemicals and materials (>3000 m^2/g) can be obtained.
- Summary of parameters and important characteristics for product post-treatments.
- Discussion on outlooks and challenges in HC product applications.

GRAPHICAL ABSTRACT

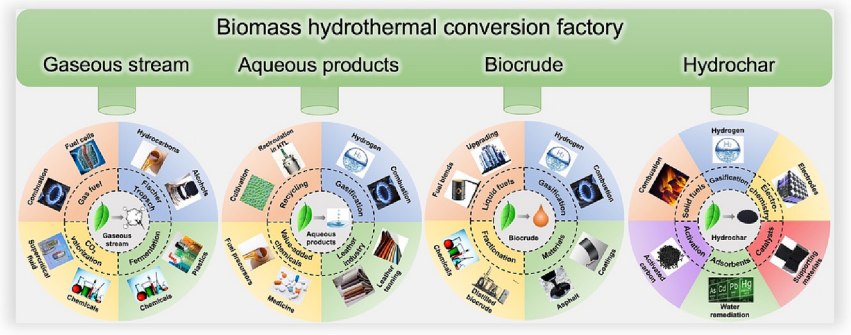

ARTICLE INFO

Editor: Daniel CW Tsang

Keywords:
Biomass
Hydrothermal conversion
Application
Biofuels
Biochemicals
Biomaterials

ABSTRACT

Biomass is a renewable and carbon-neutral resource with good features for producing biofuels, biochemicals, and biomaterials. Among the different technologies developed to date to convert biomass into such commodities, hydrothermal conversion (HC) is a very appealing and sustainable option, affording marketable gaseous (primarily containing H_2, CO, CH_4, and CO_2), liquid (biofuels, aqueous phase carbohydrates, and inorganics), and solid products (energy-dense biofuels (up to 30 MJ/kg) with excellent functionality and strength). Given these prospects, this publication first-time puts together essential information on the HC of lignocellulosic and algal biomasses covering all the steps involved. Particularly, this work reports and comments on the most important properties (e.g., physiochemical and fuel properties) of all these products from a holistic and practical perspective. It also gathers vital information addressing selecting and using different downstream/upgrading processes to convert HC reaction products into marketable biofuels (HHV up to 46 MJ/kg), biochemicals (yield >90 %), and biomaterials (great functionality and surface area up to 3600 m^2/g). As a result of this practical vision, this work not only comments on and summarizes the most important properties of these products but also analyzes and discusses present and future applications, establishing an invaluable link between product properties and market needs to push HC technologies transition from the laboratory to the industry. Such a practical and pioneering approach paves the way for the future development, commercialization and industrialization of HC technologies to develop holistic and zero-waste biorefinery processes.

* Corresponding authors.
E-mail addresses: jrn@unizar.es (J. Remón), dingwei1368@outlook.com (W. Ding).

http://dx.doi.org/10.1016/j.scitotenv.2023.163920
Received 17 February 2023; Received in revised form 12 April 2023; Accepted 29 April 2023
Available online 6 May 2023

Contents

1. Introduction

The current human development, linked with the considerable progress made in the industrialization and modernization of present societies, has led to an overconsumption of finite fossil resources and severe environmental issues (Liu and Rajagopal, 2019; Semieniuk et al., 2022). Notably, the heavy reliance on fossil resources to produce fuels, chemicals, and materials has produced an excess in the emission of exhausted gases (e.g., CO_2, SO_x and NO_x) (Zhou et al., 2022c), causing global warming and environmental contamination (Ariza et al., 2022). Therefore, seeking environmentally benign materials and technologies to furnish renewable energy and chemical and material production from renewable resources is urgently required for the sustainable development of the present and future generations (Staples et al., 2017).

As for sustainable feedstocks, biomass is an abundant, renewable (Opia et al., 2021), and carbon-neutral candidate for producing these commodities (Yang et al., 2018). In particular, lignocelluloses (He et al., 2017), algae (Zhou and Hu, 2020; Zhou et al., 2021), animal manure (Xiong et al., 2019), and municipal solid wastes (Jahromi et al., 2022) are abundant on the Earth and have fast growth/production rates. In addition, lignocellulosic and algal biomasses are photosynthetic organisms that utilize sunlight, CO_2, and water to synthesize organic nutrients stored in their cells and/or tissues (Gnanasekaran et al., 2023). Therefore, these biomasses show the ability to mitigate greenhouse gas emissions. In addition to these prospects, converting lignocellulosic wastes, algae blooms, animal manure, and urban wastes into chemicals and materials is a carbon-neutral and environmentally friendly strategy to help palliate environmental issues, ensuring the well-being and socio-economic development of future generations. Typically, biomass is composed of fats, carbohydrates (e.g., cellulose, hemicellulose, and starch), proteins, lignin, other volatiles, and ash (inorganic fraction) (Antero et al., 2020; Zhou et al., 2022a). Lignocellulosic biomass is abundant in carbohydrates and lignin (Mankar et al., 2021), whereas algal and animal biomasses contain more lipids and proteins (Devadas et al., 2021). These factors convert biomass into an excellent raw material to furnish biofuels, biochemicals, and biomaterials more sustainably than petroleum-based technologies.

With regard to the sustainable conversion of these feedstocks, many different technologies and strategies have been used for biomass conversion, with thermochemical (Gao et al., 2021) and biological (Wang et al., 2018b) processes being the most used alternatives for decades. Among these existing methods, hydrothermal technologies, classified into hydrothermal conversion and hydrothermal pretreatment, are among the most

commonly used methods for treating biomass feedstocks. Hydrothermal pretreatment is applied to enhance the enzymatic hydrolysis efficiency of lignocellulosic biomasses (Sarker et al., 2021), which has not been included due to the scope of this review. In addition, hydrothermal conversion (HC) of biomass stands out for wet biomass conversion to energy-dense carriers (Remón et al., 2022; Zhou et al., 2022b) and value-added products (Remón et al., 2021a; Remón et al., 2021b). This method utilizes hot compressed water (subcritical or supercritical) as the reaction medium, producing gases, liquids, and solids with many applications (Kumar et al., 2018). Therefore, such a technology is beneficial for treating feedstocks with high moisture contents without needing a drying pretreatment.

Typically, HC processes can be classified into different types of technologies: hydrothermal gasification (HTG), hydrothermal liquefaction (HTL), hydrothermal carbonization (HTC), and hydrothermal hydrolysis (HTH) (Remón et al., 2021a). Detailed information on these HC processes, including advantages and disadvantages, is listed in Table 1. Mainly, HTH is devoted to using carbohydrate-rich materials as the feedstock to produce water-soluble, aqueous products, mostly oligo- and monosaccharides. This process is commonly carried out at low temperatures (80–240 °C) under atmospheric or shallow pressures (<5 MPa) (Zhang et al., 2019a). HTC of biomass produces a carbonaceous solid fraction (usually called hydrochar) as the dominant product at relatively low temperatures and pressures (180–250 °C, 2–10 MPa) using long reaction times (Leng et al., 2021b). HTL is commonly conducted under moderate conditions (200–350 °C, 5–35 MPa), with biocrude being the dominant product (Fernandez-Sanroman et al., 2021). HTG, also referred to as supercritical water gasification (SCWG), occurs at near-critical temperatures (300–500 °C) and high pressures (~30 MPa), aiming to yield energy-dense gaseous fuels as the main product (Kumar et al., 2018; Sharma et al., 2022). A diagram illustrating the product distribution concerning processing temperature is depicted in Fig. 1. Based on these bespoke features, the HC of biomass can be flexibly directed to biofuels (gaseous stream, biocrude, hydrochar), biochemicals (aqueous products) and biomaterials (hydrochar) by simply changing the processing conditions or introducing specific catalysts. As shown in Fig. 1, at low temperatures, hydrolysis reactions of the components in biomass to fatty acids, monosaccharides, amino acids, and monophenols occur. Further increasing temperature leads to the repolymerization of these fractions to form hydrochar or degradation to small molecular compounds comprising of biocrude (amines, amides, fatty acids, N, O, S heterocyclic compounds, carboxylic acids, ketones, and phenolics). When the temperature augments above 300 °C, decarbonylation, decarboxylation, aqueous phase reforming, and methanation reactions might occur, forming more gaseous products (CO_2, CO, H_2, and CH_4).

In recent publications, the HC of biomass has already been achieved with high yields on a large scale (Samiee-Zafarghandi et al., 2018; Zhang et al., 2019b). Thus, the bottleneck is beyond enhancing the yields and/or the scale-up of the processes. On the contrary, the broad spectra of products (gaseous stream, biocrude, hydrochar and aqueous products), the diversity in their composition (Xu et al., 2018a), and some unfavorable fuel and physicochemical properties are the major issues limiting product applications (Wibowo et al., 2021). For example, the biocrude produced shows some unwanted characteristics, such as high viscosity, low stability (Zhang et al., 2021b), high oxygen/nitrogen contents, and low calorific value (Yang et al., 2022a). These features make biocrude unsuitable for combustion and thus limit its use in diesel engines. Besides, the hydrochar directly produced from HTC has a high proportion of volatile species and low surface area, which hampers its use as a carbon material in catalysis and/or pollutant remediation/adsorption (Sevilla et al., 2017; Sultana and Reza, 2022). As a result of these intrinsic physicochemical characteristics, these products need to be subjected to different upgrading/modification processes. Furthermore, the aqueous and gaseous fractions produced from HTL and HTC usually remain unused and have been recognized as waste in the past few decades (Das et al., 2020; Marrakchi et al., 2023), with this latter consideration needing change urgently to develop holistic zero-waste biorefinery processes.

To handle these issues, different strategies have been developed to upgrade the biocrude (Haider et al., 2018), activate the hydrochar (Wen et al., 2023), and give value to the gaseous stream and the aqueous products (Marrakchi et al., 2023). The product properties can be improved through these downstream processes, with the unused products also being transformed into bio-based commodities to achieve zero-waste processes. Many previous reviews have commented on and summarized different strategies for analyzing and optimizing HC processes, including catalyst development (Nagappan et al., 2021), product upgrading/modification (Xu et al., 2018a), recycling/reutilization (Hong et al., 2021), and fermentation of downstream products (Shen et al., 2021). However, these strategies have not been discussed holistically, i.e., publications have primarily focused on the individual utilization/optimization of only one of these fractions to produce fuels (e.g., gaseous, liquid, and solid biofuels), or value-added commodities (chemicals and materials), without a critical analysis of the possible applications for the others. This individual approach must be substituted by an all-inclusive, zero-waste, fully-product utilization perspective to achieve a multi-product optimization. Despite the above-commented publications having covered detailed information about the intrinsic characteristic of each upgrading route, the potential applications for each fraction that might help direct future research have not been

Table 1
Characteristics, advantages, and disadvantages of biomass HC process (Gao et al., 2021; Jiang et al., 2018; Kumar et al., 2018; Sharma et al., 2022).

HC process	Processing conditions	Target products	Advantages	Disadvantages
HTG	Temperature: 300–500 °C Pressure: ~30 MPa Time: 5–60 min	H_2-rich Syngas (H_2, CH_4, CO, CO_2)	No requirement for wet biomass drying Minimizing coke formation High reaction rates Higher syngas quality compared to traditional methods	High energy consumption High requirements for the equipment
HTL	Temperature: 200–350 °C Pressure: 5–20 MPa Time: 5–120 min	Biocrude oil	No requirement for wet biomass drying High conversion efficiency with moderate processing conditions Higher yields and quality of biocrude oil than pyrolysis	Low quality of biocrude, complex composition High requirements for the equipment Gaseous and aqueous products are unused
HTC	Temperature: 180–250 °C Pressure: 2–10 MPa Time: 5–300 min	Hydrochar	No requirement for wet biomass drying Low pressure and temperature required Easy to separate the product (hydrochar)	Aqueous products containing high levels of carbohydrates and organic acids are unused
HTH	Temperature: 80–240 °C Pressure: <5 MPa Time: 30–120 min	Aqueous products (oligosaccharides, monosaccharides)	No requirement for wet biomass drying Low pressure and temperature used Potential for producing value-added chemicals	Corrosion of the equipment due to the acidic catalysts used

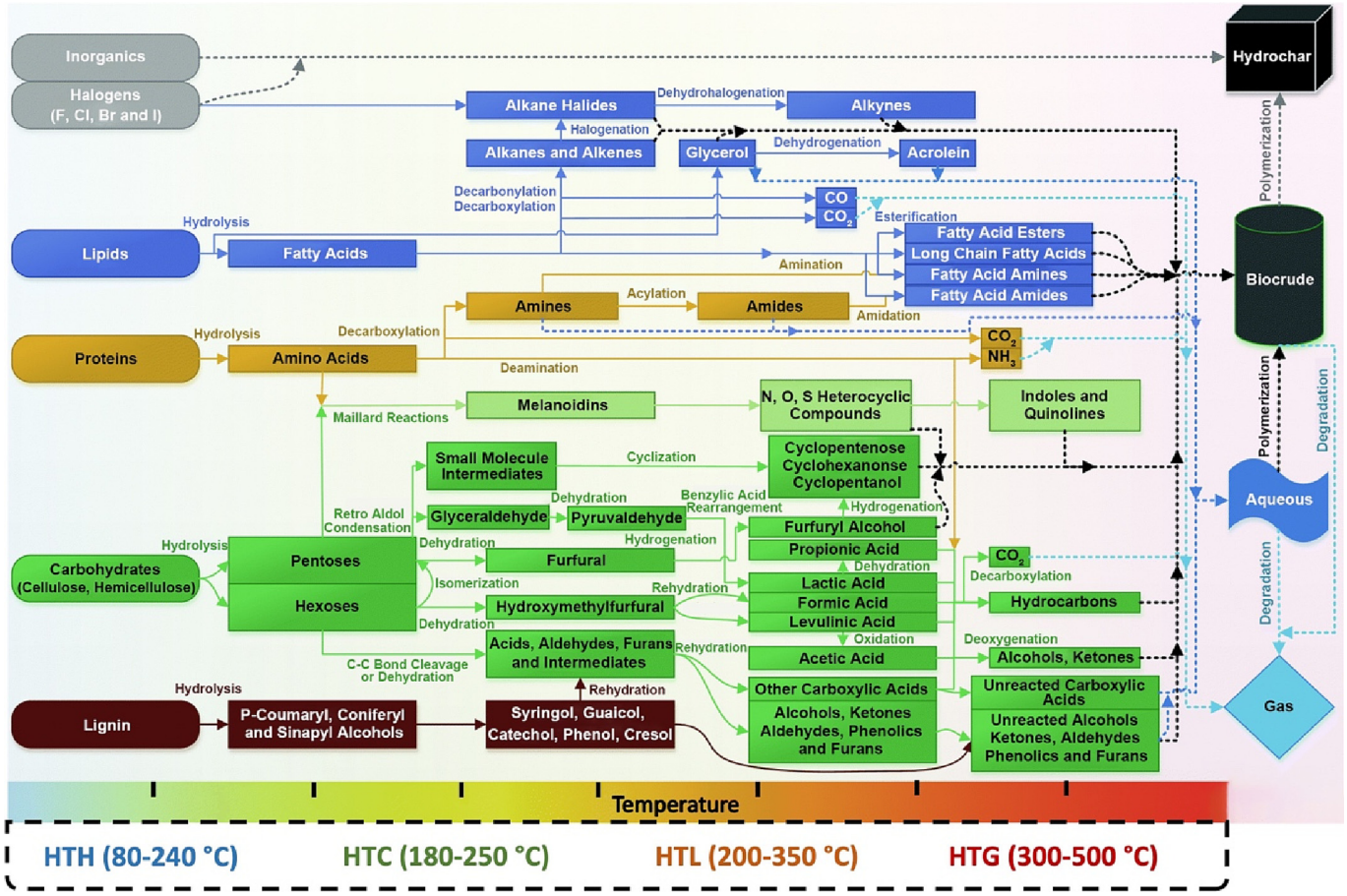

Fig. 1. Potential pathways in the hydrothermal conversion of biomass related to temperature. (Reprint from Ref. Basar et al. (2021), with permission from the Royal Society of Chemistry.)

discussed. Thus, this previous single-product strategy hampers the potential utilization of HC products and/or their integration into current biorefining processes.

Given this research opportunity, this review paper first-time analyses and discusses critically several downstream treatments, focusing on the possible commercial applications for each fraction produced during the HT of biomass, i.e., gas, biocrude, hydrochar, and aqueous product. Notably, this review emphasizes the latest developments and prospects in applying HC products as biofuels, biochemicals, and biomaterials. First, the most critical physiochemical properties of the HC products are summarized to provide the readership with helpful information on their commercial application. Then, not only the existing methods but also various potential routes to post-treat/upgrade these products to produce energy-dense biofuels, carbonaceous materials, and value-added chemicals and their application in energy, chemistry, and environment fields are summarized and compared. As a coronary, different present and future challenges and outlooks in applying HC products to achieve holistic 'waste to wealth' biorefineries are proposed and discussed.

2. Gaseous stream: physiochemical properties and present and future applications

2.1. Properties of the gaseous stream

The HC of biomass produces gaseous products via the following chemical reactions (Kumar et al., 2018; Yang et al., 2020):

$$\text{Reforming to CO}: C_xH_yO_z + (x-z)\,H_2O \leftrightarrow xCO + (x-z+y/2)\,H_2 \quad (1)$$

$$\text{Reforming to CO}_2: C_xH_yO_z + (2x-z)\,H_2O \leftrightarrow xCO_2 + (2x-z+y/2)\,H_2 \quad (2)$$

$$\text{Water} - \text{gas shift reaction}: CO + H_2O \leftrightarrow CO_2 + H_2 \quad (3)$$

$$\text{Methanation of CO}: CO + 3H_2 \leftrightarrow CH_4 + H_2O \quad (4)$$

$$\text{Methanation of CO}_2: CO_2 + 4H_2 \leftrightarrow CH_4 + 2H_2O \quad (5)$$

These reactions produce H_2, CO_2, CO, and CH_4 in the gaseous stream, whose composition is strongly influenced by the processing conditions. Notably, the (aqueous phase) reforming reaction of biomass-derived compounds (carbohydrates and polyols) occurs between 215 and 265 °C, forming CO_2, H_2, and CO as the leading products, but in a small amount (~1 vol%) (Shahbeik et al., 2022). On the contrary, operating at higher temperatures (350–400 °C, near the critical state of water), methane, forming from the methanation of CO and CO_2, is the primary product in the gaseous stream over heterogeneous catalysts (Sharma et al., 2022). Supercritical critical water gasification (SCWG) occurs above 374 °C with/without a catalyst, generating H_2 and CO_2 rather than CH_4 as the dominant products (Kumar et al., 2018). In most HTG studies, H_2-rich syngas (including H_2, CH_4, CO, and CO_2) is the target product. In addition to such gases, light hydrocarbon (C_2-C_4) formation with low proportions has also been observed during biomass HTG depending on the feedstock. A summary of the gaseous chemical composition from recent studies is presented in Table 2. These publications show that the gas yield could reach approximately 100 mol of gas/kg of biomass with the aid of a proper catalyst. As for biofuel production, some researchers have focused on controlling the gas stream to enhance the H_2 proportion in the gaseous phase

Table 2
Recent studies on the HTG of biomass.

Feedstock	Conditions	Catalyst	Gas yield	H_2	CH_4	CO_2	CO	C_{2+} alkane	Ref.
				Percentage (vol%)					
Sorbitol	300 °C, 11.5 MPa, 0.33 h^{-1} WHSV	Pt/γ-Al_2O_3	13 mol%	61.6	2.9	35.4	–	7.7	(Paida et al., 2019)
Sewage sludge-derived liquid	350 °C, 20 MPa, 25 h^{-1} LHSV	Ni/C	2.74 Nm^3/kg	40.9	51.1	8.0	–	–	(Zhang et al., 2018b)
Canola meal and polyethylene	525 °C, 22–25 MPa, 60 min	WO_3-TiO_2	~62 mmol/g	29.8	27.9	22.9	–	16.1	(Nanda et al., 2022)
Activated sludge	380 °C, 15 min, 1.5 g cat/g feedstock	Raney Ni	33 mmol/g	46	25	29	–	–	(Afif et al., 2011)
Chlorella vulgaris	500 °C, 36 MPa, 30 min	NaOH	21.9 mol/kg	68.8	23.3	–	–	7.94	(Onwudili et al., 2013)
Soybean straw	500 °C, 45 min	Ni/Ce-ZrO_2	24.3 mmol/g	44.9	15.2	37.4	–	2.5	(Okolie et al., 2021)
Chlorella vulgaris and hydrochar	650 °C, 300 bar, 120 s	–	30.99 mol/kg	23.44	20.60	41.74	6.92	5.83	(Sztancs et al., 2020)
Microbial sludge and algae	360 °C, 60 min	–	–	36.1	38.4	19	–	–	(Jayaraman et al., 2021)
Scenedesmus. sp. and sewage sludge	440 °C, 60 min	ZnO	40.7 wt%	38.27	–	–	–	–	(Arun et al., 2020)
Lignite and sorghum	500 °C, 30 min, 20 % (v/v) NMP	K_2CO_3/CaO	181.6 mol/kg	54.4	21.4	21.5	2.8	–	(Hasanoğlu et al., 2023)
Glucose	250 °C, 90 min	Pt-W	391 mL	66.5	–	17.7	15.3	–	(Saquic et al., 2022)
Waste tires	600 °C, 23.3 MPa	–	–	51.9 mmol/g	28.5	–	–	–	(Nie et al., 2022)
Sewage sludge	700 °C, 30 min	Ni@HC	–	109.2 g/kg	–	–	–	–	(Gai et al., 2019b)
Cotton stalk	360 °C, 10 min	Ni-La/SBC	–	90.4 mol%	–	–	–	–	(Song et al., 2022)
Soybean straw	500 °C, 45 min	–	14.9 mmol/g	44.4	14.9	36.6	2.1	2.0	(Okolie et al., 2020b)

due to its clean and excellent fuel properties. A detailed overview of different strategies for the gaseous stream is described as follows.

2.2. Gaseous fuel

2.2.1. Gaseous stream cleaning

An overview of different applications for the gaseous stream is illustrated in Fig. 2. This fraction is similar to syngas, containing H_2, CO_2, CH_4, and CO, along with other compounds in small amounts (Sharma et al., 2022). Attaining high proportions of H_2 and CH_4 in the gaseous stream is paramount to using this fraction as a gaseous fuel for heat and power applications due to their high calorific value, whereas the relative amount of CO_2 should be minimized to improve the fuel properties of this product (Shahbeik et al., 2022). However, the production of H_2 and CH_4 is usually accompanied by the generation of CO_2 during the HC of biomass (Sharma et al., 2022), which requires removing the CO_2 in downstream processes. Additionally to CO_2, the syngas produced from biomass includes different impurities depending on the type of feedstock, such as NH_3, HCl, and H_2S, along with tar particles and ash (Okolie et al., 2020a). These contaminants harm the environment and lead to equipment corrosion/damage and catalyst poisoning (Mondal et al., 2011). Therefore, the clean-up and/or removal of these impurities and by-products of the syngas produced

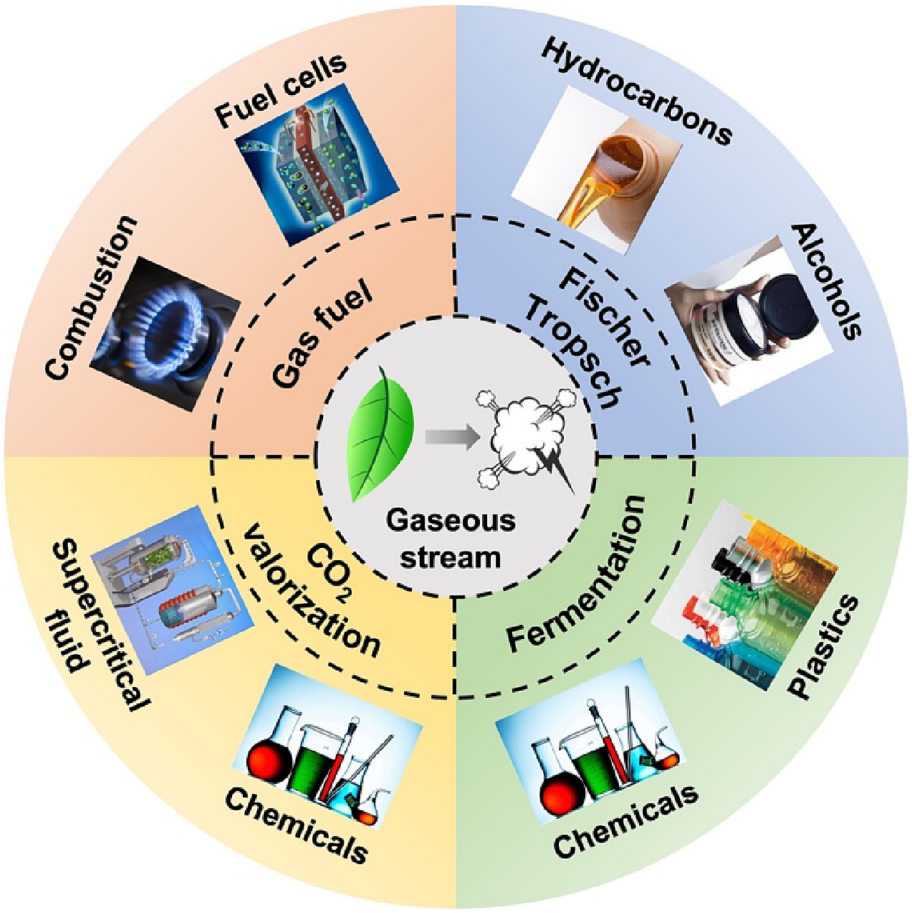

Fig. 2. An overview of gaseous stream applications.

during the HTG of biomass is essential before its application as a gaseous fuel or for further valorization.

The initial step in the purification process is syngas cleaning, i.e., removing impurities (H_2S, NH_3, HCl, tar, and ash particles). Commonly, the cleaning methods for tar (condensable organic compounds) formed during HTG of biomass are (catalytic) thermal cracking, physical separation, and non-thermal plasma separation (Shahbeik et al., 2022). Thermal cracking methods require high reaction temperatures and can be performed on an industrial scale (Shahabuddin et al., 2020; Woolcock and Brown, 2013). Introducing catalysts to such processes can reduce energy consumption and increase tar removal efficiency. However, during the thermal cracking process, the possible formation of soot might result in the deactivation of catalysts (Shahabuddin et al., 2020). Physical separation methods include using scrubbers and electrostatic precipitators at low temperatures (<100 °C). These technologies can be used on an industrial scale (Shahbeik et al., 2022), but they lead to the generation of wastewater in high amounts (Woolcock and Brown, 2013). Another method for tar removal is using non-thermal plasma (reactive atmosphere of free electrons and ions). Unfortunately, this latter is an effective but energy-intensive technique, which makes it challenging to scale up (Saleem et al., 2020).

The technologies for removing inorganic species (solid carbon and ash) include filtration, centrifuge separation with cyclones, electrostatic separation, and wet scrubbing (Woolcock and Brown, 2013). The inorganic particles in the syngas can be filtrated after a series of pretreatments (Lang et al., 2021), such as diffusion, inertial impaction, gravitational settling, and aggregation (Heidenreich, 2013). A high separation efficiency can be achieved using this method, with them being appropriate for use on an industrial scale. Based on the mass and acceleration principle, cyclones can separate heavier particulates from lighter gaseous products with a high removal efficiency on an industrial scale, but high temperatures (1100 °C) are usually required. Electrostatic separation removes particles effectively at ca. 400 °C through the difference in the dielectric properties under an electric field (Jaworek et al., 2019), with the technology being available on a pilot scale. Wet scrubbing utilizes water to trap inorganic particles at temperatures below 100 °C and has been demonstrated on an industrial scale with a removal efficiency of up to 95 % (Shahbeik et al., 2022). In 2007, Gussing (Austria) developed an industrialized gasification plant for dry dust removal via wet scrubbing (Saleem et al., 2020). For alkali impurities (Na and K), condensation, adsorption, and wet scrubbing methods are commonly applied (Shahbeik et al., 2022). Condensation requires high processing temperatures (ca. 600 °C) to nucleate and agglomerate basic vapors. In contrast, adsorption methodologies utilize solid adsorbents (e.g., kaolinite and bauxite) at ca. 800 °C with a removal efficiency of up to 99 %, and their viability has been tested on a pilot scale (Woolcock and Brown, 2013). Wet scrubbing can also be applied to separate alkali compounds using water as the trapping agent (Shahbeik et al., 2022). Despite this process being performed on an industrial scale at relatively low temperatures, it generates wastewater as the by-product.

Sulfur compounds and halides (HCl) can be separated from the syngas via chemical and physical adsorption at 400–600 °C, with the technology being tested on a pilot scale (Mondal et al., 2011). Besides, sulfur compounds can be removed by solvent adsorption methodologies (Cheah et al., 2009). Nitrogen compounds (mainly NH_3) can be removed from the syngas by thermal catalytic degradation, which converts NH_3 to N_2 and H_2 using a catalyst on an industrial scale (Shahabuddin et al., 2020). Furthermore, nitrogen-containing compounds and halides can be adsorbed by water at temperatures lower than 100 °C, with the process demonstrated on an industrial scale (Shahbeik et al., 2022).

2.2.2. CO_2 removal

The gas fraction produced during the HTG of biomass contains a high proportion (10–50 vol%) of CO_2 (Zhang et al., 2018b). This makes the raw bio-syngas unsuitable for direct combustion in engines or for synthesizing other commodities. Therefore, removing CO_2 is essential before its application as gaseous fuel or precursor for value-added products. Traditionally, physical and chemical adsorption technologies using different solids have been developed and commercialized for CO_2 removal (Wibowo et al., 2021). Common adsorbents include activated carbon, metal-organic frameworks, carbon nanotubes, and zeolites with high surface area and excellent stability and recyclability at elevated temperatures (Wibowo et al., 2021). This technology shows good resistance to sorbent loss and can be operated at high temperatures. For example, Rahimi et al. developed modified multi-walled carbon nanotubes for CO_2 adsorption with 92.71 mg/g uptake (Rahimi et al., 2019). However, some of these cannot be applied on a large scale and exhibit low adsorption selectivity to CO_2 (Wibowo et al., 2021).

Another alternative for CO_2 purification is cryogenic methods, which can separate CO_2 from the syngas stream by liquefaction with a separation efficiency higher than 99.9 % (Wibowo et al., 2021). However, this technology requires much energy to convert CO_2 into a liquid state (Baena-Moreno et al., 2019). Alternatively, CO_2 can also be captured and removed based on the pressure difference through a membrane material (selectively permeable barrier) (Wibowo et al., 2021). This technology affords low energy consumption and high separation efficiency for CO_2 separation (Solangi et al., 2021). Among these, ionic liquid membranes have attracted worldwide attention due to their low energy consumption (room temperature) and high separation efficiency (up to 500 CO_2/N_2 selectivity) (Ying et al., 2019). Wang et al. designed a process using ionic liquid for CO_2 and H_2S removal from syngas (Wang et al., 2019). They found that [bmim][Tf_2N] showed high removal rates, i.e., 97.6 % and 95.3 % for CO_2 and H_2S, respectively. Another widely-commercialized method is using liquid absorbents (e.g., amines) (Shahbeik et al., 2022). Despite this method being economically feasible, there are different operation drawbacks, such as high sorbent loss, high energy consumption and corrosion issues, hampering its commercial implementation.

2.2.3. Application of syngas in internal combustion engines

Syngas suitable for utilization in engines can be obtained after the post-treatment of the raw syngas produced during the HTG of biomass. This combustible syngas should meet the standard to limit its emission of exhausted gas fractions (non-methane organic gases, CO, NO_x, PM, and HCHO) (Azimov et al., 2011). To suit these requirements, Xu et al. optimized the syngas composition for a syngas/diesel Reactivity Controlled Compression Ignition (RCCI) engine (Jamsran et al., 2021). The results showed that syngas with a 75 vol% H_2 fraction could achieve high efficiency, moderate combustion, and low emissions.

These internal combustion engines can convert the treated, bio-derived syngas into electricity, power, and heat (Fiore et al., 2020), with this sustainable approach helping reduce the emission of greenhouse gases. Many publications have studied the combustion behavior of syngas in internal combustion engines (Karthikeyan et al., 2020), such as boosted spark-ignition engines (Park et al., 2021) and RCCI engines (Jafari et al., 2021). Commonly, these include dual-fuel, homogeneous charge spark ignition (HCSI), and direct injection (DI) engines (Fiore et al., 2020). Dual-fuel engines use conventional diesel and alternative fuels (syngas) to generate heat and power (Fiore et al., 2020). HCSI engines mix air and gaseous fuel in a carburetor (Fiore et al., 2020) and the process is limited by the gaseous fuel/air injected into the cylinder due to the low density of the gas. Due to two operational facts, DI engines have become very popular recently. One is the direct syngas injection with no limit on the amount of air introduced to the cylinder, which dramatically improves the volumetric efficiency of the engine. The other comprises the direct injection of the syngas, which can extend the operating range of the engine, allowing for operating under more streamlined conditions (Fiore et al., 2020).

2.2.4. Application of syngas in fuel cells

In addition to burning in combustion engines, the purified syngas can produce electricity in fuel cells. A fuel cell is a green and environmentally benign equipment with high electricity production efficiency and low pollutants emission (Fabbri et al., 2010). Among the different fuel cell configurations, solid oxide fuel cells (SOFC) and molten carbonate fuel cells (MCFC) have gained much attention for converting syngas to electricity

with power efficiency as high as 60 %. Additionally, the efficiency can reach up to 90 % by using a combined heat and power system (Radenahmad et al., 2020). Fig. 3 shows the electrochemical conversion of H_2 and CH_4 (Dey et al., 2014).

The performance of syngas-fueled SOFC has been thoroughly analyzed. There are many works in the literature addressing different strategies to improve the functionality of fuel cells. For example, Jin et al. analyzed the performance of a novel 550 Mwe syngas-fueled SOFC and an air turbine hybrid system (Jin et al., 2021). They found that a power output efficiency of 64 % can be attained by augmenting the pressure to 10 atm and applying a two-stage SOFC design. In another work, Habibollahzade and Rosen conducted multi-criteria optimization to select the best feedstock (gas composition) to improve the functionality of SOFC powered by syngas (Habibollahzade and Rosen, 2021). The results suggested that higher current densities and fuel utilization factors result in the optimal values of local power output and levelized cost and emissions. In general, the performance of SOFCs was affected by gas recycling at the anode and cathode and the feedstock composition. For the syngas used in fuel cells, the sulfur impurities should be controlled below 15 ppm (Radenahmad et al., 2020), as sulfur species could poison Ni anodes in SOFC. Besides, the concentration of CO_2 should be kept at a low level due to the carbon deposition on the anode caused by excess CO_2. However, when it comes to MCFC, CO_2 behaves as a feedstock for the cathode and a necessary component to form the electrolyte (De Lorenzo et al., 2017). There are no strict requirements for CO_2 concentration in MCFC.

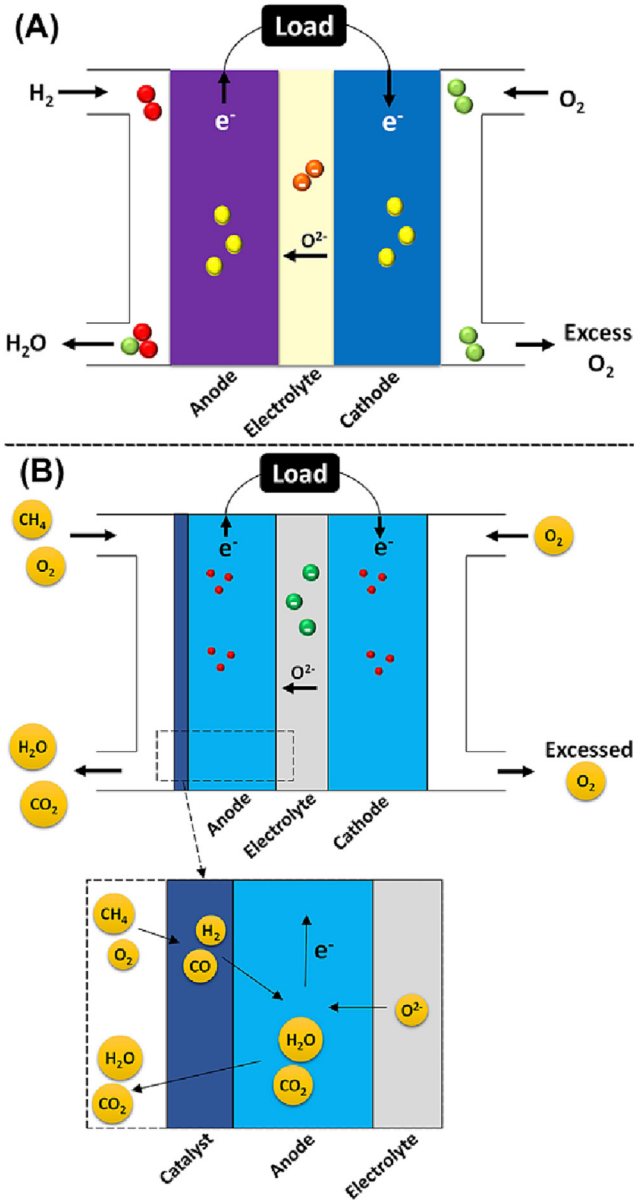

Fig. 3. Electrochemical reactions in a fuel cell with (A) H_2-O_2 and (B) CH_4-O_2. (Adapted from Ref. (Radenahmad et al., 2020), with permission from Elsevier).

2.3. Syngas valorization

2.3.1. Chemical conversion of syngas

In addition to gaseous fuel, biomass-derived syngas also shows the potential to be valorized into liquid fuels and/or value-added chemicals via gas-to-liquid technologies, which primarily include chemical conversion (Santos and Alencar, 2020) and biological fermentation (Wainaina et al., 2018). Among the chemical conversion methods, the Fischer-Tropsch synthesis (FTS) developed in the early 19th century (Fischer, 1925; Fischer and Tropsch, 1923) is a classic and mature technology to obtain liquid hydrocarbons (paraffins, olefins, and aromatics) (Santos and Alencar, 2020) and oxygenated compounds (methanol, ethanol, and long chain alcohols) (Ao et al., 2018) for syngas (mainly CO and H_2). Paraffins (gasoline) can be used as fuels in engines, whereas lower (C_{2-4}) olefins (ethylene, propylene, and butenes) are necessary platform chemicals for the manufacturing of plastics, pharmaceuticals, and paints (Zhou et al., 2019). Besides, long-chain alcohols are key raw materials for the production of paints, coatings, surfactants, and detergents (Ao et al., 2018), while short-chain alcohols (C_{2-5}) can also be applied as transportation fuels (either alone or blended) (Ao et al., 2018). In the last century, FTS plants were built in Germany, Japan, and the US, with >110,000 tons of products yielded (Santos and Alencar, 2020). In a typical FTS process, the syngas (CO and H_2) proceeds via the following routes to form longer chain hydrocarbons: (1) adsorption of CO and H_2 on the catalyst surface; (2) formation of CH_x species (x = 0–3); (3) carbon chain growth via C—C coupling reactions to form C_nH_m species ($n \geq 2$); (4) hydrogenation and dehydrogenation of the formed C_nH_m species to long chain olefins and paraffins, respectively (van Santen et al., 2013). Besides, the alkyl species (CH_x and C_nH_m) can further react with the adsorbed CO, forming acyl intermediates (CH_xCO and C_nH_mCO). These acyl species undergo hydrogenation reactions with the adsorbed H_2 to generate ethanol or C_{n+1} alcohols. In addition to this pathway, CO can be partially hydrogenated to a formyl intermediate (CHO), which subsequently inserts into the alkyl group leading to alcohols (Fang et al., 2009). The overall reactions occurring during the FTS to generate paraffins, olefins, and alcohols are as follows (Zhou et al., 2019):

$$(2n+1)H_2 + nCO \rightarrow C_nH_{2n+2} + nH_2O \quad (6)$$

$$2nH_2 + nCO \rightarrow C_nH_{2n} + nH_2O \quad (7)$$

$$2nH_2 + nCO \rightarrow C_nH_{2n+1}OH + (n-1)H_2O \quad (8)$$

Despite FTS being a mature technology investigated for decades, recent studies have focused on improving product selectivity and CO conversion (Huang et al., 2022; Li et al., 2019) and reducing the overall energy consumption of the process (Li et al., 2020b). Table 3 summarizes some recent advancements in the chemical conversion of syngas for the production of fuels and chemicals. For long-chain hydrocarbon (paraffins and olefins), bifunctional catalysts (e.g., metal supported on and/or combined with zeolite catalysts) are applied (Li et al., 2019; Li et al., 2018). These catalysts show tremendous C—C coupling, hydrogenolysis, cracking, and isomerization activity. Li et al. reported a dual metal oxide-zeolite catalysis system for synthesizing high-quality gasoline fuel (Li et al., 2019). The bifunctional Zn_2MnO_x-SAPO-11 catalyst exhibited excellent hydrocarbon productivity with 76.7 % C_5-C_7 hydrocarbon selectivity and 20.3 % CO conversion, with only 2.3 % CH_4 produced. In another work, Ni and coworkers developed a dual-bed catalyst ($ZnAlO_x$-SAPO-34) for the conversion of syngas-to-olefins, achieving a proportion of C_{2-4} olefins in the hydrocarbon

Table 3
Recent studies on the chemical conversion of syngas to produce fuels and valuable products.

Catalyst	Reaction conditions	CO conv. (%)	Product distribution (mol)	Ref.
CuCoAl|ZnO/ZrO_2	250 °C, 5 MPa, 4000 mL/(g_{cat} h), H_2/CO = 2	13.1	ROH (42.6 wt%), CO_2 (18.2 wt%), C_{2+}OH in alcohols (83.7 %)	(Huang et al., 2022)
Fe_5C_2-Cu	260 °C, 1 MPa, H_2/CO = 2, 2400 mL/(g_{cat} h)	53.2	CH_4 (3.7 %), C_{2+}H (36.5 %), ROH (29.8 %), CO_2 (30.0 %)	(Li et al., 2020b)
$Zn_2Mn_1O_x$ and SAPO-11	360 °C, 4 MPa, H_2/CO = 1, 1000 mL/(g h)	20.3	CO_2 (50.0 %), hydrocarbon (50.0 %), gasoline in hydrocarbon (76.7 %)	(Li et al., 2019)
$ZnAlO_x$/SAPO-34	390 °C, 4 MPa, H_2/CO = 1, 12,000 mL/(g h)	6.9	CO_2 (33.1 %), C_{2-4} olefins (77.0 %), CH_4 (5.5 %)	(Ni et al., 2018)
ZnO/SAPO-34	400 °C, 4 MPa, H_2/CO = 2.5, 1600 mL/(g h)	33.5	CO_2 (41 %), CH_4 (2.9 %), C_2-C_4 olefins (76.1 %), C_2-C_4 paraffins (16.4 %)	(Li et al., 2018)
CoMn | CuZnAlZr	250 °C, 6 MPa, H_2/CO = 1, 2000 mL/(g h)	29.0	CO_2 (21.6 %), ROH (58.1 %), olefins (22.5 %), paraffins (19.4 %)	(Lin et al., 2019)
$ZnAlO_x$-SAPO-11	250 °C, 6 MPa, H_2/CO = 1, 2000 mL/(g h)	34.2	CO_2 (49.8 %), C_5-C_{11} in hydrocarbons (81.6 %), *i*/*n* paraffins (38)	(Feng et al., 2022)
$ZnCr_2O_4$-HZSM-5	350 °C, 2 MPa, H_2/CO = 1, 300 mL/(g h)	37	Tetramethylbenzene in hydrocarbons (70 %)	(Arslan et al., 2019)
MnCr-Z5-Si4 (1/1)	430 °C, 4 MPa, H_2/CO = 2, 1000 mL/(g h)	33.9	Aromatics in hydrocarbons (47.2 %), xylene in aromatics (62.7 %)	(Miao et al., 2020)
Zn-Cr@SAPO	400 °C, 2 MPa, H_2/CO = 2, 6480 mL/(g h)	10.69	C_2-C_4 olefins (64.31 %), CO_2 (36.16 %)	(Tan et al., 2020)
K + −ZnO − ZrO_2|H-MOR−DA − 12MR|Pt − Sn/SiC	310 °C, 5 MPa, H_2/CO = 1, 20 h	10	EtOH (72 %), CO_2 (35 %)	(Kang et al., 2020)

fraction of 77.0 %, and 33.1 % CO_2 selectivity at 390 °C with a catalyst lifetime superior to 100 h (Ni et al., 2018).

In syngas-to-alcohol processes, catalysts with bifunctionality are also preferred. These fulfill two main requirements for the extension of such conversion, i.e., two different active sites for CO dissociation, carbon chain growth, and CO insertion and alcohol formation (Ao et al., 2018). Therefore, bimetallic and multi-metallic catalysts (e.g., Mo, Rh, Co, Fe, Zn—Cr based catalysts) have been commonly used in syngas-to-alcohol synthesis (Ao et al., 2018). Kang et al. developed a triple tandem catalyst for high-selectivity ethanol synthesis from syngas (Kang et al., 2020). The trifunctional Pt-modified ZnO-ZrO_2 combined with modified zeolite mordenite and PtSn/SiC catalysis system can efficiently convert syngas to ethanol with a selectivity of 90 %. In another publication, Li et al. reported on a Fe_5C_2-Cu nano-catalyst for converting syngas to long-chain alcohols under a pressure as low as only 1 MPa, achieving 14.8 % (mol) selectivity and 53.2 % CO conversion (Li et al., 2020b). Overall, valorizing syngas through FTS produces a wide range of products, including hydrocarbons and oxygen-containing compounds. However, FTS requires strict ratios of H_2 and CO and harsh processing conditions (high temperature and pressure). In addition to such operating requirements, the process furnishes a broad spectrum of different chemicals. Given these drawbacks, efforts should be put into designing highly active and stable heterogeneous catalysts yielding products with high selectivity.

2.3.2. Syngas fermentation

Biological approaches have also been used for syngas valorization. Such conversion routes usually take place under mild conditions in the presence of microorganisms (Sun et al., 2019). Compared to FTS, the valorization of syngas via biological processes provides the following advantages: (1) lower energy consumption at ambient temperatures and pressures; (2) enhanced product yields and selectivity due to the specificity of enzymes; (3) flexibility on the proportion of syngas components; (4) insensitive to a small amount of impurities (Gunes, 2021; Sun et al., 2019). In biological processes, acetogenic bacteria are applied to ferment the components in syngas (H_2, CO, and CO_2) with flexible composition into biofuels (e.g., ethanol (Kumar et al., 2021), butanol (Sun et al., 2022), and methane), value-added biochemicals (e.g., acetic acid, formic acid, butyrate, and caproate) (Liu et al., 2018a; Xiang et al., 2022), and biomaterials (polyhydroxyalkanoates) (Bhatia et al., 2021). The potential products and their formation mechanisms are illustrated in Fig. 4.

Table 3 provides a detailed summary of biomass fermentation into fuels and valuable products, covering the work of recent publications. As for chemical production, carboxydotrophic bacteria have been used to convert syngas molecules via the acetyl-CoA route to synthesize alcohols, organic acids, and ATPs (Sun et al., 2022). Alcohols include ethanol (Kumar et al., 2021) and butanol (Sun et al., 2022), which are promising fuel alternatives and/or additives to fossil fuels due to their high heating value, clean burning properties, and low corrosiveness (Wainaina et al., 2018). Besides, bio-derived alcohols can also be used as solvents and precursors to produce other value-added chemicals (Wainaina et al., 2018). The fermentation of syngas for alcohol production has been industrialized and performed on a full scale by LanzaTech in New Zealand, achieving a productivity of over 50,000 Mt. per year (Gunes, 2021). In addition to biofuels, producing valuable platform chemicals is also appealing. Syngas can also be fermented to carboxylic acids (e.g., acetic acid, butyric acid, and caproic acid) and/or carboxylates with added value. Acetic acid is a platform chemical for producing adhesives, inks, paints, coatings, and an antiseptic against pseudomonas infections (Asimakopoulos et al., 2018). Carboxylic acids with longer carbon chains (e.g., butyric acid and caproic acid) are also building block chemicals for the synthesis of carboxylate, cellulose acetate butyrate, poly(3-hydroxybutyrate) and are used as additives in the food industry (Li and Henson, 2019).

Furthermore, syngas can also be fermented to biomaterials (polyhydroxyalkanoates, PHAs) in the presence of phototrophic bacteria such as *Rhodospirillum rubrum* (Dhakal and Acharya, 2021). PHAs have gained wide attention due to their excellent biodegradability and

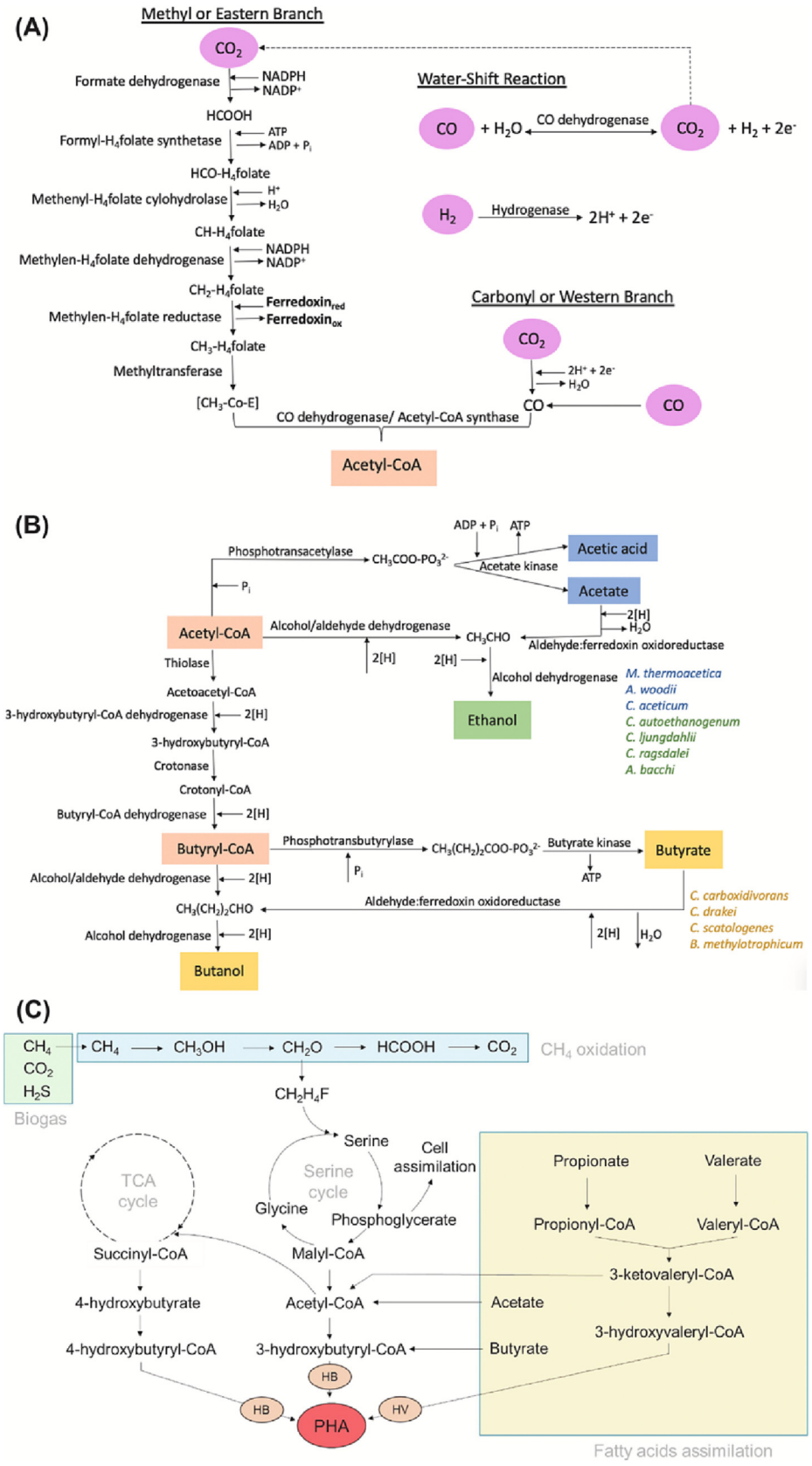

Fig. 4. Wood-Ljungdahl metabolic pathways: (A) acetogenesis phase and (B) solventogenesis phase. (C) Tentative PHA production pathway. (Adapted from Refs. (Gunes, 2021; López et al., 2018), with permission from Elsevier).

Table 4
Recent studies on syngas fermentation to produce fuels and valuable products.

Product	Microorganisms	Feed ratio (v/v %)	Growth conditions	Reactor	Yield (g/L)	Ref.
Ethanol	*Clostridium butyricum*	$CO/H_2/CO_2/N_2/CH_4$ (23/13/8/46/1)	37 °C, pH = 4–6	Tar free bioreactor	29.94 mmol/L	(Monir et al., 2020)
Ethanol, acetic acid	*Clostridium carboxidivorans*	$CO/CO_2/H_2$ (40/30/30)	37 °C, pH = 6	Batch	1.16 (ethanol), 5.12 (acetic acid)	(Sun et al., 2022)
Ethanol, butanol	*Clostridium carboxidivorans*	$CO/H_2/CO_2$ (40/30/30)	37 °C, pH = 5–7	Batch	4.09	(Sun et al., 2018)
Ethanol, butanol	*Clostridium carboxidivorans*	$CO/H_2/CO_2$ (40/40/20)	37 °C	Batch	3.11	(Cheng et al., 2019)
Butanol	Anaerobic sludge	CO (100 %)	33 °C, pH = 5–6.5	Fed batch	6.8	(He et al., 2022)
Acetate	Anaerobic sludge	$CO/H_2/CO_2/N_2$ (20/20/10/50)	37 °C, pH = 6.5, 7.5	Batch	8	(Luo et al., 2018a)
Organic acids	*Clostridium*	CO/H_2 (40/60)	35 °C	Biofilm reactors	Acetate (4.22), butyrate (1.35), caproate (0.88), caprylate (0.52)	(Shen et al., 2018a)
Volatile fatty acids	*Clostridium*	CO/H_2 (40/60)	35 °C	Biofilm reactor	61.9 mmol/L	(Wang et al., 2018a)
Organic acids	*Clostridium carboxidivorans*	$CO/H_2/CO_2/N_2$ (30/20/10/40)	33 °C, pH = 6.2	Continuous gas-fed bioreactor	11,303 mg/L	(Fernandez-Naveira et al., 2019)

compostable properties, and are a promising alternative to petroleum-based plastics such as poly(ethylene terephthalate), poly(vinyl chloride), and poly(ethylene) (Yoon and Oh, 2022). Currently, PHA-based materials have been industrialized into commercial products, such as Biopol, Nodax, Degr Pol, and Biogreen (Devadas et al., 2021). Although conducted under mild conditions, the issues in the biological fermentation processes are the long fermentation time (dozens of days) and the null reusability of the microorganisms. Therefore, future research goals should be focused on improving the fermentation efficiency and the recovery of the bacteria.

2.4. CO_2 valorization

The HC of biomass unavoidably generates high amounts of CO_2 (10–50 vol%) in addition to the target products (H_2, CO, and CH_4) due to reaction mechanisms responsible for gas formation (Zhang et al., 2018b). The proportion of CO_2 in the gaseous phase can even reach concentrations higher than 80 vol% during the HTC and/or HTL of some feedstocks, such as algae (Zhou et al., 2022b), almond hulls (Remón et al., 2021a) and face masks (Remón et al., 2022). Although CO_2 can be removed from the desired gaseous products, it is constantly emitted into the atmosphere and can aggravate global warming despite the carbon neutrality of the CO_2 produced from biomass. Thus, finding appropriate methodologies to utilize and valorize CO_2 could reduce its emission to the environment. One potential option to valorize CO_2 in the gaseous stream from HC is applying CO_2 in supercritical technologies. Supercritical CO_2 ($scCO_2$) technology has recently attracted considerable attention in many areas. These include its use as an extraction solvent for bio-reactive compounds (Sahena et al., 2009), its utilization in separation and extrusion processes (Manjare and Dhingra, 2019), and its application as a heat transfer fluid in power cycles (Liao et al., 2019). Additionally, non-toxic $scCO_2$ is an ideal solvent for extracting food-grade natural compounds (e.g., lipids, cholesterol, and carotenoids) in the food industry (Sahena et al., 2009). The earliest industrialized $scCO_2$ technology in extraction was conducted by Hag A.G. in Germany to decaffeinate green coffee beans (Sahena et al., 2009). Besides, the high volatility and low polarity of $scCO_2$ make it an ideal solvent for chemical reactions (Cabeza et al., 2017). $ScCO_2$ can also be applied in material science for extrusion processes since it is soluble in molten polymers and for processing materials such as 3D aerogels, coatings, and graphite (Cabeza et al., 2017). Additionally, a more recent application for CO_2 is to use it as a heat transfer fluid in power cycles, solar collectors, and carbon capture and storage devices (White et al., 2021). One noticeable industrialized program SunShot for concentrated-solar power plant, with a thermal efficiency of 50 % under a 10 Mw_e $scCO_2$ turbine up to 750 °C, which targets a levelized cost of electricity of 0.06 $/kWh (White et al., 2021).

Converting CO_2 to fuels and valuable chemicals is also an up-and-coming alternative to its application as a supercritical fluid (Aresta et al., 2014). Using CO_2 to synthesize chemicals dates back to the 18th century, wherein pure thermal processes were applied (Aresta et al., 2014), yet, a substantial step ahead has been taken recently. For example, a mature technology consists of using CO_2 and NH_3 to synthesize urea (H_2NCONH_2). In such a process, CO_2 and NH_3 react to form ammonium carbonate, which then decomposes into urea and H_2O (Aresta et al., 2014). Besides, CO_2 can also react with inorganic minerals (e.g., Mg and Ca oxides) to form inorganic carbonates, which can be used for CO_2 storage (Aresta et al., 2014) (Table 4).

CO_2 reduction is also an intelligent strategy to furnish value-added chemicals, with H_2 being used as the reduction agent in most cases. CO_2 reduction is a complex multistep process leading to the formation of various C_1 and C_2 products (such as carbon monoxide, methanol, formic acid, and methane) (Wang et al., 2022b), as shown in Fig. 5. In particular, C_1 and C_2 products can be formed via four main pathways: carbene, formaldehyde, formal and glyoxal (Walsh et al., 2016). The intermediate species in one pathway could also be desorbed as a final product in another. This electrochemical approach is an excellent alternative to the classical thermochemical catalysis usually used in forming these products. Such an advantageous character is accounted for by the very stable electronic structure of the CO_2

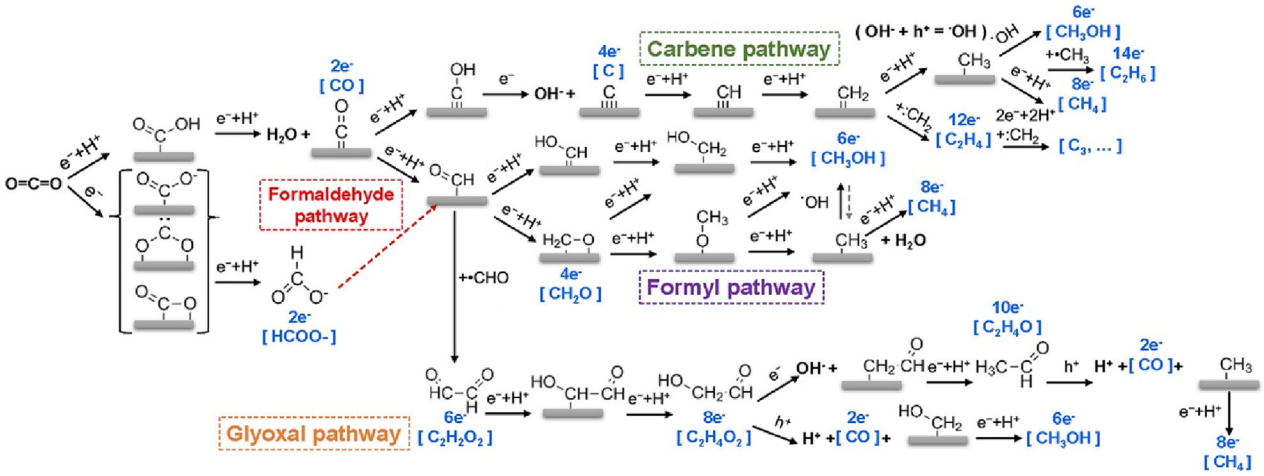

Fig. 5. Mechanisms involved in the CO_2 reduction to C_1 and C_2 products. (Reprint from Ref. Wang et al. (2022b), with permission from ACS Publications).

molecule. As a result, its thermal conversion needs harsh conditions (high temperature and pressure), leading to higher energy demand and a need for more costly apparatus (Chang et al., 2019).

For the catalytic reduction of CO_2, active metals such as Au, Ag, Pd, Sn, and Ni have been applied as the electro-/photocatalyst (Long et al., 2018; Yin et al., 2019). The catalytic process occurs at ambient temperatures and atmospheric pressures in the presence of electricity or light. Some of the most representative publications on this matter include that of Digdaya et al., who reported on the capture and reduction of CO_2 from seawater using a coupled electrochemical system (Digdaya et al., 2020). The CO_2 capture efficiency reached 71 % with an electrochemical energy consumption of 155.4 kJ/mol and a 95 % total Faradaic efficiency for CO_2 reduction to CO. In recent work, Ou et al. developed a Mn_1Co_1/CN single-atom photocatalyst for CO_2 conversion (Ou et al., 2022). They found that Mn promoted H_2O oxidation, whereas Co atoms promoted CO_2 activation. An excellent CO production rate of 47 μmol g^{-1} h^{-1} was achieved using this two-active-center single-atom photocatalyst.

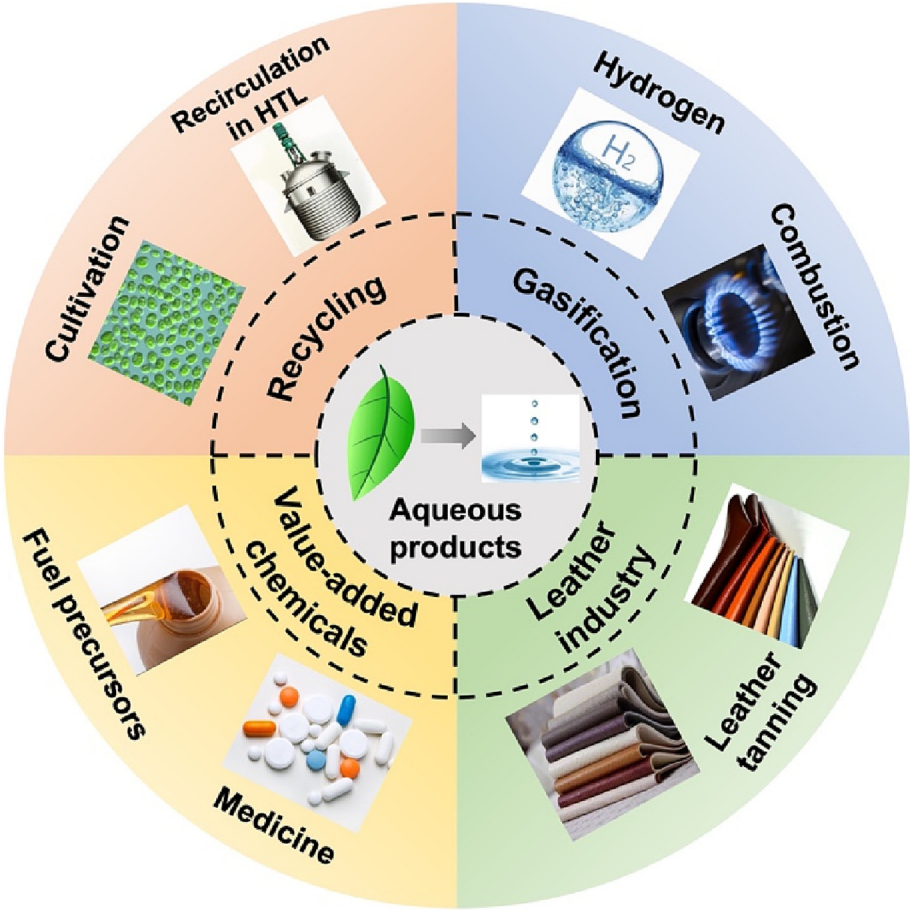

Fig. 6. An overview of different applications for the AP produced by the HC of biomass.

Table 5
Typical properties of AP from biomass HC.[a]

Feedstock	Processing conditions	pH	TOC (g/L)	COD (g/L)	TN (g/L)	TAN (g/L)	TP (g/L)	Ref.
Cellulose and bovine serum albumin (0.5:0.5)	225 °C, 8 h	8.2	18.2	61	4.8	2.5	–	(Usman et al., 2020)
Sludge	225 °C, 4 h	7.1	33.6	–	10.6	4.1	0.463	(Belete et al., 2019)
Chlorella pyrenoidosa	280 °C, 1 h, 35 wt% solid ratio	8.25	–	102	27.9	–	14.3	(Gai et al., 2015)
Sludge	350 °C, 3000 psi	6.4	1.0 wt%	40.8	0.4 wt%	–	–	(Maddi et al., 2017)
Algae	350 °C, 3000 psi	7.9	1.8 wt%	55.6	0.9 wt%	–	–	(Maddi et al., 2016)
Swine manure	270 °C, 1 h, 13 wt% solid ratio	–	–	39.8	1.85	–	–	(Si et al., 2019b)
Algae	260 °C, 1 h, 25 wt% solid ratio	–	–	52.0	80	18.8	–	(Si et al., 2019b)
Cornstalk	260 °C, 1 h, 20 wt% solid ratio	–	–	76.2	1.0	–	–	(Si et al., 2019b)
Spirulina	260 °C, 1 h, 20 wt% solid ratio	8.42	–	162.1	16.1	8.9	0.76	(Egerland Bueno et al., 2020)
Swine manure	250–270 °C, 1 h	4.53	–	27.3	1.6	0.08	–	(Wang et al., 2021b)
Wheat straw	350 °C, 58.5 L/h, 12.5 wt% solid ratio	5.4	18.7	57.1	0.43	0.1	–	(Matayeva and Biller, 2021)
Sewage sludge	325 °C, 43 L/h, 16 wt% solid ratio	4.38	12.2	35.8	1.69	0.4	–	(Matayeva and Biller, 2021)

[a] TOC: Total organic carbon; COD: chemical oxygen demand; TN: total nitrogen; TAN: total ammonia and/or ammonium nitrogen; TP: total phosphorus.

3. Aqueous phase: physiochemical properties and present and future applications

The HC of biomass leads to the formation of substantial amounts of water-soluble products. These are grouped in a water fraction, commonly referred to as the aqueous phase (AP), with a production yield ranging between 40 and 60 % (Leng et al., 2020). Such a fraction contains a high amount of water used as the reaction medium in the HC process, and it is usually unused or even recognized as waste or pollutants due to the high organic species in AP (Taghipour et al., 2021). The unmanaged disposal of this hydrothermal AP leads to a decrease in the energy balance of the process and also incurs an extra cost due to the possible post-treatments this fraction may require. The applications of AP are somehow strategies to degrade and convert these organic compounds. Therefore, current and future efforts should be put into finding alternate methods to utilize and valorize this AP. Fig. 6 depicts some examples of achieving such a valorization. In recent studies, the hydrothermal AP can be directly used as nutrients for the cultivation of microorganisms (Das et al., 2020), the feedstock for fermentation (Si et al., 2019a), and chemical conversion to fuels and value-added chemicals (Harisankar et al., 2021).

3.1. Properties of the aqueous phase

Understanding the properties of the hydrothermal AP is essential for its valorization. Table 5 summarizes the important characteristics (e.g., pH, total organic carbon) of representative APs derived from the HC of various biomass. The pH values of the AP are in the range of 4–9, depending on the nature of the original feedstock. For instance, feedstocks with high protein content, such as algae, lead to the formation of ammonia and/or nitrogen-containing compounds which increases the basicity of the AP (Egerland Bueno et al., 2020). On the contrary, the acidity of the AP mainly derives from organic acids in the aqueous phase, primarily generated from the degradation of polysaccharides (cellulose and hemicellulose) (Wang et al., 2021b). Therefore, carbohydrate-rich feedstocks, such as wood and straw, generate acidic aqueous products, while APs derived from algae are more basic (Matayeva and Biller, 2021). The Total organic carbon (TOC) and Chemical Oxygen Demand (COD) are similar standards used to reflect the total organic compounds dissolved in the AP. The TOC and COD levels are lower when an organic solvent extraction of the aqueous phase is conducted (López Barreiro et al., 2015). Besides, some publications state that proteins increase the TOC of the AP more than carbohydrates and lipids (Li et al., 2017b). For total nitrogen (TN) and total ammonia/ammonium nitrogen (TAN) contents, the amounts of proteins in the biomass impact the TN and TAN of the AP (Madsen et al., 2016). In addition to the intrinsic nature of the biomass, such AP properties are also affected by the processing conditions used in the HC process (Gai et al., 2015). On this matter, Tommaso et al. reported that increasing the reaction temperature leads to an initial increase and subsequent decrease in the TAN of the AP from HTL of wastewater algae, whereas prolonging the processing time results in an increase in TN and TAN (Tommaso et al., 2015).

During the HC of biomass, the organic components in the feedstocks are decomposed into various organic oligomers and monomers via hydrolysis, decarboxylation, dehydration, and deamination (Gu et al., 2019; Usman et al., 2019). These organic products are divided into two categories: water-soluble and insoluble. The water-insoluble fraction is the main component in biocrude, whereas water-soluble organic compounds are dissolved in the AP. As reported, oligosaccharides (Remón et al., 2020; Remón et al., 2018), monosaccharides (Remón et al., 2020), small organic acids (e.g., formic acid and acetic acid) (Luo et al., 2020; Zhang et al., 2019a) and furfurals (e.g., furfural and 5-hydroxymethylfurfural) (Luo et al., 2018b; Zhou et al., 2021) primarily constitute the APs obtained from the HC of lignocellulosic biomasses. For algal biomass, the composition of the APs is more complex as it contains higher amounts and more diverse nitrogen-containing compounds such as N-heterocycles and amides, together with organic acids, cyclic oxygenates, and other oxygenated compounds (esters, ketones, and alcohols). (Tommaso et al., 2015). Such a complex composition results from the interaction between the three main components in algal biomass (lipids, carbohydrates, and proteins) (Chacón-Parra et al., 2022; Zhang et al., 2016).

Due to the presence of ash in most biomasses, cationic and anionic inorganic compounds can lixiviate to the AP during HC. As for cations, alkaline metals, such as Na and K, are the dominant species in the AP, with Mg, Ca, Si, Fe, and Zn present in small/trace amounts (Jabeen et al., 2022). The high concentrations of Na and K in the aqueous phase result from the high solubility of their salts in water (Onwudili et al., 2013). Besides, the amounts of Mg^{2+} and Ca^{2+} are commonly far lower than those of K^+ or Na^+ (Cherad et al., 2016). As for other cations (Fe, Cu, Mn, and Zn), their contents are usually below 1 wt%. These metals are usually found in APs derived from heavy-metal-enriched biomasses (microalgae, swine manure, and industrial waste) (Shen et al., 2018b). Regarding anions, Cl^-, SO_4^{2-}, and NO_3^- are the dominant species. Their presence is ascribed to their high water solubility when coordinated with Na^+ or K^+ (Onwudili et al., 2013). Additionally to these species, sulfur and nitrate-derived compounds obtained from N- and S-containing proteins could also be part of the APs (Gu et al., 2019).

3.2. AP recycling

The AP from HC (HC-AP) is abundant in nutrients such as N, P, and K (Jabeen et al., 2022), which are essential for the cultivation of microorganisms (microalgae and other microbes) (Wagner et al., 2021). Therefore, HC-APs can be used as a medium for algae cultivation. As HC-APs have usually been recognized as wastewater, with these requiring extra cost in post-treatment downstream processes, the cultivation of microorganisms in APs is a promising strategy. This methodology not only could utilize and recover the nutrients but also eliminates the need for additional management

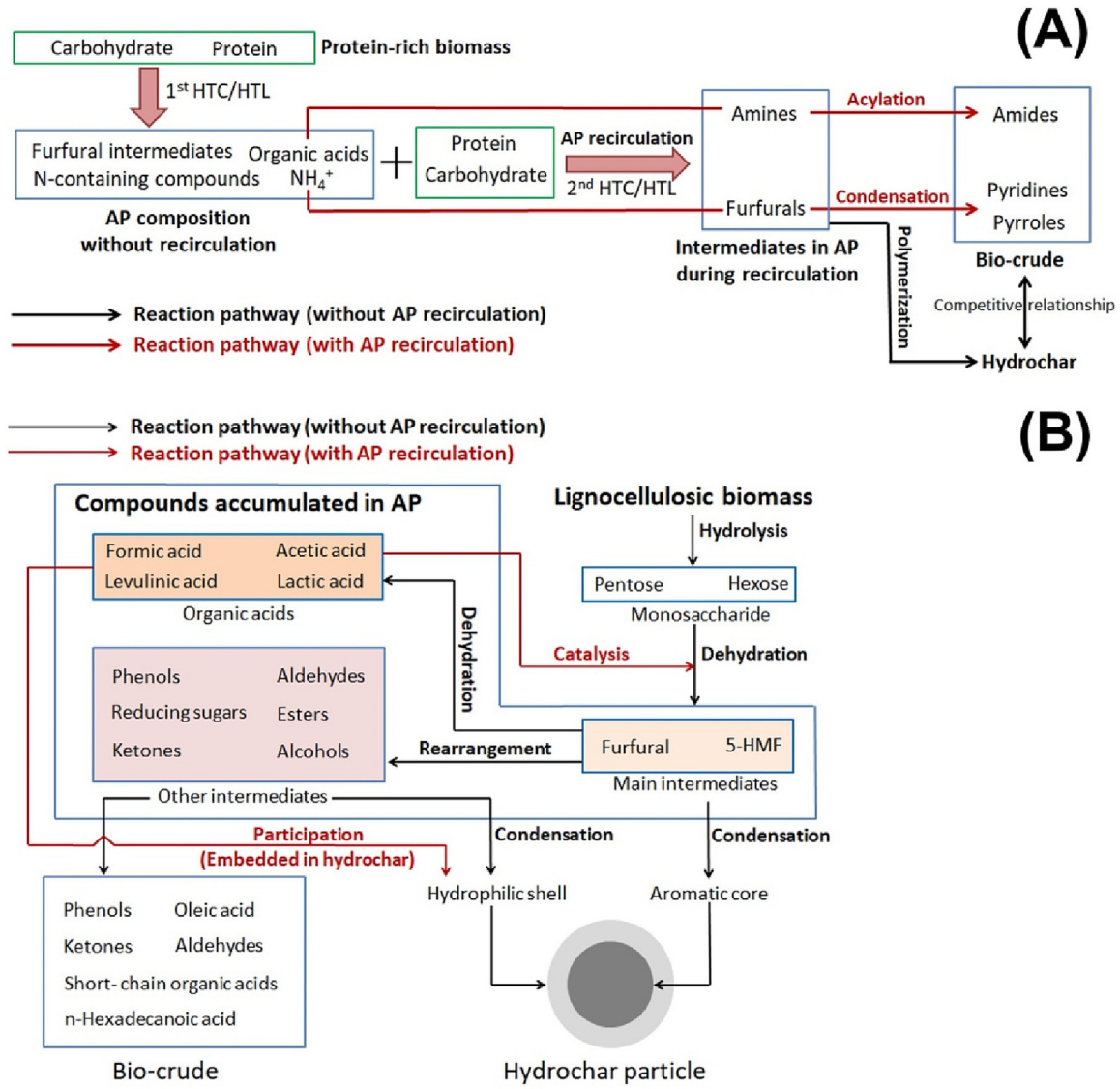

Fig. 7. Effect of the AP recirculation on biomass HC: (a) protein-abundant biomass, and (b) lignocellulosic biomass. (Adapted from Ref. (Leng et al., 2020), with permission from Elsevier).

treatments (Shanmugam et al., 2017). Algae-derived APs containing high amounts of these nutrients can potentially support algae/microbe growth (Das et al., 2020). Many recent publications reveal that some microalgae, e.g., *Chlorella* sp. are capable of uptalking N and P from HC-APs (Watson et al., 2017).

In addition to nutrients, HC-APs contain toxic compounds that negatively impact algae cultivation (Chen et al., 2020). Therefore, removing these toxic compounds becomes vital prior to applying APs as the nutrient source. Based on these ideas, Das et al. reported a strategy to utilize an AP derived from the HTL of *Tetraselmis* sp. for the semi-continuous cultivation of the same alga (Das et al., 2020). They found that replacing half of the fresh nutrients with part of the HTL-AP resulted in a slightly faster growth rate compared to control cultures comprising 100 % fresh nutrients. Chen et al. reported on a selective remediation strategy to recycle nutrients from an AP produced by the HTL of *Chlorella vulgaris*. Although the initial results were not as promising as expected, the addition of the untreated HTL-AP to the fresh medium (1: 100 dilution) led to a decrease in the growth of *C. vulgaris* by 47 % compared to the control (original) medium. However, after selective remediation using adsorption with an ion-exchange resin, the diluted HTL-AP showed an equal growth rate to that of the control medium (Chen et al., 2020).

Reutilizing the AP as the reaction medium for a subsequent HC process is also a promising option to eliminate freshwater consumption and reduce cost. Unlike recycling APs as the nutrient sources for alga growth, the recirculation/reutilization of an AP as the reaction medium for HC is not affected by the possible toxic effect exerted by dissolved species (e.g., phenols and heterocyclic chemicals) (Leng et al., 2020). On the contrary, these APs also contain a high content of organic species, and their presence in the reaction medium could exert a positive influence on the process in terms of promoting the formation of more biocrude oil/hydrochar/gaseous at the expense of water-soluble species (Fig. 7) (Hong et al., 2021; Kohansal et al., 2021). In recent years, an increasing number of studies have focused on the recirculation of the AP in the HC process. Taghipour et al. studied the influence of recycling the AP on the product yields, properties, and energy efficiency during the HTL of algal biomass using a heterogeneous catalyst (Pt/Al_2O_3) (Taghipour et al., 2021). They found that the biocrude yield increased by 17.8 %, and the nitrogen proportion decreased, with the highest energy efficiency (36.8 %) being achieved by recycling the AP twice. In another work, Kohansal et al. studied the impact of the AP recirculation on the hydrotreatment of biocrude produced from the HTL of biopulp (Kohansal et al., 2022). The experimental results confirmed an enhanced biocrude yield and more favorable energy recovery, yet, the nitrogen content in the

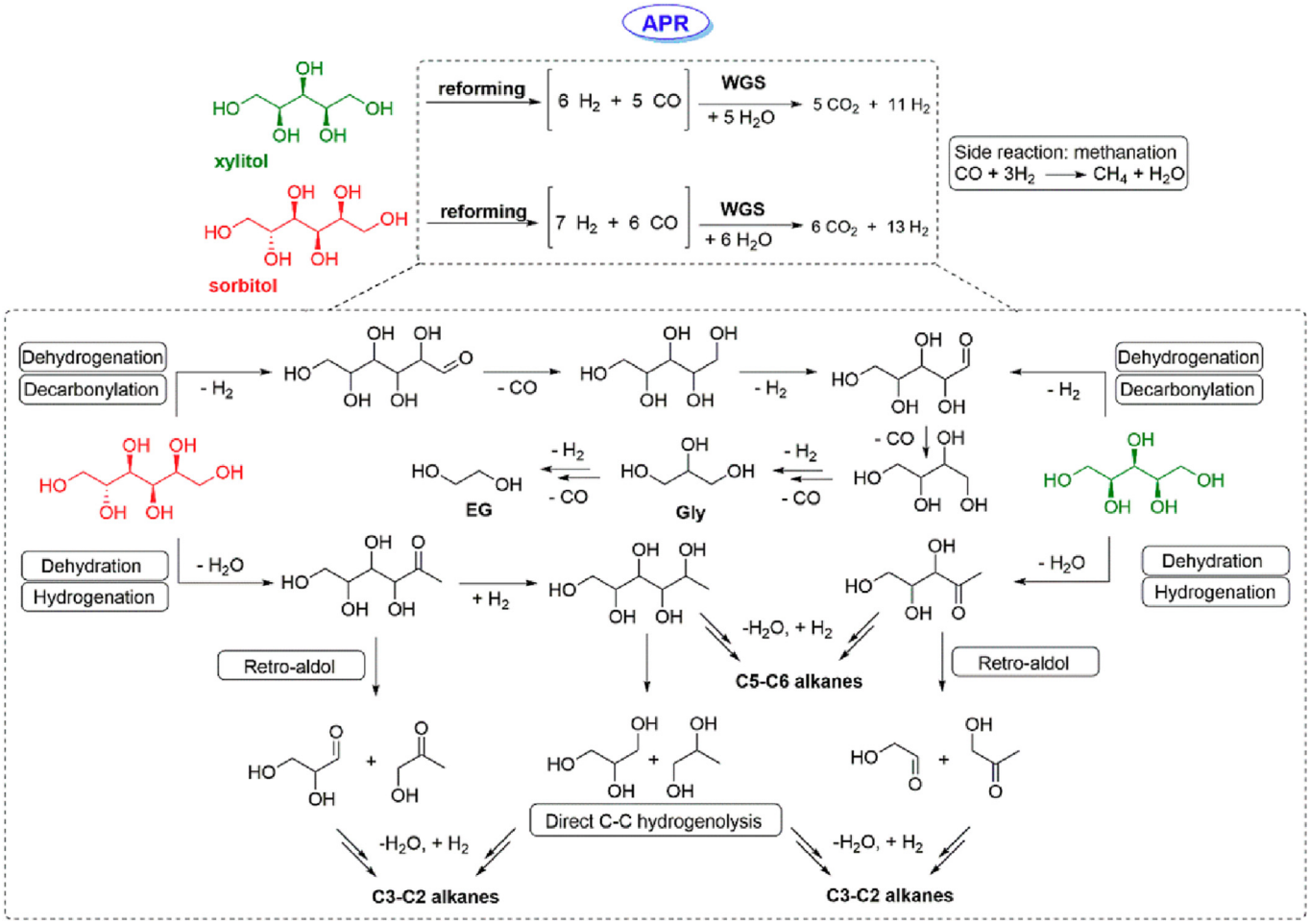

Fig. 8. Reaction pathways for the APR of model compounds. Adapted from Ref. (Fasolini et al., 2019), with permission from MDPI.

upgraded biocrude oil also increased. Despite these studies converging in promising developments, i.e., the biocrude and hydrochar yields increase with the recycling of part of the AP, organic acids and N-containing compounds also concentrate in the AP. This latter leads to biocrudes and hydrochars with increasing amounts of N-containing species, which makes it paramount to find novel recycling strategies to resolve this issue.

3.3. Aqueous phase reforming (APR)

APR is an excellent thermochemical process able to convert organic compounds into gases (H_2 and CH_4) and value-added chemicals (alkanes, alcohols, aldehydes, and ketones) in the presence of a catalyst. In some recent studies, APR has been postulated as a reliable strategy for H_2 production from different lignocellulosic biomasses and compounds derived from them (saccharides, polyols, acids, and phenols) (Aho et al., 2022; Remón et al., 2016a). Some reaction pathways occurring during the APR of model compounds are illustrated in Fig. 8. Considering that HC-APs contain substantial amounts of saccharides and phenols, the APR of HC-APs seems feasible for H_2 production. In this regard, some parametric and techno-economic studies have concluded that the feedstock type significantly determines the cost of an APR process (Sladkovskiy et al., 2018). Taking into consideration the watery nature of the APs produced from the HC of biomass, some works have challenged the economic feasibility of the APR of diluted APs based on the energy cost of the process (Oliveira et al., 2021). However, the environmental advantages must also be put on the equation balance. With that being said, the valorization of the diluted AP for clean gaseous fuel production is an environmentally benign process, and the market price of some value-added compounds could compensate for the energy requirements of this conversion route.

Table 6
Recent studies on APR of HC-AP and model compounds for H_2 production.

Feedstock	Catalyst	Processing conditions	Product distribution	Ref.
HTL-AP	Pt/C	75 mL AP, 270 °C, 2 h, 5-ButAc extraction	146 mmol H_2/g	(Di Fraia et al., 2022)
Cheese whey	Ni-Co/Al-Mg	220 °C, 44 bar, 95 g_{cat} min/g C	H_2: 32.58 vol%, CO_2: 54.9 vol%, CO: 0.63 vol%, CH_4: 10.30 vol%	(Remón et al., 2016a)
Phenol-bearing wastewater	Pt/C	220 °C, 24–28 bar, 4 h	0.2 mmol H_2/g TOC, 11.0 mmol CH_4/g TOC	(Oliveira et al., 2020)
Lactose	Ni-La/Al_2O_3	240 °C, 50 bar, 40 g_{cat} min/$g_{lactose}$	44 vol% H_2, 48 % alcohols, 6 % ketones	(Remón et al., 2016b)
Maltose	PtPd/C	200 °C, 0.3 h^{-1} WHSV	Selectivity: H_2: 53.2 %, CO_2: 72.7 %, alkanes: 27.3 %; H_2 yield: 3.4 %	(Oliveira et al., 2021)
Xylose	Pt/γ-Al_2O_3	225 °C, 29.3 bar	50 % H_2 selectivity	(Kim et al., 2020)
Cellulose	Ru/C	260 °C, 4 h	H_2 production activity: 40.8 mmol/(g_{cat} $g_{cellulose}$ h^{-1}), H_2 yield: 30.9 %	(Zhang et al., 2018a)
Alginate	Pt/C	225 °C, 6 h	H_2 yield: 6.0 %, H_2 selectivity: 32.7 %, CO_2: 57.2 %, alkanes: 10.1 %	(Pipitone et al., 2018)

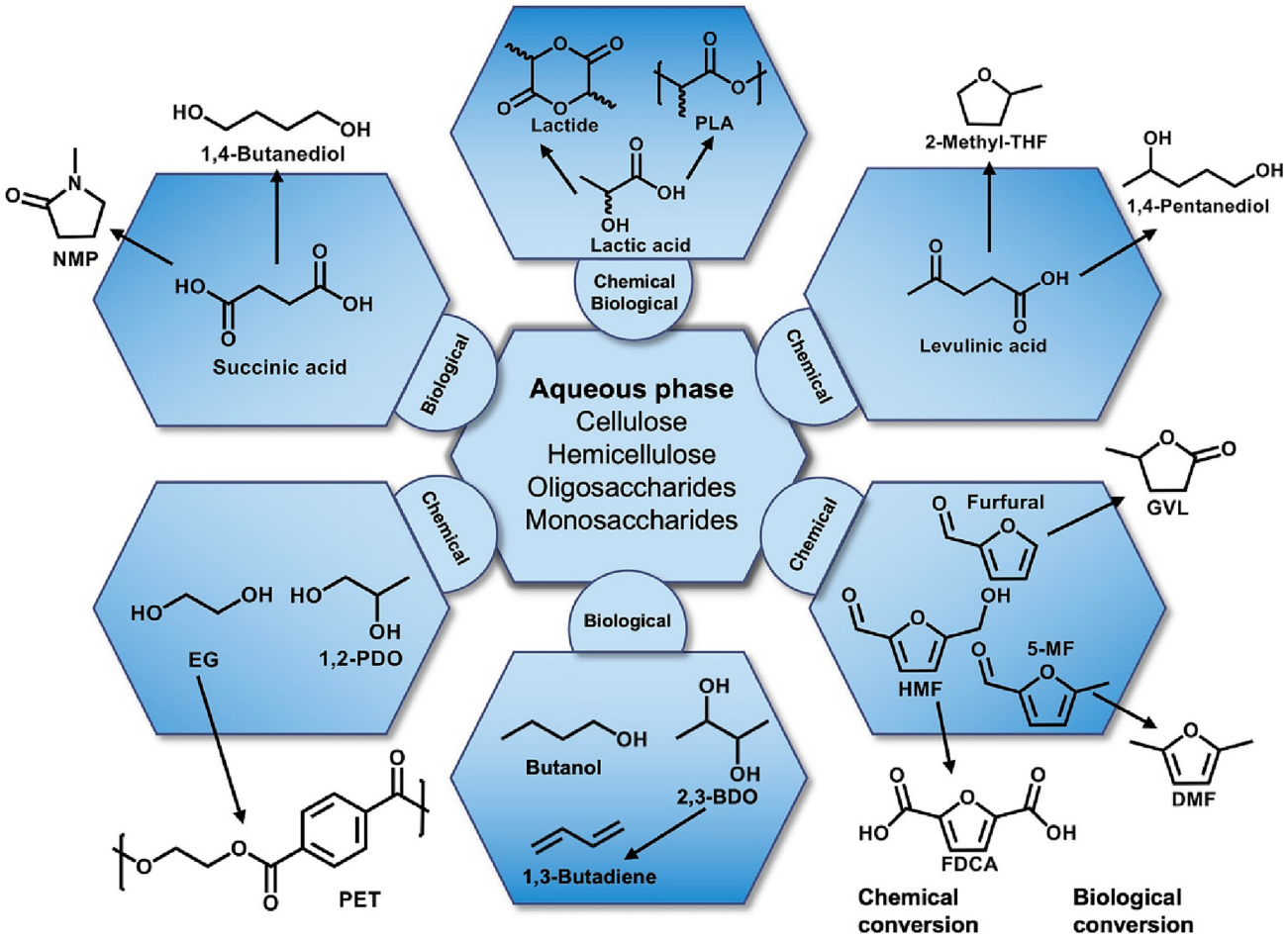

Fig. 9. Possible chemicals generated from HC-AP via chemical and biological conversion.

Table 6 summarizes recent APR advancements in HC-AP or model compounds. The APR of HC-APs and model compounds have commonly been conducted under relatively mild conditions (200–250 °C and 20–50 bar) using metal-based catalysts (Ni, Co, Pt, Pd, and Ru). These publications have also commented on catalyst stability, with catalyst deactivation being a critical issue to be yet solved. For example, Pipitone et al. investigated the APR over a Pt/C catalyst to produce H_2 of model compounds (carboxylic acids, hydroxy acids, alcohols, cyclo ketones, and aromatics), synthetic mixtures and HTL-AP from lignin-rich biomass (Pipitone et al., 2020). They found that increasing the feed concentration led to a decrease in the conversion and concluded that aromatics were the species responsible for catalyst deactivation. In another work, Zoppi et al. reported on the APR of a lignin-rich HTL by-product over a Pt/C catalyst (Zoppi et al., 2021). The results suggested that catalyst deactivation was caused by fouling. This development originated from the phenolic oligomers in the feedstock, which lowered the surface area of the catalyst.

3.4. Biological conversion

Since HC-APs produced from biomass are rich in readily biodegradable organic matter (saccharides and volatile fatty acids) (Maddi et al., 2016; Zhu et al., 2016), biological methods (Fig. 9) have also been explored as common and cost-effective strategies to furnish gaseous fuels (CH_4 and/or H_2) (Si et al., 2019a) and value-added chemicals (alcohols, organic acids or PHA) (Chen et al., 2021c; Leng et al., 2021a). However, it must be borne in mind that fermentable compounds in HC-APs coexist with toxic compounds (furans, phenols, and N-heterocycles), which could influence the efficiency of the fermentation processes (Si et al., 2019b). As for CH_4 formation, Si et al. studied the anaerobic conversion of a HTL-AP to produce CH_4 (Si et al., 2019b). After anaerobic conversion, the remaining organics in the liquid phase were mainly N-containing polymers (>1000 Da), which can be depolymerized into oligomers (100–300 Da) after subsequent treatment with anaerobic microbes; yet, the conversion of these latter species into CH_4 was still difficult. However, they found that an additional ozone pretreatment and the addition of granule-activated carbon improved the methane yield by 109 % and 298 %, respectively. In other studies, the oleaginous yeast *Yarrowia lipolytica* was used to valorize an HTL-AP toward valuable chemicals. For example, Cordova et al. reported on producing chemicals (itaconic acid and polyketide tri-acetic acid lactone) and lipids via biological conversion of a HTL-AP using the oleaginous yeast *Yarrowia lipolytica* (Cordova et al., 2020). Under optimum conditions, a triacetic acid lactone yield as high as 21.6 g/L was attained using a reaction medium of 20 wt% HTL-AP and 80 wt% sugar hydrolysate.

3.5. Leather industry

Tanning is an essential step in the leather industry that improves the physiochemical properties of raw skin, such as mechanical strength and stability against heat, chemicals, and putrefaction, to obtain commercial leather goods (Ding et al., 2022). Traditionally, leather tanning has been conducted worldwide using chrome salts Cr(III) as the tanning agent (Jiang et al., 2021a). However, the possible oxidation of Cr(III) to hazardous and carcinogenic Cr(IV) might result in many environmental and human health issues (Jiang et al., 2021b). Therefore, researchers have recently searched for green and more sustainable alternatives for leather tanning. On this matter, biomass-based aqueous products (aqueous fractions containing oligosaccharides (Jiang et al., 2020), aldehydes (Ding et al., 2022), polyols (Hao et al., 2023) and carboxylic acids (Yu et al., 2022))

Table 7
Recent studies on platform chemicals production via chemical conversion of AP and AP-derived carbohydrates.

Product	Feedstock	Catalyst	Processing conditions	Yield	Ref.
Sugar-rich solution	Wheat straw and *Laminaria saccharina*	Catalyst-free	57 wt% seaweed, 215 °C, 37 min	90C-wt%	(Remón et al., 2020)
Hemicellulosic monosaccharides	Almond shells	Sulfuric acid	150–200 °C, 0–20 min, MTHF-H_2O system	205.3 g/kg	(Davila et al., 2021)
Xylooligosaccharides	Mango seed shell	Catalyst free	180 °C, 2.5 MPa, 15 min	393.44 mg/g	(Monteiro et al., 2021)
5-HMF	Watermelon peel	1 % HCl	135 °C, 6 min, liquid/solid = 12/1	3.8 %	(Shao et al., 2019)
5-HMF	Fructose	Acid functionalized carbon	70 °C, atmospheric pressure, 5 min, microwave	97.8 % conv., 90.6 % selectivity	(Lyu et al., 2022)
5-HMF	Chlorella sp.	$Al_2(SO_4)_3$	165 °C, 30 min	23.46 %	(Jeong and Kim, 2021)
Levulinic acid	*Gracilaria lemaneiformis*	0.2 M H_2SO_4	180 °C, 20 min, microwave	16.3 wt%	(Cao et al., 2019)
5-HMF and LA	Corn straw	Sulfonated carbon	200 °C, 1 h	16.2 mg 5-HMF/g, 65.4 mg LA/g	(Ozsel et al., 2019)
Acetic acid	Microalgae and extracted residue	CuO	300 °C, 2 h, 2 mol/L NaOH	35 %	(Zhong et al., 2020)
Lactic acid (LaA)	Corn stover	MgO	220 °C, 0.5 h, 3 mmol pre-added D-LaA	57.9 %	(Xu et al., 2021a)
Xylitol	Xylose	Ru/ZP-A	90 °C, 7 h	97 %	(Musci et al., 2020)
Furfural alcohol	Xylose	Zr-SBA-15	130 °C, 6 h, 30 bar N_2	41 %	(Perez et al., 2021)
D-xylonic acid	D-xylose	N-doped defect-rich carbon	100 °C, 30 min	57.4 %	(Li et al., 2022)

have arisen as new materials to develop alternative Cr-free tanning processes. For example, Jiang et al. investigated the application as a tanning agent of an AP containing Al-oligosaccharide complexes produced from the HC of cellulose (Jiang et al., 2020). A combined experimental and theoretical study revealed that oligosaccharides complexed with Al species. These species behaved as a 'Trojan horse' penetrating the leather matrix. This prevented the overload of Al species onto the leather surface and enhanced their penetration into the leather matrix. Once inside, the released Al species coordinated with amino groups of the collagen, resulting in an enhanced tanning performance. Similarly, Gao et al. studied the application in the leather industry of another AP (oligosaccharide-rich aqueous liquid) produced from pubescen hemicellulose degradation using $ZrOCl_2$ as a catalyst (Gao et al., 2022). They found that $ZrOCl_2$ facilitated the disruption of hydrogen bonds in hemicellulose and inhibited the condensation and repolymerization of xylooligosaccharides into macromolecules. Furthermore, Zr-oligosaccharides were applied as a Cr-free tanning agent, which helped the penetration of Zr species into the collagen matrix and increased the thermal stability of the leather.

3.6. Platform chemicals via chemical conversion of AP

HC-APs produced from biomass and lignocellulosic waste contain a high fraction of carbohydrate-derived compounds, such as oligosaccharides, polysaccharides, organic acids, and furans (Gao et al., 2021). Therefore, these HC-APs can synthesize plenty of value-added carbohydrate-based chemicals, with some listed as building block chemicals by the United States Department of Energy (US DOE) (Werpy and Petersen, 2004). Compared to fossil-based chemicals, biomass-derived chemicals possess the advantages as follows: (1) higher sustainability; (2) the carbon-neutrality of the production/application process of biomass-based chemicals; (3) higher biodegradability; (4) no requirements for introducing extra oxygen into biomass-based chemicals due to the high oxygen content in biomass. Fig. 9 illustrates some of the most representative species resulting from the HC of biomass and platform chemicals that can be produced from them. The chemical conversion of AP-derived carbohydrates comprises an initial depolymerization of polysaccharides and oligosaccharides into monosaccharides via hydrolysis. Then, these latter molecules can undergo different conversion processes, such as dehydration, hydrogenation, or oxidation, to generate other products. These conversion routes take place under the action of solvents and/or acidic catalysts, which significantly influence the depolymerization of poly- and oligosaccharides into monosaccharides (Davila et al., 2021; Xiong et al., 2021).

The monosaccharide units mainly comprise glucose and xylose (Jing et al., 2019). Besides, some algal biomass contains rhamnose, mannose, galactose, and fucose (Ramachandra and Hebbale, 2020). In most cases, hexoses are the most representative and abundant monosaccharide unit. These can be dehydrated into 5-hydroxymethylfurfural (5-HMF) and levulinic acid. 5-HMF is one of the most desired platform chemicals from those that can be produced via biomass conversion. The production of 5-HMF from sugars via HC technology has already been commercialized based on the patents developed by AVALON Industries and AVA Biochem (Fernandez-Sanroman et al., 2021). They could produce crystalline 5-HMF with purity levels up to food grade. Such desirability is accounted for by the wide spectrum of products that can be achieved from its conversion, including dimethylfuran (DMF) via hydrogenation (Thananatthanachon and Rauchfuss, 2010), ethoxymethylfurfural (EMF) via etherification (Liu et al., 2018b), and 2,5-furan-dicarboxylic acid (FDCA) via oxidation (Motagamwala et al., 2018). These compounds are essential precursors for the production of fuels and materials. Besides, levulinic acid (LA), also included within the top 12 building block chemicals by the US DOE, has the potential to be converted to other valuable compounds for the chemical industry, such as 2-methyl tetrahydrofuran, γ-valerolactone (GVL) and 1,4- pentanediol (Werpy and Petersen, 2004). Hemicellulose in lignocellulosic biomass is composed of xylose units, which can be dehydrated to furfural (Luo et al., 2019). Furfural is another crucial platform molecule that can synthesize fuels and chemicals

(furfural alcohol, 2-methyl furan, and succinic acid) with a niche market in the fuel, plastic, and pharmaceutical industries (Luo et al., 2019). In addition to these dehydrated products, these carbohydrates can be transformed into small organic acids (formic acid, acetic acid, and lactic acid), which are widely used in pharmaceutical, polymer, leather, and dyeing industries (Ding et al., 2018; Ma et al., 2021a). Furthermore, the catalytic hydrogenation of saccharides to polyols has gained increasing attention in recent years. Polyols (e.g., ethylene glycerol, 1,2-propanediol, and sorbitol) are multifunctional chemicals serving as precursors for producing antifreeze agents, fine chemicals, cosmetics, medicines, and food additives (Torres-Mayanga et al., 2019).

Given these bespoke alternatives, the appropriate selection of the processing parameters and catalyst type is vital to obtain target products with high yield and selectivity. Table 7 summarizes commonly used processing conditions and catalysts for producing value-added chemicals from converting saccharides in HC-APs. As for the catalysts, acidic catalysts (Brønsted and Lewis acids) have been widely used to convert saccharides into dehydrated products (5-HMF, furfural, and LA), whereas metal oxide catalysts (CuO and MgO) have been generally applied in organic acid production (acetic acid and lactic acid). Additionally to these common catalysts, carbon-based materials and halides also occupy a niche in the catalyst market. For example, Lyu et al. reported on a microwave-assisted and energy-efficient strategy for 5-HMF production from fructose using surface functionalized carbon superstructures (SCS) (Lyu et al., 2022). Based on the characterization, the SCS catalyst showed acidic properties with surface sulfonic and carboxy groups. In the catalytic activity tests, these SCS catalysts achieved a fructose conversion of 97.8 % and 5-HMF selectivity of 90.6 % under mild conditions (70 °C, atmospheric pressure, 5 min) with excellent recyclability. In another work, Xu et al. studied the selective conversion of hemicellulose in various lignocellulosic biomasses to lactic acid in the presence of YCl_3, with ~60 % yield achieved (Xu et al., 2020). A combined experimental and theoretical study revealed that H^+ and $[Y(OH)_2(H_2O)_2]^+$ were the active species responsible for lactic acid production. The hydrogenation of carbohydrate-based compounds has been commonly conducted over active metals (e.g., Pt, Pd, Ru, Ni, and Co). For instance, Wang et al. developed a Ru(III) single-site micellar catalyst to hydrogenate biomass-derived carbonyl compounds in the aqueous phase (Wang et al., 2022a). Compared to conventional metal catalysts, this Ru catalyst exhibited excellent catalytic activity and product selectivity in hydrogenating a wide range of carbonyl compounds.

These publications have paved the way for converting HC-APs from biomass to valuable chemicals. However, in most of these cases, model compounds (e.g., glucose, fructose, furfural) have been used as the feedstock due to the complexity of raw biomass-derived AP, accounted to some extent for by the presence of some unwanted co-products which might result in catalyst deactivation. Besides, HC-APs also contain a high fraction of repolymerized and undergraded oligomers and polymers, namely humins, which could result in the loss of the carbon balance and poison the catalyst by carbon deposition. Therefore, suitable catalytic systems are required to tolerate the impurities and enhance the carbon balance. Given these, the challenge is investigating the conversion/valorization of actual HC-APs produced from biomass and lignocellulosic waste. The work conducted so far is transferable, yet, there is a long and exciting path to go.

4. Biocrude: physiochemical properties and present and future applications

The biocrude produced by HC of biomass is an energy-dense, crude-like viscous liquid product with wide applications. This liquid is commonly recovered from the aqueous reaction medium through liquid-liquid

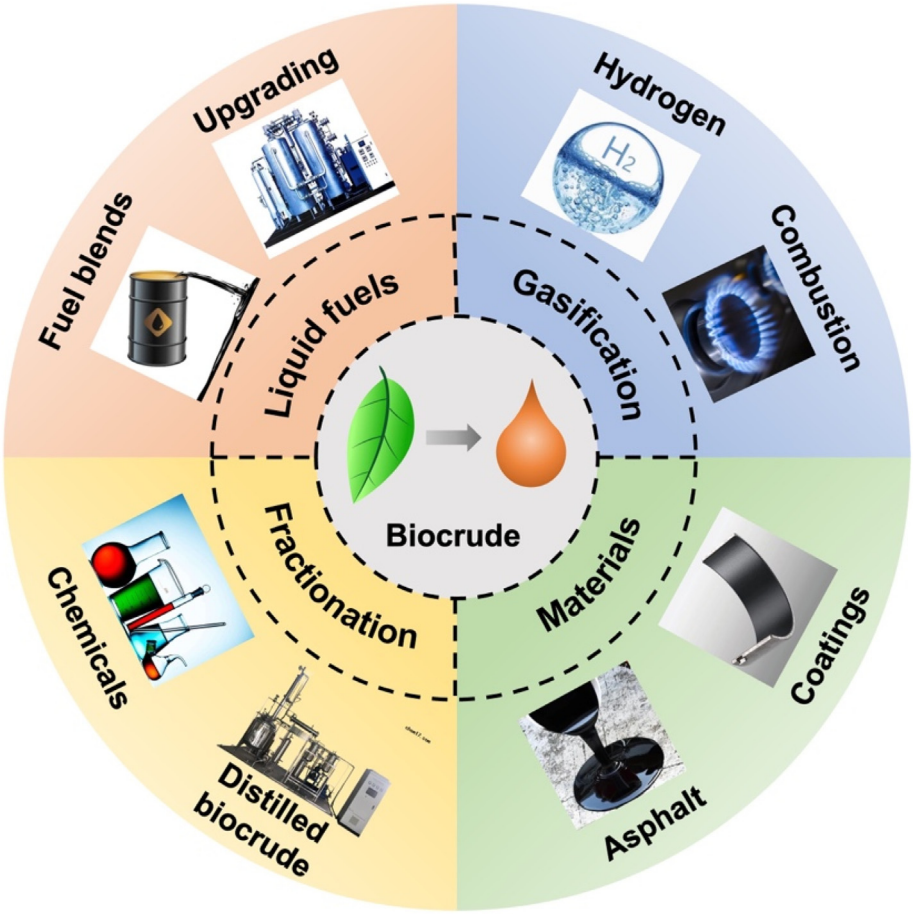

Fig. 10. An overview of biocrude applications.

Table 8
Typical properties of biocrude from biomass HTL.

Feedstock	Processing conditions	Biocrude yield (wt%)	C (wt%)	H (wt%)	O (wt%)	N (wt%)	HHV (MJ/kg)	Chemical composition	Ref.
Eucalyptus	300 °C, 30 min, KOH	40.5	69.7	6.1	24.1	0.1	28.0	Acids: 5.7 %, furan and pyrroles: 1.5 %, esters: 35 %, phenols: 12.1 %, ketones: 19 %, amines and amides: 0.3 %, hydrocarbons: 1.8 %, others: 24.6 %	(Wu et al., 2019)
Food waste	350 °C, 1 h, H_2, 3%NiMo/Al_2O_3	58	75.2	11.8	6.4	6.6	40.0	Amides: 36 %, acids: 52 %, ketones: 1 %, N-heterocycles: 3 %, phenols: 2 %, hydrocarbons: 6 %	(Ahmed Ebrahim et al., 2022)
Sewage sludge	340 °C, 10 min	54.4	72.4	9.0	11.9	3.5	35.4	Phenols, N-heterocycles, amides, acids, ketones, hydrocarbons, esters	(Xu et al., 2018b)
Spirulina	300 °C, 20 min	–	69.3	9.2	14.1	7.5	34.0	Hydrocarbons: 11.4 %, esters: 7.4 %, acids: 45 %, alcohols and phenols: 6.1 %, ketones: 5 %, N-containing compounds: 25 %	(Wang et al., 2021a)
Cornstalk	290 °C, 0 min	–	70.0	6.9	22.0	1.1	29.6	Hydrocarbons: 1.2 %, esters: 1.8 %, acids: 39.7 %, alcohols and phenols: 42.2 %, ketones: 5 %, N-containing compounds: 1.9 %, others: 6.5 %	(Wang et al., 2021a)
Swine manure	340 °C, 30 min	–	75.8	9.1	10.1	5.0	36.8	Hydrocarbons: 8.2 %, acids: 63.9 %, alcohols, and phenols: 5.0 %, ketones: 5 %, N-containing compounds: 22.9 %	(Wang et al., 2021a)
Nannochloropsis	300 °C, 30 min	41	70.2	7.6	14.5	7.5	32.6	Hydrocarbons: 8 %, aromatics: 3.5 %, aldehyde: 1 %, fatty acids: 9 %, esters: 22 %, amides: 12.5 %, heterocyclics: 16 %	(Liu et al., 2021a)
Rice straw and *Nannochloropsis*	350 °C, 10 min, K_2CO_3	42.2	77.2	7.1	11.1	4.6	32.6	Fatty acids: 30.9 %, ketones: 10.22 %, nitrogenous compounds: 9.1 %, phenols: 2.9 %, alcohols: 2.0 %, esters: 5.1 %	(Xia et al., 2022)
Cladophora socialis	350 °C, 8 min, Fe catalyst	36.2	77.2	8.9	10.1	3.8	37.1	Carbonyls: 51 %, alcohols: 1.8 %, acids: 0.2 %, esters: 1.8 %, phenols: 6.2 %, furans: 2.3 %, N-containing: 2 %, HCs: 9 %	(Nguyen et al., 2021)

extractions using organic solvents. The production of biocrude has already been achieved on an industrial scale in some companies, such as UPM refinery (Finland), Pyrovac (Canada), and Kior (USA) (Hu and Gholizadeh, 2020). Thus, the downstream treatment and sustainable application of biocrude are the significant bottlenecks nowadays instead of enhancing its yield or process scale-up. The renewable-based nature and physicochemical properties of biocrude have potentiated their use to furnish liquid biofuels and value-added compounds. Notably, in the vast majority of studies addressing biofuel production by HC, the fuel properties (Peng et al., 2017) and combustion behaviors (Choi et al., 2016) of biocrudes have been evaluated. Besides, some researchers have also explored different upgrading/hydroprocessing treatments to enhance the fuel properties of these liquids (Liu et al., 2022b). The following sections summarize the latest progress in applying biocrude to produce biofuels and synthesizing value-added/platform chemicals (aromatics, aldehydes, and acids) and commercial products (asphalt and adhesive). An overview of some representative applications for biomass-derived biocrudes is illustrated in Fig. 10.

4.1. Properties of biocrude

The chemical and fuel properties of representative biocrudes extracted from recent publications are summarized in Table 8. The biocrudes obtained from HC of biomass comprise a pool of organic compounds, which are usually classified into different categories: hydrocarbons, carboxylic acids, esters, ketones, aldehydes, alcohols, phenols and N-containing compounds (Wang et al., 2021a; Xu et al., 2018b). Gas chromatography-mass spectrometry (GC–MS) has commonly been used to characterize the biocrude chemical composition using a semiquantitative methodology based on chromatographic areas (Ahmed Ebrahim et al., 2022). The proportions of organic compounds in the biocrudes depend on the biochemical composition of the original feedstock and processing conditions (temperature, time, and type/amount of catalyst) used in the HC.

As for the feedstock, the biochemical composition (lipids, carbohydrates, lignin, and proteins) of biomass affects the reaction pathways during the HC, with this latter influencing the yields and properties of the reaction products (Gao et al., 2021). In general, lignocellulosic biomass produces biocrudes with higher proportions of aldehydes, furans, and phenols, whereas the HC of algae results in the formation of more carboxylic acids, esters and N-containing compounds (Wang et al., 2021a). On this matter, Wang et al. reported on the properties and stability of a biocrude produced by the HTL of three types of biomasses (cornstalk, swine manure, and microalgae) (Wang et al., 2021a). They found that the biocrudes produced from microalgae and swine manure contained more hydrocarbons, carboxylic acids, and N-containing compounds, whereas that obtained from cornstalk comprised higher proportions of alcohols and phenols. These different chemical compositions also influenced the stability of the biocrude produced. Remarkably, phenols in the biocrude from cornstalk tend to be oxidized and repolymerized to a solid phase after one-day storage at 80 °C, resulting in a biocrude with a higher viscosity. Xu et al. studied the effect of the temperature (260–350 °C) on the product properties of a biocrude obtained by HTL of sewage sludge (Xu et al., 2018b). The results showed that increasing reaction temperature augmented the gas and biocrude yields and Higher Heating Value (HHV) of this latter at the expense of the aqueous (AP) and solid yields. The presence of a catalyst also influences the chemical composition of the biocrude. In this regard, catalysts could promote specific reactions (e.g., hydrodeoxygenation, hydrolysis) during HTL, which impacts the chemical composition of the biocrude produced. Nguyen et al. reported on the influence of various catalysts (KOH, K_2CO_3, H_2PO_4, HCOOH, H-ZSM-5, Raney Ni, Ru/C, and Fe metal) during the HC of *Cladophora Socialis* macroalgae at 350 °C (Nguyen et al., 2021). They found that metallic Ni promoted hydride reduction and decarboxylation, thus enhancing the proportions of phenols and hydrocarbons in the biocrude.

The fuel properties of biocrudes are commonly evaluated by making use of their elemental composition and higher heating values (HHV). The

Table 9
Recent studies on catalytic upgrading of HTL-biocrude.

Catalyst	Feedstock	Upgrading conditions	Yield (wt%)	Performance	Ref.
$NiMoS/Al_2O_3$	Microalgal biocrude	340–400 °C, 2.5–10 h, 120 bar H_2	69–82	Decrease in the content of phenols, anilines, indoles, amides, and N, increase in C and H content, a high percentage of *n*-, *i*- and cyclic alkanes (short and long chain)	(Rathsack et al., 2019)
CoMo oxide/Al_2O_3	Biocrude from pine, microalgae, and sewage sludge	400 °C, 1500 psi H_2	–	Increase in C (>80 wt%) and H (>10 wt%) contents, decrease in O (<2 wt%) and N (<0.05 wt%) contents, and viscosity, density and moisture content, and a high proportion of *n*-alkanes	(Jarvis et al., 2018)
NiMo/γ-Al_2O_3	Microalgal biocrude	350 °C, 2–4 h, 40–80 bar H_2	–	Optimum HHV: 44 MJ/kg, N: 3 wt%, O: complete removal	(Haider et al., 2018)
CoMo/Al_2O_3	Animal carcass biocrude	400 °C, 4 h, 6 MPa H_2	68.03	C: 84.4 wt%, H, 12.9 wt%, O: 1.5 wt%, N: 1.2 wt%, HHV: 46.7 MJ/kg; Main composition: alkanes, small amount of nitriles	(Yang et al., 2022a)
NiMo/Al_2O_3	Sewage sludge biocrude	400 °C, 4 h, 8 MPa H_2	72	C: 85.3 wt%, H: 13.8 wt%, N: 0.9 wt%, O: 0 wt%, HHV: 46.1 MJ/kg; abundant in diesel-range hydrocarbons	(Castello et al., 2019)
NiMo/Al_2O_3	Algal biocrude	400 °C, 4 h, 8 MPa H_2	63	C: 83.7 wt%, H: 12.3 wt%, N: 4.1 wt%, O: 0 wt%, HHV: 43.7 MJ/kg; difficulty in complete denitrogenation	(Castello et al., 2019)
NiMo/Al_2O_3	Miscanthus biocrude	400 °C, 4 h, 8 MPa H_2	61	C: 87.4 wt%, H: 10.3 wt%, N: 1.5 wt%, O: 0.8 wt%, HHV: 42.2 MJ/kg; abundant in gasoline-range hydrocarbons and aromatics	(Castello et al., 2019)
CoNiMoW/γ-Al_2O_3	Microalgal biocrude	400 °C, 4 h, 3.4 MPa H_2	46.9	C: 70.2 wt%, H: 8.3 wt%, N: 9.1 wt%, O: 12.2 wt%, HHV: 33.4 MJ/kg; more small molecular compounds	(He et al., 2018b)
Ni-Cu-Re/γ-Al_2O_3	Algae biocrude	350 °C, 4 h, 75 bar H_2	58.5	C: 81.4 wt%, H: 12.1 wt%, N: 1.3 wt%, O: 5.2 wt%, HHV: 41 MJ/kg; energy recovery: 64.6 %, 20 % improvement in bio-oil HHV	(Pongsiriyakul et al., 2021)
Pt/C	Algal biocrude	400 °C, 4 h, 8 MPa H_2, H_2 replacement, tetralin	89	C: 88.9 wt%, H: 9.9 wt%, N: 4976 ppm, O: 0.7 wt%, HHV: 44 MJ/kg; excellent removal efficiency of O, S and N	(Chen et al., 2021b)
Ni-Mo/Al_2O_3	Biocrude from *Chlorella vulgaris*	400 °C, 4 h, 6 MPa H_2	~50	C: 83.7 wt%, H: 11.4 wt%, N: 3.6 wt%, O: 1 wt%, HHV: 42.9 MJ/kg; increase in the amount of gasoline, kerosene, and diesel oil	(Guo et al., 2019)
NiW/Al_2O_3	Biocrude from Nannochloropsis	400 °C, 4 h, 6 MPa H_2	~80	C: 80.9 wt%, H: 11.9 wt%, N: 4.4 wt%, O: 2.6 wt%, HHV: 42.3 MJ/kg; increase in the amount of gasoline, kerosene, and diesel oil	(Guo et al., 2019)
Ni/HY + Zn-H_2O	Oakwood biocrude	330 °C, 3 h	80	C: 77.0 wt%, H: 6.9 wt%, O: 16.1 wt%, HHV: 33.1 MJ/kg, TAN: 12.4 mg KOH/g oil, density: 1.08 kg/L, viscosity: 794 Pa.s	(Hamidi et al., 2022)
Ni/SiO_2-Al_2O_3	Solvent-extracted biocrude from sewage sludge	350 °C, 1 h, 1000 psig H_2	86	C: 81.3 wt%, H: 11.8 wt%, N: 2.1 wt%, O: 4.8 wt%, HHV: 43.5 MJ/kg	(Jahromi et al., 2022)

elemental composition of biocrude usually varies between 60 and 78 wt% for C, 6–12 wt% for H, 8–20 wt% for O, and 2–6 wt% for N (Basar et al., 2021). The hydrothermal conditions, feedstock, and catalyst also influence the elemental composition. It is generally agreed that augmenting the temperature, prolonging the reaction time, and adding catalysts increase the proportions of C and H and decrease the O content, resulting in an increment in the HHV of the biocrudes (Gao et al., 2021). The research goal for high-quality liquid biofuel production is to maximize the C and H contents and minimize the O and N contents. However, the relatively high amounts of O and N in lignocellulosic and algal biomasses lead to biocrudes containing high amounts of these two latter species (Basar et al., 2021). The presence of O in the biocrude results in a decrease in the HHV, whereas the presence of N could cause the formation of NO_x during its combustion, which leads to pollution issues (Zhou and Hu, 2020). Therefore, post-treatment of biocrudes is frequently required before their possible usage as transportation fuels.

4.2. Biocrude upgrading

Biocrudes from biomass comprise higher proportions of oxygen and nitrogen-containing species than petroleum-based liquid fuels (Qu et al., 2021). Such differences are responsible for some of the unwanted characteristics (e.g., high viscosity, poor stability, NO_x emission, and low energy density) of these bioliquids (Zhang et al., 2021b). These adverse properties make these biocrudes not meet the standards to be used as combustible fuels (Jones et al., 2014). Therefore, eliminating O and N in biocrudes is essential to improve the fuel properties and product selectivity to tackle these issues. To date, two catalytic strategies have been primarily used to upgrade biomass-derived biocrudes: (i.) in-situ biocrude upgrading through catalytic HTL and (ii.) post-catalytic upgrading of the obtained HTL-biocrude. Due to the scope of this review, this section only collects essential information covering the catalytic upgrading/hydrotreatment of the obtained biocrude in the presence of heterogeneous catalysts. More information regarding in-situ catalytic HTL can be found elsewhere (Nagappan et al., 2021; Scarsella et al., 2020). The catalysts used for catalytic upgrading of HC-biocrudes possess high activity in deoxygenation reactions and an excellent denitrogenation capability to effectively remove O and N atoms in the biocrude. In such processes, O and N are removed from the biocrude in the forms of H_2O, CO (Qu et al., 2021), and NH_3 (Liu et al., 2022b). These transformations occur in the presence of hydrogen molecules or hydrogen donors (methanol, isopropanol, and formic acid) (Scarsella et al., 2020; Zhang et al., 2021b). Besides, oxygen can be removed from biocrudes via decarboxylation in the absence of hydrogen sources, generating CO_2 as the co-product (Zhuang et al., 2022b).

Many publications have investigated the catalytic upgrading of HTL-biocrudes to date (Table 9). Generally, the biocrude upgrading process performs at relatively high temperatures (300–400 °C) and pressures (3–12 MPa initial H_2 pressure) in the presence of supported transition metal catalysts. The upgraded biocrude shows improved physiochemical and fuel properties, with enhanced HHV and hydrocarbon proportions, lower viscosity, and heteroatom contents than the original liquid. Masoumi et al. explored the hydrodeoxygenation of an algal biocrude using a catalyst consisting of NiMo carbide supported on an algae-derived activated carbon. (Masoumi and Dalai, 2021a). Among these, the NiMo carbide prepared via co-impregnation and carbothermal reduction in N_2 performed the best. This catalyst had high acidity and a large surface area, combined with a sufficient amount of active phase (Mo_2C), which provided the catalyst with high oxygen removal efficiency. Once the catalyst was selected, these authors also used a surface response methodology to optimize the processing conditions and found that up to 94 wt% of the original O content could be removed, which led to an upgraded biocrude with a HHV as high as 43.9 MJ/kg.

In another work, Yan et al. studied the effect of the support of several Ru-based catalysts in the hydrodeoxygenation (HDO) of a biocrude derived from radiata pine softwood (abundant in polyaromatic compounds) and guaiacol (Yan et al., 2021). Among the prepared Ru-based catalysts (Ru/

BEA, Ru/ZSM-5 and Ru/Al_2O_3, and Ru/SiO_2 with different Si/Al ratios), Ru/BEA with a Si/Al ratio of 12.5 exhibited the highest activity. Such a remarkable activity was ascribed to a high content of strong Brønsted acid sites, which facilitated hydrogenation, deoxygenation, and ring-opening reactions to form cycloalkanes in high yields. Despite these publications attaining high oxygen and nitrogen removals, with the proportions of these heteroatoms being lower than 1 %, they still did not meet the US DOE standards for biomass-based biofuels. This latter regulation limits the amounts of N, O, and S in the biocrude to 0.05 wt%, 1 wt% and 0 wt %, respectively (Jones et al., 2014). These publications still report N and S contents in the upgraded biocrudes higher than these standards; therefore, efforts must be put into developing more advanced processes and strategies to remove these heteroatoms.

4.3. Liquid biofuels or blends in engines

Biomass-derived biocrudes have the potential to be used in combustion engines either alone or blended. Nonetheless, the presence of impurities (primarily N and S-containing compounds) along with their relatively lower HHVs (30–35 MJ/kg) compared to petroleum fuels hampers this approach. This latter is accounted for by the possible emission of exhausted gases (NO_x and SO_x) and the low combustion efficiency achieved with liquids with low calorific values (Zhang et al., 2021b). For example, Red Arrow Products (USA) burnt biocrude directly for heat with 5 MWth plant capacity. However, exhausted gas emissions were high, with CO (17 %), NO_x (1.2 %), and formaldehyde (0.2 %) generated (Hu and Gholizadeh, 2020). Moreover, the high viscosity and low flash and pour points of biomass-derived biocrudes also result in storage difficulties and possible incompatibilities with current combustion engines (Hu and Gholizadeh, 2020).

Despite these unwanted characteristics, some researchers have investigated the engine performance of biomass-derived biocrudes, with the information gathered being paramount for developing new and more efficient upgrading processes. For example, Obeid et al. studied the engine performance and emissions of N-containing diesel fuels (Obeid et al., 2020). The presence of nitrogen resulted in a slight increase in the density and decrease in the viscosity, flash point, and HHV of biocrudes. These properties led to more difficult storage and less CO and unburned hydrocarbons emission but more NO_x at 25 % engine load. In another work, Peng et al. investigated the combustion performance of a biocrude obtained from the HTL of algae in a reaction medium comprising an ethanol-water mixture (Peng et al., 2017). They found that the reaction medium significantly influenced the combustion properties of the biocrude. Mainly, the ignition temperature of the biocrude produced in the ethanol-water mixture was lower than that of another biocrude obtained in pure water. Both studies agreed that biomass-derived biocrudes have the potential to be used in combustion engines. However, more research and development are needed before directly applying these liquids in combustion engines.

Blending with petroleum-derived liquid fuels is a more plausible option for biocrude utilization in engines. On this matter, Chen et al. blended a renewable biowaste-based-HTL-biocrude with diesel and tested the fuel properties of such a mixture (Chen et al., 2018). They found that the biocrude could be distilled into petroleum diesel-like fractions and that the acidity of the distillates could be efficiently reduced via esterification to meet fuel standards. The blends containing 10–20 wt% of upgraded distillates and diesel showed 96–100 % power output, 101–102 % more NO_x, 89–91 % more CO, 92–125 % more unburned hydrocarbon, and 109–115 % higher soot emissions compared with pure diesel. In another work, Choi et al. studied the flame stability and exhaust emission of biocrude/ethanol blends in a spray burner (Choi et al., 2016). The results showed that stable combustion with lower CO and higher NO_x emissions was achieved with the biocrude/ethanol blends compared to those of ethanol alone.

4.4. H_2 production from biocrudes

Similarly to the strategies described in Sections 2 and 3 to produce H_2/syngas from HC-APs, biocrudes containing abundant organic compounds (phenols, oxygen heterocycles) can also be converted into H_2-rich gases. This strategy is also supported by the higher energy densities of biomass-derived biocrudes than those of the original biomass feedstocks, which converts H_2 production into a promising route with low feedstock transportation costs (Hu and Gholizadeh, 2020). Among the different processes for H_2 production from biomass-derived liquids, supercritical water gasification (SCWG) has been intensively investigated to produce hydrogen from biocrude. Tushar et al. studied the catalytic SCWG of a biocrude produced from the HTL of cattle manure and related model compounds over a dual metal-dual support (Ni-Ru/Al_2O_3-ZrO_2) catalyst using a tubular flow reactor (Tushar et al., 2016). The highest H_2 yield was 1.34 mol/mol C for glucose (model compound) and 1.01 mol/mol C for biocrude. The highest carbon gasification efficiencies were 88 % for glucose and 92 % for biocrude, with a stability of 20 h on stream at optimum conditions. In another study, Hu et al. investigated the SCWG of a biocrude produced from the HTL of lipid-extracted algae in a batch reactor using K_2CO_3, NaOH, and Ru/C as the catalysts (Hu et al., 2020). The best results were attained at 500 °C, using a reaction time of 60 min, with a 10 wt% catalyst (K_2CO_3) loading. Under such conditions, 8 % of the biocrude was converted to gaseous products, with 1.08 mmol/g H_2 produced.

4.5. Biocrude fractionation

As mentioned in previous sections, biomass-derived biocrudes are very complex mixtures containing a substantial number of different chemical species, including oxygenates and N-containing compounds. This heterogeneity hinders their direct application as transportation fuels and the selective production of value-added chemicals. On the bright side, this diverse chemical composition facilitates biocrude fractionation due to the different physiochemical characteristics (boiling point, polarity, and solubility) of the different chemical groups in biocrudes. As a result, these liquids can be efficiently fractionated using different technologies, such as solvent extraction (Chan et al., 2020), adsorption (Drugkar et al., 2022), and membrane separation (Pinheiro Pires et al., 2019). Additionally, distillation can also be used to separate high-quality fractions from biocrude (Goswami et al., 2022). Up-to-date information on these separation technologies is collected and compared comprehensively in this section, with detailed information on technologies available for biocrude fractionation listed in Table 10.

As described in Table 10, liquid-liquid extraction is a traditional and common strategy for biocrude fractionation. This technology uses solvents as fractionation agents and separates the different types of components according to their solubility and polarity under mild conditions (Drugkar et al., 2022). Based on the solvents used, the liquid-liquid extraction method can be classified into organic solvent extraction, water extraction, and SCF extraction (Drugkar et al., 2022). The commonly used organic solvents in biocrude extraction are chloroform, dichloromethane, alcohols, ethyl acetate, and hexane (Hu and Gholizadeh, 2020). Among the organic solvents, chloroform and ethyl acetate show extraordinary extraction efficiency toward furans, ketones, phenols, and carboxylic acids (Drugkar et al., 2022). The low boiling points of these organic solvents make the separation of solvents easy to achieve. However, using some organic solvents (chloroform and dichloromethane) with high volatility is not environmentally friendly. Water extraction is a greener process to extract water-soluble fractions (carbohydrate-derived compounds and polar compounds). In most cases, water extraction was conducted to separate water and water-soluble fractions from biocrudes (Oasmaa et al., 2015; Vitasari et al., 2011). In addition, $scCO_2$ extraction has gained increasing attention in recent years due to the non-toxic and non-flammable properties of CO_2. (Manjare and Dhingra, 2019). This technology allows flexible extraction selectivity for hydrophobic compounds by simply varying the temperature and pressure (Drugkar et al., 2022). After $scCO_2$ extraction, CO_2 returns to the gaseous phase by depressurizing the system, resulting in a simple separation of the dissolved products. Based on these premises, Montesantos et al. studied the extraction of biocrude produced by HTL of pinewood, investigating the influence of temperature and pressure (Montesantos et al.,

Table 10
Fractionation technologies for biocrude and their key characteristics (Chan et al., 2020; Drugkar et al., 2022; Pinheiro Pires et al., 2019).

Fractionation technology	Description	Working principles	Advantages(s)	Disadvantage(s)
Liquid-liquid extraction				
Organic solvent extraction	Selective extraction of target component based on the polarity and affinity with a solvent	Low temperatures (20–70 °C), variable extraction efficiency	Low operation temperature Easy to separate the product	The use of harmful organic solvents (chloroform)
Water extraction	Separation and isolation of water-soluble and polar components	80–90 % recovery of polar compounds	A viable method to recover polar chemicals Simplicity and inexpensiveness	Suitability and practicality for commercialization are doubtful
SCF extraction	Stabilization and selective extraction of the components of interest	Supercritical state of the solvent (40–120 °C)	Green process Speed and altered selectivity Easy to remove the solvent ($scCO_2$) Affinity to hydrophobic constituents	High costs High pressure
Distillation				
Atmospheric distillation	Separation of different components from a mixture based on their boiling point and volatility	80–250 °C, atmospheric pressure	Favorable for recovery of acids, alcohols, and aldehydes High efficiency and flexibility	High temperature and long residence time Destroying the instinct properties of unstable chemicals via polymerization
Vacuum distillation		~20–160 °C	Milder temperature Less degree of polymerization	Energy-intensive
Molecular distillation		50–160 °C, high vacuum	Separation of thermally unstable components High efficiency and yield of biocrude distillates	Energy-intensive High cost of equipment
Adsorption	Physisorption or chemisorption of selected compounds by solid adsorbents	<100 °C	Low energy requirement Good economic viability Low waste generation	
Membrane separation	Separation of mixture via semi-permeable layer or filter based on the molecular sizes	25–150 °C	Flexibility Operational simplicity Low energy requirement Facile scalability	High cost and complex maintenance
Fractional condensation	Separating biocrude into heavy and light fractions	25–550 °C	Flexibility High separation efficiency	High energy consumption

2019). They found that augmenting temperature led to higher process operability and extraction efficiency. The extract obtained under optimal conditions was rich in ketones, 1-ring phenols, and fatty acids. Nevertheless, this technology requires high pressure, which can be costly and require special units.

Distillation separates different components from the biocrude based on their boiling point and volatility. Conventional distillation technologies include atmospheric and vacuum distillations, which perform under atmospheric pressure (101 kPa) and vacuum conditions (<10 kPa), respectively (Chan et al., 2020). In these processes, the distillation temperature depends on the boiling points of the target compounds, which vary from 20 to 250 °C (Pinheiro Pires et al., 2019). Owing to the high temperatures needed for atmospheric distillation, some undesirable reactions, such as polymerization and condensation of the oxygenated compounds (phenols and furans) in biocrude, could occur (Zhang et al., 2013). On the contrary, a vacuum distillation taking place at a lower temperature prevents the biocrude from undertaking such transformations. Molecular distillation is a separation technology occurring at a high vacuum (as low as 0.001 mbar) (Shan Ahamed et al., 2021). This low pressure allows the distillation to be conducted at a low temperature for a short period. Therefore, molecular distillation is suitable for the separation of thermally sensitive chemicals. However, the shallow pressure of this technology results in high costs and dedicated equipment.

Other biocrude fractionation technologies include fractional condensation, adsorption, and membrane separation. Fractional condensation separates biocrude into light (C1-C4, phenols, and sugars) and heavy (oligomers) fractions (Drugkar et al., 2022). Despite this technology having high separation efficiency, which is commonly used to improve the physicochemical properties of biocrudes, it is very energy-intensive. Adsorption, also known as solid-liquid extraction, uses solid adsorbents (e.g., resins, silica, zeolites, biochar, and activated carbon) to extract chemicals via chemisorption or physisorption selectively (Chan et al., 2020). Adsorption of chemicals shows several advantages, such as low energy requirement, low costs, and low waste generation. Furthermore, membrane separation fractionates biocrudes depending on their molecular sizes. This methodology comprises different technologies, i.e., microfiltration (0.05–10 μm), ultrafiltration (1–100 nm), and nanofiltration (<2 nm) (Buonomenna and Bae, 2015). These methodologies are flexible, simple, energy-efficient, and can be scaled up, but the cleaning and maintenance of the membranes are complex and costly.

4.6. Other applications

Biocrudes can also be used as alternatives or additives for petroleum-derived asphalt binders with improved properties. For example, Lv et al. investigated the influence of biocrude and rock asphalt contents and shear time on the properties of modified asphalt (Lv et al., 2020). They found that combining biocrude and rock asphalt could improve the low- and high-temperature resistance of neat asphalt and the low-temperature crack resistance of composite-modified asphalt. Using biocrudes in asphalt saves energy and provides greener construction material in road engineering. In another work, Zhang et al. developed a bio-oil-derived Al adhesive from low temperature (<200 °C) microwave-assisted pyrolysis of waste office paper (Zhang et al., 2015). The application of bio-oil to aluminum plates (50 × 50 cm) followed by curing under various conditions suggested that the optimal tensile strength of 2300 N could be achieved at 160 °C for 8 h cure. Biocrudes also show potential to be used as a source of bio-based lubricants and antioxidants to improve the oxidation properties of biodiesel. Chandrasekaran et al. (2016) used Mihaljevic, Rancimat, and PDSC test methods to evaluate the antioxidant properties of different phenolic fractions extracted from biocrude. The results showed that the phenolic extracts possessed similar antioxidant activity in biodiesel and soybean oils to the commercial antioxidant butylated hydroxytoluene. Notably, the antioxidant activity might depend on dimers of phenols with molecular weights of 302, 316, 330, and 344.

Some publications also report on utilizing biocrude as a source of carbonaceous materials in various fields. For example, Ye et al. developed a

carbon-based slow-release fertilizer coated by biocrude for farmland applications (Ye et al., 2019). They found that the biocrude coating decreased the fertilizer release speed in the water by 15 %, and the leaching rate in soil decreased by 3–5 %. These developments confirmed that the coating treatment enhanced the release capacity of the fertilizer. On this matter, Du et al. developed lignin-based nanofibers from biocrude (Du et al., 2020). They found that the nanofibers prepared from the biocrude had similar surface characteristics, crystallinity, and mechanical properties compared with polyacrylonitrile carbon nanofibers.

5. Hydrochar: physiochemical properties and present and future applications

The HC of biomass also produces an ignite-like solid product known as hydrochar. As this solid material is abundant in carbon and possesses a similar HHV to lignite and coke, it can be used as a solid fuel. For fuel purposes, HTC is similar to the definition of wet torrefaction (He et al., 2018a), which is also included in this review and regarded as HTC hereafter. Besides, the produced hydrochar can be subjected to different upgrading/activation processes to produce carbonaceous materials with enhanced properties, which can be applied in various fields, such as catalysis, electrochemistry, and remediation. The advantages of hydrochar-based materials compared to conventional materials applied in these fields are listed in Table 11. This section collects and compares vital information about the application of hydrochar and activated hydrochar to develop biofuels and carbonaceous materials. An overview of hydrochar applications is depicted in Fig. 11.

5.1. Properties of hydrochar

Table 12 summarizes the most important properties (fuel, chemical, and structural properties) of hydrochars produced from the HC of biomass. These include fuel properties, along with morphology and surface functional characteristics. The fuel properties are evaluated by the elemental composition, HHV, flame stability, and thermalgravimetric (TG) analysis. The elemental composition is very useful for gathering structural information about hydrochars. According to previous studies, a H/C ratio below 0.3 represents highly condensed aromatic ring systems, whereas above 0.7 indicates non-condensed aromatic ring systems (Tasca et al., 2019). The morphological and textural properties of biomass-derived hydrochars are characterized by scanning/transmission electron microscope and N_2 physisorption, respectively. Generally, the hydrochars produced by HC have varied BET surface areas (10–300 m^2/g) (Son Le et al., 2022), depending on the processing conditions (Xiao et al., 2018) and inherent properties of the original feedstocks (Liu et al., 2019).

For example, Xiong et al. studied the effect of processing conditions on the hydrochar yield and properties of HTC of swine manure (Xiong et al., 2019). The optimization results were 260 °C, 0.1 g/mL solid-liquid ratio, and 30 min, where 53.2 wt% hydrochar with 15.9 MJ/kg HHV could be obtained. Increasing HTC temperatures led to an increment in the P content in hydrochars. Wang et al. assessed the influence of the co-HTC process on the hydrochar properties of food waste and woody sawdust (Wang et al., 2020a). The results showed that a high food waste blend ratio and HTC temperature weakened the oxygen-containing functional groups (-OH and C—O) and enhanced C═C and C—N groups. Besides, Liu et al. investigated the influence of how and to what extent a swelling pretreatment impacted the properties of a hydrochar produced from cellulose (Liu et al., 2019). The results showed that an initial increase in the HC temperature from 220 to 260 °C augmented the BET surface area while further increasing the temperature to 280 °C led to a decrease. When it comes to morphology, hydrochars produced from the HC of biomass show a more irregular surface compared to their original biomasses. Such a feature results from a collapse of their structures during HC (Wang et al., 2018b) and requires further activation processes to improve the physicochemical properties of these solids. The surface functionality of hydrochars is qualitatively analyzed using Fourier Transform Infrared Spectroscopy (FT-IR) and X-ray photoelectron spectroscopy (XPS). Based on these technologies, several authors have addressed and reported on the mechanistic understanding of the evolution of biomass components during HC. In some cases, in-situ Diffuse Reflection Infrared Fourier Transform Spectroscopy (DRIFTS) has also been conducted to monitor the change in the functional groups during the HTC process (Lin et al., 2022). Some essential applications for hydrochars produced from biomass are described as follows.

5.2. Solid biofuels

For obtaining solid biofuels, The HC or torrefaction of biomass removes a certain amount of alkaline ash and oxygen-rich compounds, resulting in improved fuel properties and higher energy densities compared to the raw biomass, which leads to hydrochars with HHVs similar to lignite (29 MJ/kg) and coke (33 MJ/kg), in some cases (Li et al., 2017a). Based on these improved fuel properties, some hydrochars are suitable for energy generation via combustion, which has been widely investigated in recent years. Ma et al. synthesized hydrochars from the HTC of pomelo peel and evaluated their combustibility blended with coal (Ma et al., 2021b). They found that the pomelo peel hydrochars obtained at 220 °C and 240 °C showed low ash contents. The combustibility study of a solid comprising 70 wt% hydrochar and 30 wt% coal indicated that the synergistic interaction between hydrochar and coal enhanced the combustibility with emissions of only small amounts of H_2O, CH_4, CO, and phenols and reduced amounts of CO_2. These results demonstrated that the combustion behavior of hydrochars could be enhanced through a co-HTC strategy.

In another work, Xu et al. studied the interaction mechanisms and combustion behaviors of hydrochar from the *co*-HTC of cotton textile waste (CTW) and polyvinyl chloride waste (PVCW) (Xu et al., 2021b). They found that the interactions between the two feedstocks during co-HTC improved the aromatic degree of the hydrochars produced. In particular, hydrochloric acid generated from PVCW promoted the depolymerization of CTW, whereas the surface functionality of hydrochars was improved by the C—Cl bonds inserted into the polymer skeleton. These synergies produced hydrochar with a HHV as high as 30.7 MJ/kg, a fuel ratio of 0.68, and a dichlorination efficiency of 91 %. In addition to these encouraging results, the TG analysis of the hydrochar revelated that the co-HTC of CTW and PVCW led to a hydrochar with improved ignition and burnout

Table 11
Advantages of hydrochar-based materials compared to conventional materials.

Application	Conventional material	Advantages of hydrochar-based material
Solid biofuels	Coal	Sustainable and clean energy source, similar calorific value to coal, waste management
Electrode materials	Activated carbon, graphene (oxide), carbon nanotubes, noble metals, transition metals, metal oxides, metal nitrides, RuO_2/MnO_2/V_2O_5	Low preparation cost, higher treatment efficiency, good chemical stability, high surface area, high electronic conductivity, abundant sources, adjustable properties, sustainability, carbon neutral
Catalysts	SiO_2, Al_2O_3, zeolites, metal oxides, carbon-based materials	High surface area, inherent abundant oxygen-containing functional groups, uniformed size, high mechanical strength, low cost, sustainability, adjustable surface functional groups, resistance to acid/alkali corrosive
Bio-adsorbents	Coal-derived activated carbons, pyrochar, and silicate material with an anionic framework	Low cost, energy-saving, sustainable, high surface area, good stability, particular morphology, abundant oxygen-containing functional groups, adjustable surface functional groups, intense chemical reactivity, and less aromaticity

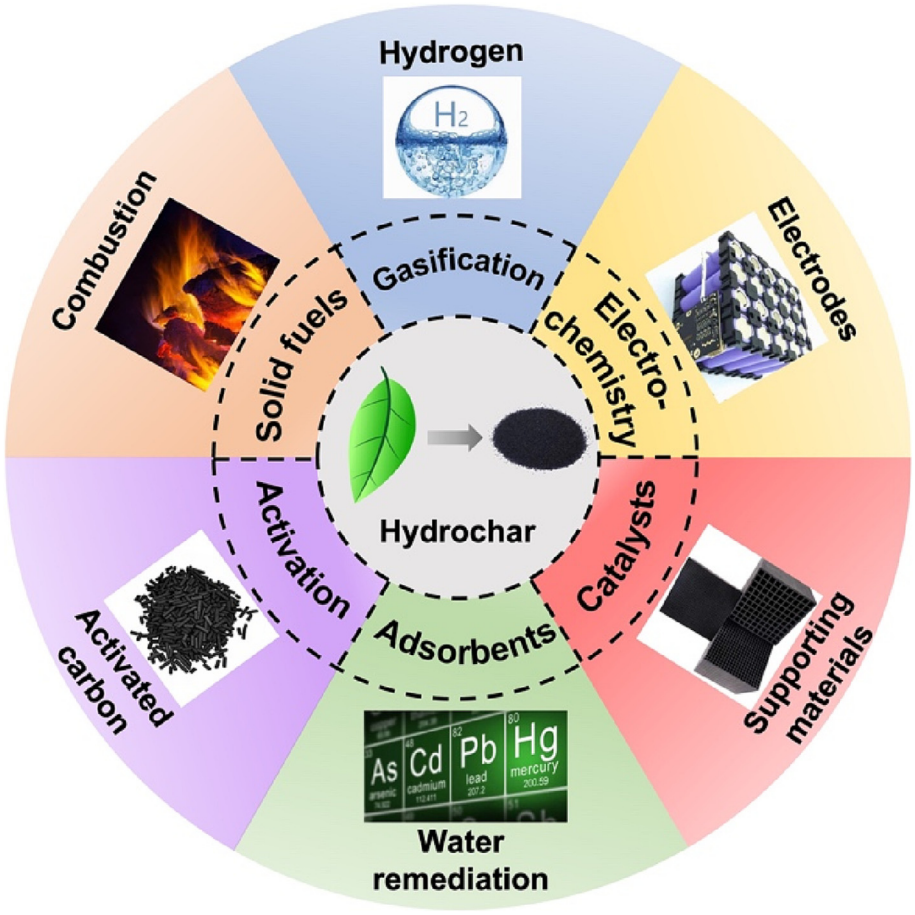

Fig. 11. An overview of hydrochar applications.

temperatures. Despite these promising results in energy production, the main issue in using hydrochar as a solid fuel is the possible pollution derived from undesired impurities (nitrogen, sulfur, and ash). The existence of these impurities might cause emissions of exhausted gases (NO_x and SO_x) and metal (oxide) particulates (Si, K, Na, S, Cl, P, Ca, Mg, Fe), fouling, slag, and corrosion in combustors. Thus, developing technologies for removing these heteroatoms in hydrochar is still necessary to achieve clean combustion. For industrial applications as solid fuel, CarboREN technology in SunCoal industries could achieve the HTC of municipal solid waste of 705 kg/h at 215 °C and 2 MPa, with a low energy consumption of 7 %. This means that HTC technology has already industrialized with excellent economic viability and environmental impacts (He et al., 2018a).

5.3. Hydrochar gasification

Hydrochars are more energy-dense and easier to store and transport than the original biomass from which these are produced. These inherent advantages make hydrochar a promising feedstock for post-treatment for energy production. As the hydrochar shows similar or enhanced characteristics compared to raw biomass, it can also be used for gaseous biofuel production via gasification. In the past few years, many studies have investigated a two-step process comprising an initial HC of biomass followed by the gasification of the hydrochar produced to produce a H_2-rich gaseous biofuel. On this matter, Zhuang et al. reported on the gasification characteristics of a biowaste-derived hydrochar (Zhuang et al., 2020). They compared three types of biowaste (herb tea waste (HTW), penicillin mycelial waste (PMW), and sewage sludge (SS)) in this two-step strategy. The results indicated that initial HTC promoted the syngas quality (increased the H_2 and CH_4 concentrations) and the conversion degree of the hydrochar in the gasification, which led to less tar formation. Lin et al. investigated the co-gasification of PVC-derived hydrochar and alkali coal. Higher yields of H_2 and CH_4, as well as a high H_2/CO ratio (1.65–3.96), were obtained, whereas the yield of CO_2 decreased by blending PVC with coal (Lin et al., 2021).

5.4. Hydrochar activation

Despite biomass-derived hydrochars produced by HC showing enhanced energy density compared to raw biomass, they have a low surface area (<10 m^2/g) and poor thermal stability. Besides, their textural properties, functionality, and thermal stability still need to be improved by further treatments to be utilized in the fields of catalysis, electrochemistry, and pollutant remediation. Such enhancements can be achieved using different activation methods, including physical and thermal activation, chemical activation, and functionalization. Table 13 summarizes some of the most widespread activation methodologies used for hydrochar activation.

Physical and thermal methods utilize reactive gases (e.g., CO_2, diluted O_2) as the activation agent. These technologies have several advantages, such as avoiding acidic or basic chemicals, no need to wash after activation, and no waste generation (Shen et al., 2021). Some relevant publications on these strategies include the work of Ahmad et al., who reported the activation of hydrochar produced from the HTC of lincomycin residue in a CO_2 flow at 700 °C for 1.5 h (Ahmad et al., 2020). They focused on the activation effect on the transformation of phosphorous and nitrogen species in hydrochar/activated hydrochar. The results showed that the N content decreased after HTC and activation. Phosphorous species (P-$NaHCO_3$ and P-NaOH) were stabilized and transformed into more stable species (P-residue) after CO_2 activation. These evolutions led to enhanced Pb (II) removal from the solution. In another work, Huang et al. investigated the influence of the oxygen concentration and temperature on the properties of thermal-

Table 12
Typical properties of hydrochar from biomass HTC or wet torrefaction.

Feedstock	Processing conditions	Hydrochar yield (wt%)	Elemental composition (wt%)				HHV (MJ/kg)	Physiochemical and structural properties	Ref.
			C	H	O	N			
Swine manure (SW) and sawdust	220 °C, 10 h, 1:3	61.84	57.05	6.11	28.05	1.89	24.05	Surface groups: hydroxyl, carboxyl, aliphatic methylene, carbonyl groups, aromatic ring in lignin	(Lang et al., 2018)
Pomelo peel and PVC	220 °C, 6 h, 1:1	39	60.87	4.36	32.38	0.72	22.58	Surface groups: alkyl chloride, aromatic C═O, C═C in carbonyls; enhanced flame stability and combustion properties	(Wei et al., 2022)
Sewage sludge and banana stalk	280 °C, 1 h, 3:10	43.29	51.11	NA	NA	2.37	21.09	Superior combustion performance of co-HTC hydrochar reduced contamination degree of heavy metals in hydrochar	(Zhang et al., 2021a)
Orange peel	240 °C, 2 h	~42	68.34	5.04	23.69	1.56	–	BET surface area: 13.51 m^2/g, pore volume: 0.06 cm^3/g, pore diameter: 21.75 nm; surface groups: COOR, C═O, C—O, CH_x	(Xiao et al., 2018)
Swelled cellulose	260 °C, 4 h	32.43	71.7	4.6	23.7	–	–	BET surface area: 203.5 m^2/g, pore volume: 0.26 cm^3/g, pore diameter: 4.51 nm; spherical particle; more stable chemical structure	(Liu et al., 2019)
Corn stover	220 °C, 4 h, 2 % acid	32.86	71.2	4.5	20.3	0.2	–	Surface groups: O—H, C═O, C—O, C═C, COOH; Formation of carbon spheres	(Zhang et al., 2019b)
Cellulose and AP bio-oil	210 °C, 1 h	~54	75.1	5.5	19.4	–	30.2	High hydrogen content and low aromatization degree; ignition temperature: 170 °C, burnout temperature: 600 °C; high hydrophobicity	(Lin et al., 2022)
Leather waste	180 °C, 30 min	86.1	53.7	8.5	25.2	1.1	6058 kcal/kg	Stable combustion characteristics at a high temperature; surface groups: hydroxyl, carboxyl, carbonyl groups	(Lee et al., 2019)
Municipal solid waste	200 °C, 30 min	69.7	66.6	8.8	23.9	0.7	33.01	Energy yield of 89 %	(Triyono et al., 2019)
Chlorella pyrenoidosa	200 °C, 30 min	30.2	59.0	7.4	21.3	6.4	28.32	Surface groups: C═O, C═C, C═N, -C-O, N—H, -C-O-R	(Farobie et al., 2022)
Whitewood	200 °C	~50	49	~7	~44	<1 %	~20	A strong cellulose-lignin structure	(Güleç et al., 2022)

oxidation-activated hydrochar for tetracycline adsorption (Huang et al., 2020). They found that increasing the temperature from 300 to 700 °C augmented the BET surface area of the activated hydrochar. Among the different conditions tested, the hydrochar activated in 0.5 vol% O_2 at 500 °C showed the best adsorption capacity of tetracycline measured by the micropore filling and π-π interaction methodologies.

Chemical methods have been more frequently investigated for hydrochar activation compared with physical or thermal methods. The chemical activation of hydrochars generally produces activated carbonaceous materials with better porosity. The chemicals used for hydrochar activation can be classified into acids, alkalis, and inorganic salts. Hydrochloric (He et al., 2021) and phosphoric acids (Wang et al., 2022c) are the most commonly utilized agents in acid activation. For example, Wang et al. developed a phosphoric acid-activated hydrochar from the HTC of livestock waste for ammonia adsorption (Wang et al., 2022c). The characterization of the activated hydrochars indicated that phosphoric acid extended the pores and introduced acidic groups into the hydrochar. The P-containing groups improved NH_3 adsorption by activated chars. As for alkali activation, KOH is the most frequently reported agent for hydrochar activation, leading to activated hydrochars with excellent porosity (Yu et al., 2019). An example of this technology includes the work of Sultana et al., who investigated different conditions for hydrochar activation from the HTC of loblolly pine and its application in hydrogen storage (Sultana and Reza, 2022). A BET surface area as high as 3666 m^2/g, along with total pore and micropore volumes of 1.56 cm^3/g and 1.32 cm^3/g, were achieved at 800 °C, conducting the treatment for 2 h. This hydrochar could achieve a hydrogen storage capacity of 10.2 wt% at 77 K and 55 bar.

The salts commonly used for hydrochar activation include $KHCO_3$, $K_2C_2O_4$, and $ZnCl_2$. Shi et al. addressed the synthesis of carbon spheres from glucose-derived hydrochar by $KHCO_3$ activation, exploring their CO_2 capture capabilities (Shi et al., 2022). The hydrochar produced at 200 °C was subjected to chemical activation by $KHCO_3$ with urea. An ultrahigh BET surface area of 3576 m^2/g was achieved by activating at 800 °C. The experimental results revealed that the activated carbon spheres could capture CO_2 up to 35 mmol/g, regardless of the pressure. In another work, hydrochar from orange peel waste was activated with $K_2C_2O_4$ at 800 °C for 2 h, with the activated hydrochar resembling a microporous carbon with a BET surface area of 2130 m^2/g, a micropore volume of 1.12 cm^3/g and a CO_2 uptake capability of 6.67 mmol/g at 0 °C and 1 bar (Rehman et al., 2022). In this line, Susanti et al. synthesized an activated carbon (AC) using $ZnCl_2$ from cocoa pods husk hydrochar (Susanti et al., 2022), achieving an activated carbon material with a mesoporous structure.

5.5. Hydrochar in electrochemistry

Carbonaceous materials produced by the HC of biomass can also be used in electrochemical energy storage devices due to their excellent electrochemical performance. The high BET surface area, tunable porous structures, high electric conductivity, and mechanical strength of these carbon materials account for such applications. These excellent features convert hydrochars into a promising renewable option to replace traditional materials commonly used in electrical energy storage devices, such as supercapacitors (SCs) (Amar et al., 2021; Wang et al., 2020b) and batteries (Yu et al., 2021).

Given these favorable prospects, plenty of work has studied the application of hydrochar-derived carbons as SCs. Esteban et al. devised a facile method to synthesize hydrochar/gold nano grapes (C/Au NGs) and explored their applications as tunable supercapacitor materials (Arenas Esteban et al., 2020). Microporous carbon nanospheres/Au were synthesized by carbonizing Au/polymeric glucose spheres at 500 and 700 °C for 1 h using KOH as the activation agent. The carbon nanospheres (CNSs) containing Au nanoparticles (Au NPs) produced at 500 °C showed a high volumetric capacitance, affording similar gravimetric capacitances (205 F/g at 5 mV) to the CNSs without Au NPs. Interestingly, the C/Au NGs obtained at 700 °C exhibited higher capacitance (435 F/g). These authors also

Table 13
Hydrochar activation methods.

Feedstock[a]	Activation conditions	Surface area (m^2/g)	Improvements	Ref.
Physical or thermal methods				
Peanut shell	900 °C, 2 h, 150 mL/min CO_2	1308	Enhanced surface area (8 to 1308 m^2/g) and adsorption capacity	(Zhang et al., 2020)
Lincomycin	700 °C, 10 °C/min 1.5 h, 200 mL/min CO_2	–	Stabilization of P species (from P-$NaHCO_3$ and P-NaOH to P-residue)	(Ahmad et al., 2020)
Poplar	500 °C, 10 °C/min 3 h, 160 mL/min 0.5 %O_2 in N_2	618.02	Enhanced adsorption by micropore filling and π-π interactions	(Huang et al., 2020)
Chemical methods				
Sawdust	$K_2C_2O_4$ and melamine, 800 °C, 3 °C/min, 1 h, N_2	2600–3000	Pore volume: 1.3–1.6 cm^3/g, pore size: <3 nm, good electronic conductivity	(Sevilla et al., 2017)
Glucose	$KHCO_3$ and urea, 800 °C, 5 °C/min, 2 h, 60 mL/min N_2	3576	Promoted pore formation, superior CO_2 capture performance (35.57 mmol/g)	(Shi et al., 2022)
Livestock manure	H_3PO_4, 550 °C, 2 h, N_2	464.45	Increased P-containing groups on the surface, enhanced NH_3 adsorption	(Wang et al., 2022c)
Sludge	Fenton oxidation, 30 % H_2O_2/Fe^{2+}	5.18	Increased acidic group concentration and surface area	(Belete et al., 2021)
Loblolly pine	KOH, 800 °C, 2 h	3666	Pore volume: 1.56 cm^3/g	(Sultana and Reza, 2022)
Pinecones	$KHCO_3$ and K_2FeO_4, 500 °C, 2 h, N_2	703.97	Remarkable microporous structures; loading of Fe_0 and Fe_3O_4	(Ahmad et al., 2020)
Sucrose	KOH, 800 °C, 10 °C/min, 2 h, 100 mL/min N_2	2604	Microporous surface area: 1318 m^2/g, pore volume: 1.685 cm^3/g	(Yu et al., 2019)
Tobacco stem	KOH, 800 °C, 5 °C/min, 90 min, N_2, $(NH_4)C_2O_4$ modified	2875	Micropore volume/total pore volume = 0.7, high degree of disorder	(Wen et al., 2023)
Food waste	KOH, 800 °C, 2 h, 1 L/min N_2	2885	Total pore volume: 1.93 cm^3/g	(Sultana et al., 2021)
Orange peel waste	$K_2C_2O_4$, 800 °C, 2 h, N_2	2130	Micropore volume: 1.1166 cm^3/g, high pyrrolic nitrogen content (46.1 %)	(Rehman et al., 2022)

[a] The feedstock for hydrochar production.

reported that extraordinarily high gravimetric and volumetric capacitances of 210 F/g and 114 F/cm^3 were achieved using these materials in a symmetrical two-electrode cell.

Hydrochar-derived carbon can also be applied as electrodes in lithium-ion batteries. Yu et al. reported the application of a spent Pb-adsorbed hydrochar as an anode for lithium batteries (Yu et al., 2021). CO_2 activation and alkali treatment were conducted to remove the remaining biocrude and ash in the hydrochar. This activated material was first used for Pb (II) adsorption, with the solid produced in this step subsequently used as an anode in a Li-ion battery. This latter exhibited a high reversible capacity (358 mAh/g at 0.1 A/g for 100 cycles) and an extraordinary rate capacity (383 mAh/g at 0.1 A/g).

5.6. Hydrochar in catalysis

Activated hydrochars are also considered promising materials for developing renewable-based, carbon-neutral catalysts. They possess a high surface area for active metal dispersion and modifiable surface functional groups. These characteristics provide hydrochar-based catalysts with excellent activity in some chemical reactions, such as molecule activation and bond cleavage. Table 14 recaps some recent progress in the application of hydrochar in catalysis. To this end, hydrochars produced by HC of biomass are first subjected to pyrolysis and/or chemical/physical activation at a high temperature (500–900 °C). Then, the activated carbonaceous materials produced with these treatments are functionalized with active metals or functional agents.

For example, Liu et al. obtained a hydrochar-derived material from cellulose and used it to synthesize an Al-hydrochar-supported catalyst for glucose isomerization to fructose (Liu et al., 2021b). Cellulose was initially subjected to swelling using trifluoroacetic acid and then carbonized under hydrothermal conditions at 260 °C for 4 h. The as-prepared hydrochar was impregnated with $AlCl_3$ and then calcined at 300 °C for 1 h. The catalytic tests showed the process achieved a 26.3 % fructose yield at 160 °C, using a reaction time of 20 min in the presence of the Al-hydrochar catalyst. They found that the amorphous aluminum species were responsible for the catalytic activity in glucose isomerization, whereas the crystalline aluminum species inhibited such reaction. Nickel-based hydrochar catalysts are another good example of how hydrochars can be used in catalysis. For example, Gai et al. developed different bimetallic Ni-Cu/hdyrochar catalysts to produce H_2 by steam-reforming acetic acid (Gai et al., 2019a). Among these, a Ni-Cu/hydrochar catalyst with Ni:Cu ratio of 6:4 showed the best catalytic activity on acetic acid stream reforming with 95 % H_2 concentration. The catalyst characterization results demonstrated that quinones and hydroquinones formed on the hydrochar surface promoted the formation of metal-carbon conjugated bonds via metal-support interactions, with these developments being responsible for such excellent catalytic behavior.

Other authors have also explored using hydrochar-supported catalysts for amination reactions. Zhuang et al. developed a cobalt hydrochar-supported catalyst for the reductive amination of benzaldehyde (Zhuang et al., 2022a). They compared the catalytic performance on the reductive amination of benzaldehyde to benzylamine of a series of hydrochar-supported metal catalysts synthesized via two different methodologies, i.e., impregnation and one-pot synthesis (Fig. 12). They found that the former method led to the formation of outer-sphere surface complexes with metal nanoparticles. At the same time, the latter produced an inner sphere with amorphous metallic species. The catalyst prepared by impregnation showed higher catalytic activity with an optimal yield of benzylamine of 93.7 % and high stability with up to five consecutive runs achieved. Recent publications have emphasized the use of biomass-derived materials in thermocatalysis (esterification (Araujo et al., 2019), hydrogenation (Madduluri et al., 2020)), electrocatalysis (oxygen reduction (Han et al., 2020) and hydrogen evolution reactions (Cui et al., 2015)) and photocatalysis (toxic pollutants) (Zhu et al., 2020). Given the fact that biomass-derived hydrochars resemble some common characteristics and features of these materials, the application of hydrochar-based catalysts could be expanded to more chemical transformations. This opens the door to exciting new catalytic applications for carbon-based materials produced by the HC of biomass.

5.7. Hydrochar as a bio-adsorbent material

Hydrochars derived from the HC of biomass comprise a tunable surface with abundant oxygen-containing functional groups (carbonyl, carboxylic, hydroxyl groups) with excellent adsorption capabilities. The adsorption efficiency of hydrochars is related to the surface area and aromaticity (Zhang et al., 2019c). Given these features, many authors have explored the use of hydrochars to adsorb and remove several kinds of contaminants in wastewater and soils. These applications include removing heavy metals (Cu, Ni, Cd, Pb) and organic contaminants (pesticides, drugs, and dyes) (Antero et al., 2020). Table 15 summarizes the latest progress on the application of hydrochars as adsorbents.

Biomass-derived hydrochar can efficiently adsorb a wide range of heavy metals. Adsorption is a physiochemical process based on electrostatic attraction, complexation, ion exchange, and H-bonding interactions. These interactions are caused by the abundant oxygen-containing groups (carboxyl and hydroxyl groups) on the surface of hydrochars. Xia et al. developed a H_2O_2 modified hydrochar for the adsorption of Pb^{2+} in the aqueous phase (Xia et al., 2019). They found that the maximum adsorption

Table 14
Recent studies on hydrochar-based catalysts and their catalytic performance.

Hydrochar catalyst	Catalytic reaction	Processing conditions	Catalytic performance	Ref.
Pyrolyzed hydrochar (water hyacinth)	Glucose isomerization	120 °C, 45 min	31 % fructose yield and 89 % selectivity; recyclability: 3 runs	(Yang et al., 2022b)
Al/hydrochar (corn stover)	Glucose isomerization	160 °C, 20 min	35.1 % fructose yield and 77.4 % selectivity; recyclability: 4 runs	(E et al., 2022)
Al-doped hydrochar (corn stover)	Glucose isomerization	180 °C, 5 min, microwave	42.6 % fructose yield and 83.6 % selectivity	(Liu et al., 2022a)
Cu/hydrochar (chitosan)	Ullmann C—N coupling	90 °C, 24 h, K_2CO_3, H_2O	90 % yield; recyclability: 5 runs	(Ge et al., 2020)
Co@HC (glucose)	Reduction amination of benzaldehyde	80 °C, 2 h, 2 MPa H_2, 7 mol/L NH_3 in MeOH	93.7 % yield of benzylamine	(Zhuang et al., 2022a)
Ni@HC (pinewood sawdust)	Catalytic reforming of sewage sludge	700 °C, 30 min	109.2 g H_2/kg sludge, 2.12 mg tar/g	(Gai et al., 2019b)
NiFe/HC (Pinewood sawdust)	Stream reforming of sewage sludge	700 °C, 0.5 h	113.7 g H_2/kg sludge, 2.3 mg tar/g	(Gai et al., 2018)
Ni-Cu/HC (sawdust)	Stream reforming of acetic acid	600 °C, 30 min	95 % concentration of H_2	(Gai et al., 2019a)
Ni/SB-C (sugarcane bagasse)	Methane dry reforming	850 °C, 72 h	CH_4/CO_2 conversions of 81.32/93.93 %, 99.86 % carbon balance	(Zhao et al., 2021)
Ni/hydrochar (glucose)	APR of methanol	250 °C, 1.5 h	Turnover frequency: 89.5 mol_{H2}/mol_{Ni}/min, recyclability: 10 runs	

capacity of Pb (II) was 92.8 mg/g at 25 °C and pH = 5. According to the mechanistic investigation, the modified hydrochar adsorbed Pb (II) via surface complexation with accessible -OH and -COOH groups and Pb^{2+}-π interactions. Besides, introducing other functional groups by surface modification could also facilitate the removal of heavy metals. Li et al. synthesized a dithiocarbamate-modified hydrochar for lead ions adsorption (Li et al., 2020a). During the modification, the prepared hydrochar was subjected to an alkali treatment with a NaOH solution (0.25 mol/L), followed by etherification with epichlorohydrin, amination with diethylene tetramine water solution (1:1), and dithiocarbamate with CS_2 and NaOH. After these modifications, amine and dithiocarbamate groups were introduced onto the hydrochar surface. These species promoted Pb^{2+} removal via inner-sphere surface complexation of lead ions with dithiocarbamate, carboxylate, amine, and sulfonate groups, and ion exchange between Na^+ and Pb^{2+}. The presence of these surface groups on the hydrochar provided it with an adequate adsorption capacity of 151.51 mg Pb(II)/g.

In addition to heavy inorganic metals, hydrochars can also adsorb and remove organic pollutants. The adsorption of organics is ascribed to several interactions, including electrostatic attraction, complexation, ion exchange, hydrophobic interactions, H-bonding, n-π, and π-π interactions (Guan et al., 2021; Ighalo et al., 2022). Guan et al. compared the chemical and physical aging (i.e., high temperature and freeze-thaw cycles aging, oxidation, and acidification) on the hydrochar properties and adsorption capacities for norfloxacin and Cu(II) (Guan et al., 2021). They found that chemical aging (oxidation and acidification) significantly influenced the hydrochar properties. Aging increased the polarity and concentration of O-containing surface functional groups, which improved the sorption of norfloxacin via hydrophobic partition and H-bonding. For hydrochar treated by acidification and physical methods, the existence of Cu^{2+} prohibited the adsorption of norfloxacin. However, due to the hydrophobic partition effect, Cu^{2+} promoted the adsorption of norfloxacin using oxidative hydrochar.

6. Techno-economic and life cycle analyses

In biomass hydrothermal conversion processes, despite the gas yield being low (1–5 wt%), the gas can contain a high proportion of CO_2 (80 vol%) at HTC and HTL processing temperatures (180–350 °C). Besides, in biomass HTG, although the CO_2 in the gaseous products accounts for lower proportions (10–40 vol%), the gas yield is much higher. Given this CO_2 release, there are doubts about whether HC processes could mitigate CO_2 emissions. In this regard, it must be borne in mind that the photosynthesis of biomass uptakes CO_2, which converts biomass HC into a carbon-neutral process. To further analyze this issue, life-cycle analyses (LCA) of

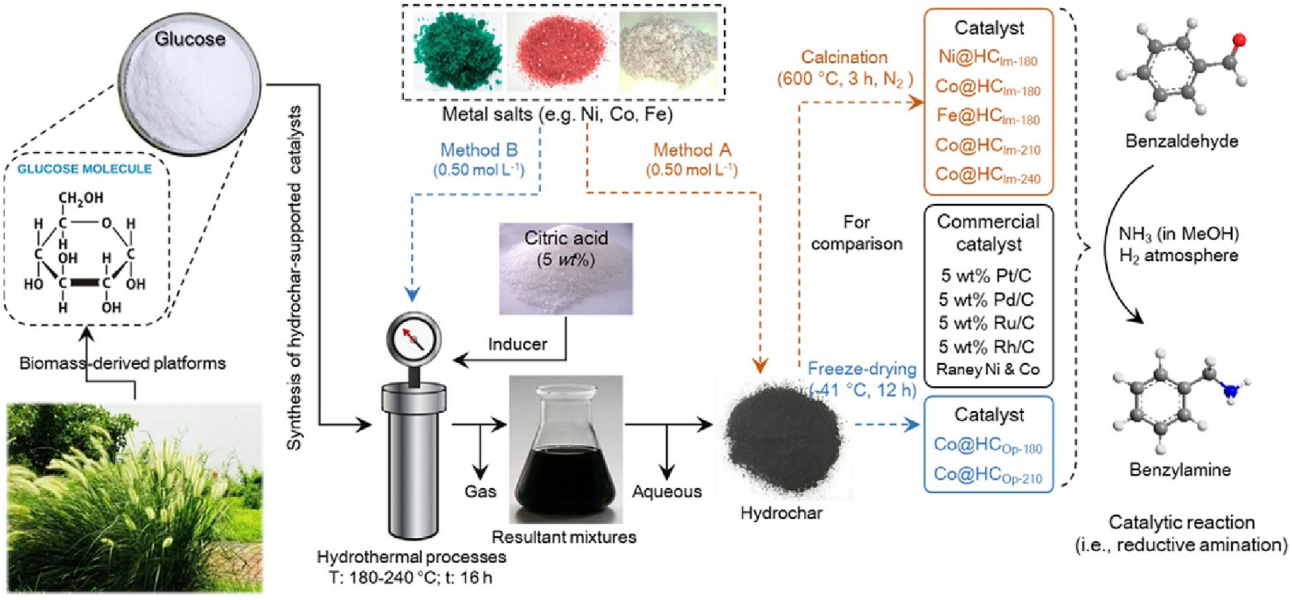

Fig. 12. Schematic diagram for preparing hydrochar-supported metal catalysts via two methods. Adapted from Ref. Zhuang et al. (2022a), with permission from Elsevier.

Table 15
Recent studies on hydrochar-based adsorbents.

Contaminant	Feedstock	HTC Conditions	Modification	Performance	Ref.
Inorganic contaminants					
As(V)	Cattle manure	0.8 M thiourea, 0.8 M Fe $(NO_3)_3$, 240 °C, 4 h	–	44.8 mg As(V)/g, 38.44 L/g	(Chen et al., 2021a)
Cd(II)	Poplar sawdust	220 °C, 1 h	15 % HNO_3 impregnation, 25 °C, 2 h	19.9 mg Cr(II)/g in 50 mg/L	(Li et al., 2021)
Cu(II) and Zn(II)	Corn straw	200 °C, 30 min	KOH (3 M) at 30 °C for 1 h; polyethyleneimine/methanol (10 % w/v) at 30 °C for 24 h; glutaraldehyde (1 % w/v) for 30 min	207.6 mg Zn(II)/g, 56.1 g Cu(II)/g	(He et al., 2021)
Pb(II)	Sawdust	260 °C, 2 h	20 % H_2O_2, 30 °C, 6 h	92.80 mg Pb^{2+}/g at 25 °C, pH 5.0	(Xia et al., 2019)
Pb(II)	Sugarcane bagasse	$ZnCl_2$, 180 °C, 11.5 h	2 M KOH, 25 °C, 1 h	q_{max} = 90.1 mg Pb(II)/g	(Malool et al., 2021)
Ni(II), Pb(II) and Cu(II)	Avocado seed	250 °C, 12 h	–	0.12–0.35 mmol/g	(Dhaouadi et al., 2021)
Pb(II)	Fenton sludge	340 °C, 1 h	–	359.83 mg Pb(II)/g	(Tong et al., 2021)
Pb(II)	Bamboo powder	200 °C, 24 h	0.25 mol/L NaOH; epichlorohydrin, 80 °C, 4 h; 50 % diethylenetriamine, 60 °C, 4 h; CS_2, 14 % NaOH, room temperature, 24 h	151.51 mg Pb(II)/g	(Li et al., 2020a)
Cd(II) and Pb(II)	Pinecone	200 °C, 5 h	$FeCl_3$, CH_3COONa, $Na_3C_6H_5O_7$, ethylene glycerol, 200 °C, 1 h; NaOH, 25 °C, 90 min; CS_2, 1 h	62.49 mg Cd(II)/g, 149.33 mg Pb(II)/g	(Zhang et al., 2022)
Cu(II) and NH_4^+	Miscanthus	180 °C, 1 h	–	310 mg Cu^{2+}/g, 71 mg NH_4^+/g	(Georgiou et al., 2021)
Organic contaminants					
Cu(II), Zn(II) and tetracycline	Pine sawdust	0.5 M Sodium silicate, 0.5 M $MgCl_2$, 180 °C, 12 h	–	214.7 mg Cu(II)/g, 227.3 mg Zn(II)/g, 361.7 mg tetracycline/g, 5 cycles	(Deng et al., 2020)
Cu(II) and benzotriazole	Sawdust	N-cyclohexyl sulfamic acid, 25 °C, 6 h; 190 °C, 12 h	–	159.91 mg benzotriazole/g, 298.86 mg Cu(II)/g	(Deng et al., 2019)
Cr(VI) and Congo Red	Poplar sawdust	200 °C, 12 h; 3 M KOH, 1 h, room temperature	$FeCl_3$, CH_3COONa, ethylene glycol, 180 °C, 12 h	1019.2 mg Congo red/g, 287.7 mg Cr(IV)/g	(Wu et al., 2022)
Methylene blue	Corncobs	180 °C, 6 h	1 M KOH, 130 °C, 2 h; 800 °C, 2 h, N_2	489.56 mg methylene blue/g	(Hien Tran et al., 2022)
Methylene blue	Bamboo	Acrylic acid, ammonium persulfate, 200 °C, 24 h; 0.1 M NaOH, 2 h	–	717.78 mg methylene blue	(Lv et al., 2022)
Methylene blue	Chili seeds	215 °C, 8 h	–	145 mg methylene/g blue	(Parra-Marfil et al., 2020)
Rhodamine B	Corn stover	230 °C, 30 min, 9 recycles	–	23.6 mg Rhodamine B/g	(Islam et al., 2022)
2-nitrophenol	Avocado seed	200 °C, 12 h	–	562 mg 2-nitrophenol/g	(Pauletto et al., 2021)
Toluene and iodine	Orange peel	210 °C, 2 h, urea	KOH, 800 °C, 3 °C/min, 2 h	724 mg toluene/g, 2252 mg iodine/g	(Xiao et al., 2020)

HC processes were addressed in the literature. These were accomplished in parallel with a techno-economic analysis (TEA) to assess the commercial feasibility of the process. Marangon et al. studied the environmental performance of microalgae HTL. They reported that aqueous phase recirculation, biomass humidity reduction, and enhancing heat recovery lead to a 45 % decrease in the negative impacts of the HTL process, with 0.1349 kg of CO_2eq per MJ emitted (Marangon et al., 2022). Masoumi et al. studied the LCA and TEA of biofuel production via HTL and hydrotreatment using hydrochar-based catalysts (Masoumi and Dalai, 2021b). The results showed that the minimum fuel selling price was 2.2 $/L to breakeven the cost of operation, and the estimated greenhouse gas emission of the process (-1.13 g CO_2eq MJ^{-1}) was much lower compared to the production of petroleum-based fuels. Besides, Roy et al. evaluated the life cycle of hydrochar from the co-HTC of peat moss and miscanthus for energy and soil amendment applications (Roy et al., 2020). They found that the hydrochar produced from miscanthus exhibited a lower global warming potential than peat moss and blended biomasses. Hydrochar applied in soil amendment was more environmentally friendly compared with energy application. Furthermore, Okolie et al. studied the LEA of three scenarios based on biomethane and bioethanol production via an integrated process including HTG, syngas fermentation, and bio methanation (Roy et al., 2020). Scenario 1 was based on bioethanol production via HTG and syngas fermentation; scenario 2 coupled scenario 1 with a CO_2 capture unit; scenario 3 added bio methanation and electrolytic units. The TEA of these scenarios indicated that the minimum selling price of bioethanol decreased in the following order: scenario 2 ($1.4 L^{-1}) > scenario 1 ($1.32 L^{-1}) > scenario 3 ($0.31 L^{-1}). Overall, the operating conditions of hydrothermal and downstream processes influence the cost and profit. LCA studies of the process indicated that CO_2 emission from biomass HTL could be reduced compared to those of petroleum-based production processes.

7. Conclusions

Hydrothermal conversion of biomass is one of the most promising routes to obtain renewable, carbon-neutral products to furnish biofuels, biochemicals, and biomaterials. This review has collected vital information, covering the most relevant studies on applying the products obtained during the hydrothermal conversion of biomass, i.e., gas, aqueous phase, biocrude, and hydrochar. A holistic, zero-waste approach has been followed in this review to comment on the present and possible future applications of these products industrially. This practical vision emphasizes how these products can be used in various fields to achieve comprehensive commercialized biorefineries, providing the readers with a deep insight into the development of integrative processes to develop novel 'waste to wealth' integrative strategies.

The gaseous stream, primarily containing H_2, CO, CH_4, and CO_2, along with other minor impurities, can be subjected to a gas cleaning process to remove unwanted impurities. The cleaned gas abundant in H_2, CH_4, and CO can be directly applied as gaseous biofuels for power generation. It can also be chemically and/or biologically transformed into value-added chemicals (alkanes, alkenes, alcohols, and organic acids) via Fischer-Tropsch synthesis and fermentation. The aqueous phase, with abundant organics (carbohydrates and protein-derived compounds) and inorganics (Na, K, Ca, Mg, Cl, S), can be used for biomass/microorganism cultivation and/or recycled to be used as the reaction medium for a subsequent HC process. Other applications for the AP include its chemical and biological conversion into fuel (H_2, CH_4, alcohols), chemicals (acids and furans), and/or masking agents for leather tanning.

As for biocrude, this is an energy-dense liquid comprising a pool of complex chemicals with potential application to furnish fuels and chemicals. To be used as a transportation biofuel (alone or blended) in

internal combustion engines, the biocrude must be upgraded through catalytic hydrotreatment/hydrodeoxygenation to remove O and N selectively. It can also be used for the production of gaseous fuels (H_2-rich gas) via gasification and value-added chemicals (phenols, ketones, acids) via fractionation (including distillation, fractional condensation, solvent extraction, and membrane separation). Hydrochar is an energy-dense solid material with fuel properties similar to lignite and coke, which makes it an auspicious solid biofuel for energy generation. Additionally, the thermal stability, mechanical strength, porosity, and functionality of this solid can be enhanced via chemical and physical activation strategies. In this manner, the activated hydrochar shows potential to be applied as a biomaterial with many applications in electrochemistry, catalysis, and pollution remediation.

8. Opportunities and challenges

Despite these promising features, the hydrothermal conversion of biomass and industrial utilization of these products still offer challenging research opportunities. Some gaps and research opportunities to develop zero-waste processes via biomass hydrothermal conversion are as follows.

(1) *Stability of the catalyst under hydrothermal conditions*. Catalysts with good stability under hydrothermal conditions can be recycled, reducing material costs. However, the processing conditions used during the hydrothermal conversion or subsequent product upgrading are usually severe (200–500 °C). These high temperatures cause carbon deposition on the catalyst surface, which might block the pores and active species. Besides, collapse, support hydrolysis, leaching, sintering, and poisoning could also occur during the hydrothermal conversion of biomass. Therefore, it is vital to study the variations in the morphology and surface physiochemical properties and address how these changes influence the catalytic activity to understand, analyze and prevent the possible deactivation of the catalyst.

(2) *Integrated systems for the production and separation of products*. The post-treatment (separation, purification) of the hydrothermal products requires complex procedures and expensive equipment. To simplify the procedures and reduce costs, integrated reaction systems or reactors should be designed to in-situ or ex-situ produce and separate the products.

(3) *Enhancing product purity*. Due to the inherent complexity of lignocellulosic and algal biomass, the HC products comprise a plethora of many different compounds. Still, some reaction products, such as the biocrude and aqueous fraction, are made up of a complex mixture of different compounds. Thus, the existing separation technologies can hardly obtain one specific product with high purity. Given this, investigating more efficient ways to separate and purify these products is essential. Another approach consists of finding holistic applications for these products based on their overall physicochemical/fuel properties rather than only focusing on their chemical compositions to obtain a few valuable chemicals.

(4) *Searching for alternative green solvents to water*. Hydrothermal biomass conversion consumes massive freshwater (1.9–5.9 m^3/m^3 biofuel) (Fang et al., 2015). This is not sustainable in some regions with a freshwater shortage. A possible solution to this issue is utilizing globally abundant seawater as the reaction medium. The inorganic species in seawater might exhibit some catalytic and/or promotional effect on the formation of products during hydrothermal treatment. However, the ions in the seawater might corrode the equipment for traditional HC. Therefore, the reactors might need to be redesigned using other materials. This is an emerging and exciting research area to increase the sustainability of hydrothermal conversion processes.

(5) *Searching for technologies for the application of N-containing products*. Some biomasses are abundant in proteins. Nitrogen-rich biocrudes, and mainly, aqueous fractions, have been commonly used as a source of nutrients for biomass/microorganism cultivation. On the contrary, future work should explore how to take advantage of the abundant nitrogen content in biomass to produce nitrogen-containing products (N-containing chemicals and N-doped carbon) with commercial applications.

(6) *Technical-economic analysis and life cycle assessment*. Some technical-economic analyses (TEA) and life cycle assessments (LCA) have been conducted to evaluate the economic benefit and environmental impacts of hydrothermal conversion processes. However, the existing TEA and LCA have only addressed the HC process. Due to the differences between the HC process and the post-treatment/application processes needed to upgrade the reaction products, further analyses and assessments of these processes need to be conducted and included to analyze hydrothermal conversion as a whole, from the biomass to the final products.

CRediT authorship contribution statement

Yingdong Zhou: Conceptualization, Methodology, Validation, Investigation, Data curation, Writing – original draft. **Javier Remón:** Conceptualization, Methodology, Validation, Formal analysis, Investigation, Data curation, Writing – review & editing, Supervision, Project administration, Funding acquisition. **Xiaoyan Pang:** Investigation, Writing – review & editing. **Zhicheng Jiang:** Investigation, Writing – review & editing. **Haiteng Liu:** Investigation, Writing – review & editing. **Wei Ding:** Conceptualization, Methodology, Validation, Formal analysis, Investigation, Data curation, Writing – review & editing, Supervision, Project administration, Funding acquisition.

Data availability

Data will be made available on request.

Declaration of competing interest

The authors declare that they have no known competing financial interests or personal relationships that could have appeared to influence the work reported in this paper.

Acknowledgments

This work is financially supported by the National Foreign Expert Project (G2022056002), the Chengdu University of Technology Teachers Development Research Fund (10912-KYQD2022-09753), and the National Natural Science Foundation of China (22108297). Javier Remón is very grateful to MCIN/AEI/10.13039/501100011033 and the European Union "NextGenerationEU"/"PRTR" for the Ramón y Cajal Fellowship (RYC2021-033368-I) awarded.

References

Afif, E., Azadi, P., Farnood, R., 2011. Catalytic hydrothermal gasification of activated sludge. Appl. Catal. B Environ. 105 (1–2), 136–143.

Ahmad, S., Zhu, X., Luo, J., Zhou, S., Zhang, C., Fan, J., Clark, J.H., Zhang, S., 2020. Phosphorus and nitrogen transformation in antibiotic mycelial residue derived hydrochar and activated pyrolyzed samples: effect on pb (II) immobilization. J. Hazard. Mater. 393, 122446.

Ahmed Ebrahim, S., Robertson, G., Jiang, X., Baranova, E.A., Singh, D., 2022. Catalytic hydrothermal liquefaction of food waste: influence of catalysts on bio-crude yield, asphaltenes, and pentane soluble fractions. Fuel 324, 124452.

Aho, A., Alvear, M., Ahola, J., Kangas, J., Tanskanen, J., Simakova, I., Santos, J.L., Eranen, K., Salmi, T., Murzin, D.Y., Grenman, H., 2022. Aqueous phase reforming of birch and pine hemicellulose hydrolysates. Bioresour. Technol. 348, 126809.

Amar, V.S., Houck, J.D., Maddipudi, B., Penrod, T.A., Shell, K.M., Thakkar, A., Shende, A.R., Hernandez, S., Kumar, S., Gupta, R.B., Shende, R.V., 2021. Hydrothermal liquefaction (HTL) processing of unhydrolyzed solids (UHS) for hydrochar and its use for asymmetric supercapacitors with mixed (Mn, Ti)-perovskite oxides. Renew. Energy 173, 329–341.

Antero, R.V.P., Alves, A.C.F., de Oliveira, S.B., Ojala, S.A., Brum, S.S., 2020. Challenges and alternatives for the adequacy of hydrothermal carbonization of lignocellulosic biomass in cleaner production systems: a review. J. Clean. Prod. 252, 119899.

Ao, M., Pham, G.H., Sunarso, J., Tade, M.O., Liu, S., 2018. Active centers of catalysts for higher alcohol synthesis from syngas: a review. ACS Catal. 8 (8), 7025–7050.
Araujo, R.O., Chaar, J.D.S., Queiroz, L.S., da Rocha Filho, G.N., da Costa, C.E.F., da Silva, G.C.T., Landers, R., Costa, M.J.F., Gonçalves, A.A.S., de Souza, L.K.C., 2019. Low temperature sulfonation of acai stone biomass derived carbons as acid catalysts for esterification reactions. Energy Convers. Manag. 196, 821–830.
Arenas Esteban, D., Guerrero Martínez, A., Carretero González, J., Birss, V.I., Otero-Díaz, L.C., Ávila Brande, D., 2020. Tunable supercapacitor materials derived from hydrochar/gold nanograpes. ACS Appl. Energy Mater. 3 (9), 9348–9359.
Aresta, M., Dibenedetto, A., Angelini, A., 2014. Catalysis for the valorization of exhaust carbon: from CO2 to chemicals, materials, and fuels. Technological use of CO2. Chem. Rev. 114 (3), 1709–1742.
Ariza, A., Lengaigne, M., Menkes, C., Lebourges-Dhaussy, A., Receveur, A., Gorgues, T., Habasque, J., Gutiérrez, M., Maury, O., Bertrand, A., 2022. Global decline of pelagic fauna in a warmer ocean. Nat. Clim. Chang. 12 (10), 928–934.
Arslan, M.T., Qureshi, B.A., Gilani, S.Z.A., Cai, D., Ma, Y., Usman, M., Chen, X., Wang, Y., Wei, F., 2019. Single-step conversion of H2-deficient syngas into high yield of tetramethylbenzene. ACS Catal. 9 (3), 2203–2212.
Arun, J., Gopinath, K.P., Vo, D.-V.N., SundarRajan, P., Swathi, M., 2020. Co-hydrothermal gasification of scenedesmus sp. with sewage sludge for bio-hydrogen production using novel solid catalyst derived from carbon-zinc battery waste. Bioresour. Technol. Rep. 11, 100459.
Asimakopoulos, K., Gavala, H.N., Skiadas, I.V., 2018. Reactor systems for syngas fermentation processes: a review. Chem. Eng. J. 348, 732–744.
Azimov, U., Tomita, E., Kawahara, N., Harada, Y., 2011. Effect of syngas composition on combustion and exhaust emission characteristics in a pilot-ignited dual-fuel engine operated in PREMIER combustion mode. Int. J. Hydrog. Energy 36 (18), 11985–11996.
Baena-Moreno, F.M., Rodríguez-Galán, M., Vega, F., Vilches, L.F., Navarrete, B., Zhang, Z., 2019. Biogas upgrading by cryogenic techniques. Environ. Chem. Lett. 17 (3), 1251–1261.
Basar, I.A., Liu, H., Carrere, H., Trably, E., Eskicioglu, C., 2021. A review on key design and operational parameters to optimize and develop hydrothermal liquefaction of biomass for biorefinery applications. Green Chem. 23 (4), 1404–1446.
Belete, Y.Z., Leu, S., Boussiba, S., Zorin, B., Posten, C., Thomsen, L., Wang, S., Gross, A., Bernstein, R., 2019. Characterization and utilization of hydrothermal carbonization aqueous phase as nutrient source for microalgal growth. Bioresour. Technol. 290, 121758.
Belete, Y.Z., Ziemann, E., Gross, A., Bernstein, R., 2021. Facile activation of sludge-based hydrochar by Fenton oxidation for ammonium adsorption in aqueous media. Chemosphere 273, 128526.
Bhatia, S.K., Otari, S.V., Jeon, J.M., Gurav, R., Choi, Y.K., Bhatia, R.K., Pugazhendhi, A., Kumar, V., Rajesh Banu, J., Yoon, J.J., Choi, K.Y., Yang, Y.H., 2021. Biowaste-to-bioplastic (polyhydroxyalkanoates): conversion technologies, strategies, challenges, and perspective. Bioresour. Technol. 326, 124733.
Buonomenna, M.G., Bae, J., 2015. Membrane processes and renewable energies. Renew. Sust. Energ. Rev. 43, 1343–1398.
Cabeza, L.F., de Gracia, A., Fernández, A.I., Farid, M.M., 2017. Supercritical CO2 as heat transfer fluid: a review. Appl. Therm. Eng. 125, 799–810.
Cao, L., Yu, I.K.M., Cho, D.W., Wang, D., Tsang, D.C.W., Zhang, S., Ding, S., Wang, L., Ok, Y.S., 2019. Microwave-assisted low-temperature hydrothermal treatment of red seaweed (Gracilaria lemaneiformis) for production of levulinic acid and algae hydrochar. Bioresour. Technol. 273, 251–258.
Castello, D., Haider, M.S., Rosendahl, L.A., 2019. Catalytic upgrading of hydrothermal liquefaction biocrudes: different challenges for different feedstocks. Renew. Energy 141, 420–430.
Chacón-Parra, A.D., Hall, P.A., Lewis, D.M., Glasius, M., van Eyk, P.J., 2022. Elucidating the maillard reaction mechanism in the hydrothermal liquefaction of binary model compound mixtures and spirulina. ACS Sustain. Chem. Eng. 10 (33), 10989–11003.
Chan, Y.H., Loh, S.K., Chin, B.L.F., Yiin, C.L., How, B.S., Cheah, K.W., Wong, M.K., Loy, A.C.M., Gwee, Y.L., Lo, S.L.Y., Yusup, S., Lam, S.S., 2020. Fractionation and extraction of bio-oil for production of greener fuel and value-added chemicals: recent advances and future prospects. Chem. Eng. J. 397, 125406.
Chandrasekaran, S.R., Murali, D., Marley, K.A., Larson, R.A., Doll, K.M., Moser, B.R., Scott, J., Sharma, B.K., 2016. Antioxidants from slow pyrolysis bio-oil of birch wood: application for biodiesel and biobased lubricants. ACS Sustain. Chem. Eng. 4 (3), 1414–1421.
Chang, K., Zhang, H., Cheng, M.-J., Lu, Q., 2019. Application of ceria in CO2 conversion catalysis. ACS Catal. 10 (1), 613–631.
Cheah, S., Carpenter, D.L., Magrini-Bair, K.A., 2009. Review of mid- to high-temperature sulfur sorbents for desulfurization of biomass- and coal-derived syngas. Energy Fuel 23 (11), 5291–5307.
Chen, H., Xu, J., Lin, H., Zhao, X., Shang, J., Liu, Z., 2021a. Arsenic removal via a novel hydrochar from livestock waste co-activated with thiourea and gamma-Fe(2)O(3) nanoparticles. J. Hazard. Mater. 419, 126457.
Chen, L., Wang, Z.-C., Chen, D., Yin, L.-X., Duan, P.-G., 2021b. Hydro-upgrading of algal bio-oil in tetralin for the production of high-quality liquid fuel: process intensification. Fuel Process. Technol. 224, 107034.
Chen, P.H., Venegas Jimenez, J.L., Rowland, S.M., Quinn, J.C., Laurens, L.M.L., 2020. Nutrient recycle from algae hydrothermal liquefaction aqueous phase through a novel selective remediation approach. Algal Res. 46, 101776.
Chen, W.-T., Zhang, Y., Lee, T.H., Wu, Z., Si, B., Lee, C.-F.F., Lin, A., Sharma, B.K., 2018. Renewable diesel blendstocks produced by hydrothermal liquefaction of wet biowaste. Nat. Sustain. 1 (11), 702–710.
Chen, Z., Rao, Y., Usman, M., Chen, H., Bialowiec, A., Zhang, S., Luo, G., 2021c. Anaerobic fermentation of hydrothermal liquefaction wastewater of dewatered sewage sludge for volatile fatty acids production with focuses on the degradation of organic components and microbial community compositions. Sci. Total Environ. 777, 146077.
Cheng, C., Li, W., Lin, M., Yang, S.T., 2019. Metabolic engineering of clostridium carboxidivorans for enhanced ethanol and butanol production from syngas and glucose. Bioresour. Technol. 284, 415–423.
Cherad, R., Onwudili, J.A., Biller, P., Williams, P.T., Ross, A.B., 2016. Hydrogen production from the catalytic supercritical water gasification of process water generated from hydrothermal liquefaction of microalgae. Fuel 166, 24–28.
Choi, S.K., Choi, Y.S., Kim, S.J., Jeong, Y.W., 2016. Characteristics of flame stability and gaseous emission of biocrude-oil/ethanol blends in a pilot-scale spray burner. Renew. Energy 91, 516–523.
Cordova, L.T., Lad, B.C., Ali, S.A., Schmidt, A.J., Billing, J.M., Pomraning, K., Hofstad, B., Swita, M.S., Collett, J.R., Alper, H.S., 2020. Valorizing a hydrothermal liquefaction aqueous phase through co-production of chemicals and lipids using the oleaginous yeast yarrowia lipolytica. Bioresour. Technol. 313, 123639.
Cui, W., Liu, Q., Xing, Z., Asiri, A.M., Alamry, K.A., Sun, X., 2015. MoP nanosheets supported on biomass-derived carbon flake: one-step facile preparation and application as a novel high-active electrocatalyst toward hydrogen evolution reaction. Appl. Catal. B Environ. 164, 144–150.
Das, P., AbdulQuadir, M., Thaher, M., Khan, S., Chaudhary, A.K., Al-Jabri, H., 2020. A feasibility study of utilizing hydrothermal liquefaction derived aqueous phase as nutrients for semi-continuous cultivation of tetraselmis sp. Bioresour. Technol. 295, 122310.
Davila, I., Diaz, E., Labidi, J., 2021. Acid hydrolysis of almond shells in a biphasic reaction system: obtaining of purified hemicellulosic monosaccharides in a single step. Bioresour. Technol. 336, 125311.
De Lorenzo, G., Milewski, J., Fragiacomo, P., 2017. Theoretical and experimental investigation of syngas-fueled molten carbonate fuel cell for assessment of its performance. Int. J. Hydrog. Energy 42 (48), 28816–28828.
Deng, J., Li, X., Wei, X., Liu, Y., Liang, J., Song, B., Shao, Y., Huang, W., 2020. Hybrid silicate-hydrochar composite for highly efficient removal of heavy metal and antibiotics: coadsorption and mechanism. Chem. Eng. J. 387, 124097.
Deng, J., Li, X., Wei, X., Liu, Y., Liang, J., Tang, N., Song, B., Chen, X., Cheng, X., 2019. Sulfamic acid modified hydrochar derived from sawdust for removal of benzotriazole and Cu(II) from aqueous solution: adsorption behavior and mechanism. Bioresour. Technol. 290, 121765.
Devadas, V.V., Khoo, K.S., Chia, W.Y., Chew, K.W., Munawaroh, H.S.H., Lam, M.K., Lim, J.W., Ho, Y.C., Lee, K.T., Show, P.L., 2021. Algae biopolymer towards sustainable circular economy. Bioresour. Technol. 325, 124702.
Dey, T., Singdeo, D., Pophale, A., Bose, M., Ghosh, P.C., 2014. SOFC power generation system by bio-gasification. Energy Procedia 54, 748–755.
Dhakal, N., Acharya, B., 2021. Syngas fermentation for the production of bio-based polymers: a review. Polymers (Basel) 13 (22), 3917.
Dhaouadi, F., Sellaoui, L., Hernández-Hernández, L.E., Bonilla-Petriciolet, A., Mendoza-Castillo, D.I., Reynel-Ávila, H.E., González-Ponce, H.A., Taamalli, S., Louis, F., Lamine, A.B., 2021. Preparation of an avocado seed hydrochar and its application as heavy metal adsorbent: properties and advanced statistical physics modeling. Chem. Eng. J. 419, 129472.
Di Fraia, A., Miliotti, E., Rizzo, A.M., Zoppi, G., Pipitone, G., Pirone, R., Rosi, L., Chiaramonti, D., Bensaid, S., 2022. Coupling hydrothermal liquefaction and aqueous phase reforming for integrated production of biocrude and renewable H_2. AICHE J. 69, 1–14.
Digdaya, I.A., Sullivan, I., Lin, M., Han, L., Cheng, W.H., Atwater, H.A., Xiang, C., 2020. A direct coupled electrochemical system for capture and conversion of CO2 from oceanwater. Nat. Commun. 11 (1), 4412.
Ding, K., Le, Y., Yao, G., Ma, Z., Jin, B., Wang, J., Jin, F., 2018. A rapid and efficient hydrothermal conversion of coconut husk into formic acid and acetic acid. Process Biochem. 68, 131–135.
Ding, W., Liu, H., Remón, J., Jiang, Z., Chen, G., Pang, X., Ding, Z., 2022. A step-change toward a sustainable and chrome-free leather production: using a biomass-based, aldehyde tanning agent combined with a pioneering terminal aluminum tanning treatment (BATTAT). J. Clean. Prod. 333, 130201.
Drugkar, K., Rathod, W., Sharma, T., Sharma, A., Joshi, J., Pareek, V.K., Ledwani, L., Diwekar, U., 2022. Advanced separation strategies for up-gradation of bio-oil into value-added chemicals: a comprehensive review. Sep. Purif. Technol. 283, 120149.
Du, B., Chen, C., Sun, Y., Yu, M., Liu, B., Wang, X., Zhou, J., 2020. Lignin bio-oil-based electrospun nanofibers with high substitution ratio property for potential carbon nanofibers applications. Polym. Test. 89, 106591.
E, S., Jin, C., Liu, J., Yang, L., Yang, M., Xu, E., Wang, K., Sheng, K., Zhang, X., 2022. Engineering functional hydrochar based catalyst with corn stover and model components for efficient glucose isomerization. Energy 249, 123668.
Egerland Bueno, B., Americo Soares, L., Quispe-Arpasi, D., Kimiko Sakamoto, I., Zhang, Y., Amancio Varesche, M.B., Ribeiro, R., Tommaso, G., 2020. Anaerobic digestion of aqueous phase from hydrothermal liquefaction of spirulina using biostimulated sludge. Bioresour. Technol. 312, 123552.
Fabbri, E., Pergolesi, D., Traversa, E., 2010. Materials challenges toward proton-conducting oxide fuel cells: a critical review. Chem. Soc. Rev. 39 (11), 4355–4369.
Fang, C., Thomsen, M.H., Brudecki, G.P., Cybulska, I., Frankaer, C.G., Bastidas-Oyanedel, J.R., Schmidt, J.E., 2015. Seawater as alternative to freshwater in pretreatment of date palm residues for bioethanol production in coastal and/or arid areas. ChemSusChem 8 (22), 3823–3831.
Fang, K., Li, D., Lin, M., Xiang, M., Wei, W., Sun, Y., 2009. A short review of heterogeneous catalytic process for mixed alcohols synthesis via syngas. Catal. Today 147 (2), 133–138.
Farobie, O., Anis, L.A., Fatriasari, W., Karimah, A., Nurcahyani, P.R., Rahman, D.Y., Nafisyah, A.L., Amrullah, A., Aziz, M., 2022. Simultaneous production of nutritional compounds and hydrochar from Chlorella pyrenoidosa via hydrothermal process. Bioresour. Technol. Rep. 20, 101245.
Fasolini, Cucciniello, Paone, Mauriello, Tabanelli, 2019. A short overview on the hydrogen production via aqueous phase reforming (APR) of cellulose, C6-C5 sugars and polyols. Catalysts 9 (11), 917.

Feng, J., Miao, D., Ding, Y., Jiao, F., Pan, X., Bao, X., 2022. Direct synthesis of isoparaffin-rich gasoline from syngas. ACS Energy Lett. 7 (4), 1462–1468.
Fernandez-Naveira, A., Veiga, M.C., Kennes, C., 2019. Selective anaerobic fermentation of syngas into either C2–C6 organic acids or ethanol and higher alcohols. Bioresour. Technol. 280, 387–395.
Fernandez-Sanroman, A., Lama, G., Pazos, M., Rosales, E., Sanroman, M.A., 2021. Bridging the gap to hydrochar production and its application into frameworks of bioenergy, environmental and biocatalysis areas. Bioresour. Technol. 320 (Pt B), 124399.
Fiore, M., Magi, V., Viggiano, A., 2020. Internal combustion engines powered by syngas: a review. Appl. Energy 276, 115415.
Fischer, F., 1925. The Conversion of Coal Into Oils. E. Benn Limited.
Fischer, F., Tropsch, H., 1923. The preparation of synthetic oil mixtures (synthol) from carbon monoxide and hydrogen. Brennstoff-Chem 4, 276–285.
Gai, C., Yang, T., Liu, H., Liu, Z., Jiao, W., 2019a. Hydrochar-supported bimetallic Ni–Cu nanocatalysts for sustainable H2 production. ACS Appl. Nano Mater. 2 (11), 7279–7289.
Gai, C., Zhang, F., Yang, T., Liu, Z., Jiao, W., Peng, N., Liu, T., Lang, Q., Xia, Y., 2018. Hydrochar supported bimetallic Ni–Fe nanocatalysts with tailored composition, size and shape for improved biomass steam reforming performance. Green Chem. 20 (12), 2788–2800.
Gai, C., Zhang, Y., Chen, W.T., Zhou, Y., Schideman, L., Zhang, P., Tommaso, G., Kuo, C.T., Dong, Y., 2015. Characterization of aqueous phase from the hydrothermal liquefaction of Chlorella pyrenoidosa. Bioresour. Technol. 184, 328–335.
Gai, C., Zhu, N., Hoekman, S.K., Liu, Z., Jiao, W., Peng, N., 2019b. Highly dispersed nickel nanoparticles supported on hydrochar for hydrogen-rich syngas production from catalytic reforming of biomass. Energy Convers. Manag. 183, 474–484.
Gao, M., Jiang, Z., Ding, W., Shi, B., 2022. Selective degradation of hemicellulose into oligosaccharides assisted by ZrOCl2 and their potential application as a tanning agent. Green Chem. 24 (1), 375–383.
Gao, Y., Remón, J., Matharu, A.S., 2021. Microwave-assisted hydrothermal treatments for biomass valorisation: a critical review. Green Chem. 23 (10), 3502–3525.
Ge, X., Ge, M., Chen, X., Qian, C., Liu, X., Zhou, S., 2020. Facile synthesis of hydrochar supported copper nanocatalyst for ullmann C N coupling reaction in water. Mol. Catal. 484, 110726.
Georgiou, E., Mihajlovic, M., Petrovic, J., Anastopoulos, I., Dosche, C., Pashalidis, I., Kalderis, D., 2021. Single-stage production of miscanthus hydrochar at low severity conditions and application as adsorbent of copper and ammonium ions. Bioresour. Technol. 337, 125458.
Gnanasekaran, L., Priya, A.K., Thanigaivel, S., Hoang, T.K.A., Soto-Moscoso, M., 2023. The conversion of biomass to fuels via cutting-edge technologies: explorations from natural utilization systems. Fuel 331, 125668.
Goswami, G., Kumar, R., Sinha, A., Birazee, B., Chandra Dutta, B., Bhutani, S., Das, D., 2022. ALGLIQOL: a two stage integrated process towards synthesis of renewable transportation fuel via catalytic hydrothermal liquefaction of lipid enriched microalgae biomass and distillation. Energy Convers. Manag. 263, 115696.
Gu, Y., Zhang, X., Deal, B., Han, L., Zheng, J., Ben, H., 2019. Advances in energy systems for valorization of aqueous byproducts generated from hydrothermal processing of biomass and systems thinking. Green Chem. 21 (10), 2518–2543.
Guan, J., Liu, Y., Jing, F., Ye, R., Chen, J., 2021. Contrasting impacts of chemical and physical ageing on hydrochar properties and sorption of norfloxacin with coexisting Cu(2). Sci. Total Environ. 772, 145502.
Güleç, F., Williams, O., Kostas, E.T., Samson, A., Lester, E., 2022. A comprehensive comparative study on the energy application of chars produced from different biomass feedstocks via hydrothermal conversion, pyrolysis, and torrefaction. Energy Convers. Manag. 270, 116260.
Gunes, B., 2021. A critical review on biofilm-based reactor systems for enhanced syngas fermentation processes. Renew. Sust. Energ. Rev. 143, 110950.
Guo, B., Walter, V., Hornung, U., Dahmen, N., 2019. Hydrothermal liquefaction of Chlorella vulgaris and nannochloropsis gaditana in a continuous stirred tank reactor and hydrotreating of biocrude by nickel catalysts. Fuel Process. Technol. 191, 168–180.
Habibollahzade, A., Rosen, M.A., 2021. Syngas-fueled solid oxide fuel cell functionality improvement through appropriate feedstock selection and multi-criteria optimization using Air/O2-enriched-air gasification agents. Appl. Energy 286, 116497.
Haider, M., Castello, D., Michalski, K., Pedersen, T., Rosendahl, L., 2018. Catalytic hydrotreatment of microalgae biocrude from continuous hydrothermal liquefaction: heteroatom removal and their distribution in distillation cuts. Energies 11 (12), 3360.
Hamidi, R., Tai, L., Paglia, L., Scarsella, M., Damizia, M., De Filippis, P., Musivand, S., de Caprariis, B., 2022. Hydrotreating of oak wood bio-crude using heterogeneous hydrogen producer over Y zeolite catalyst synthesized from rice husk. Energy Convers. Manag. 255, 115348.
Han, L., Cui, X., Liu, Y., Han, G., Wu, X., Xu, C., Li, B., 2020. Nitrogen and phosphorus modification to enhance the catalytic activity of biomass-derived carbon toward the oxygen reduction reaction. Sustainable Energy Fuels 4 (6), 2707–2717.
Hao, D., Wang, X., Liang, S., Yue, O., Liu, X., Hao, D., Dang, X., 2023. Sustainable leather making - an amphoteric organic chrome-free tanning agents based on recycling waste leather. Sci. Total Environ. 867, 161531.
Harisankar, S., Francis Prashanth, P., Nallasivam, J., Vishnu Mohan, R., Vinu, R., 2021. Effects of aqueous phase recirculation on product yields and quality from hydrothermal liquefaction of rice straw. Bioresour. Technol. 342, 125951.
Hasanoğlu, A., Faki, E., Seçer, A., Türker Üzden, Ş., 2023. Co–solvent effects on hydrothermal co–gasification of coal/biomass mixtures for hydrogen production. Fuel 331, 125693.
He, C., Tang, C., Li, C., Yuan, J., Tran, K.-Q., Bach, Q.-V., Qiu, R., Yang, Y., 2018a. Wet torrefaction of biomass for high quality solid fuel production: a review. Renew. Sust. Energ. Rev. 91, 259–271.
He, X., Zhang, T., Xue, Q., Zhou, Y., Wang, H., Bolan, N.S., Jiang, R., Tsang, D.C.W., 2021. Enhanced adsorption of Cu(II) and Zn(II) from aqueous solution by polyethyleneimine modified straw hydrochar. Sci. Total Environ. 778, 146116.
He, Y., Lens, P.N.L., Veiga, M.C., Kennes, C., 2022. Selective butanol production from carbon monoxide by an enriched anaerobic culture. Sci. Total Environ. 806 (Pt 2), 150579.
He, Y., Li, X., Xue, X., Swita, M.S., Schmidt, A.J., Yang, B., 2017. Biological conversion of the aqueous wastes from hydrothermal liquefaction of algae and pine wood by rhodococci. Bioresour. Technol. 224, 457–464.
He, Z., Xu, D., Wang, S., Zhang, H., Jing, Z., 2018b. Catalytic upgrading of water-soluble biocrude from hydrothermal liquefaction of chlorella. Energy Fuel 32 (2), 1893–1899.
Heidenreich, S., 2013. Hot gas filtration – a review. Fuel 104, 83–94.
Hien Tran, T., Le, A.H., Pham, T.H., Duong, D., Nguyen, X.C., Nadda, A.K., Chang, S.W., Chung, W.J., Nguyen, D.D., Nguyen, D.T., 2022. A sustainable, low-cost carbonaceous hydrochar adsorbent for methylene blue adsorption derived from corncobs. Environ. Res. 212 (Pt B), 113178.
Hong, C., Wang, Z., Si, Y., Li, Z., Xing, Y., Hu, J., Li, Y., 2021. Effects of aqueous phase circulation and catalysts on hydrothermal liquefaction (HTL) of penicillin residue (PR): characteristics of the aqueous phase, solid residue and bio oil. Sci. Total Environ. 776, 145596.
Hu, X., Gholizadeh, M., 2020. Progress of the applications of bio-oil. Renew. Sust. Energ. Rev. 134, 110124.
Hu, Y., Qi, L., Tirumala Venkateswara Rao, K., Zhao, B., Li, H., Zeng, Y., Xu, C., 2020. Supercritical water gasification of biocrude oil from low-temperature liquefaction of algal lipid extraction residue. Fuel 276, 118017.
Huang, C., Zhu, C., Zhang, M., Chen, J., Fang, K., 2022. Design of efficient ZnO/ZrO2 modified CuCoAl catalysts for boosting higher alcohol synthesis in syngas conversion. Appl. Catal. B Environ. 300, 120739.
Huang, H., Niu, Z., Shi, R., Tang, J., Lv, L., Wang, J., Fan, Y., 2020. Thermal oxidation activation of hydrochar for tetracycline adsorption: the role of oxygen concentration and temperature. Bioresour. Technol. 306, 123096.
Ighalo, J.O., Rangabhashiyam, S., Dulta, K., Umeh, C.T., Iwuozor, K.O., Aniagor, C.O., Eshiemogie, S.O., Iwuchukwu, F.U., Igwegbe, C.A., 2022. Recent advances in hydrochar application for the adsorptive removal of wastewater pollutants. Chem. Eng. Res. Des. 184, 419–456.
Islam, M.T., Chambers, C., Toufiq Reza, M., 2022. Effects of process liquid recirculation on material properties of hydrochar and corresponding adsorption of cationic dye. J. Anal. Appl. Pyrolysis 161, 105418.
Jabeen, S., Gao, X., Hayashi, J.-I., Altarawneh, M., Dlugogorski, B.Z., 2022. Systematic characterization of biocrude and aqueous phase from hydrothermal carbonization of algal biomass. J. Environ. Chem. Eng. 10 (3), 107953.
Jafari, B., Seddiq, M., Mirsalim, S.M., 2021. Impacts of diesel injection timing and syngas fuel composition in a heavy-duty RCCI engine. Energy Convers. Manag. 247, 114759.
Jahromi, H., Rahman, T., Roy, P., Adhikari, S., 2022. Hydrotreatment of solvent-extracted biocrude from hydrothermal liquefaction of municipal sewage sludge. Energy Convers. Manag. 263, 115719.
Jamsran, N., Park, H., Lee, J., Oh, S., Kim, C., Lee, Y., Kang, K., 2021. Influence of syngas composition on combustion and emissions in a homogeneous charge compression ignition engine. Fuel 306, 121774.
Jarvis, J.M., Albrecht, K.O., Billing, J.M., Schmidt, A.J., Hallen, R.T., Schaub, T.M., 2018. Assessment of hydrotreatment for hydrothermal liquefaction biocrudes from sewage sludge, microalgae, and pine feedstocks. Energy Fuel 32 (8), 8483–8493.
Jaworek, A., Sobczyk, A.T., Krupa, A., Marchewicz, A., Czech, T., Śliwiński, L., 2019. Hybrid electrostatic filtration systems for fly ash particles emission control. A review. Sep. Purif. Technol. 213, 283–302.
Jayaraman, R.S., Gopinath, K.P., Arun, J., Malolan, R., Adithya, S., Ajay, P.S., Sivaramakrishnan, R., Pugazhendhi, A., 2021. Co-hydrothermal gasification of microbial sludge and algae kappaphycus alvarezii for bio-hydrogen production: study on aqueous phase reforming. Int. J. Hydrog. Energy 46 (31), 16555–16564.
Jeong, G.-T., Kim, S.-K., 2021. Hydrothermal conversion of microalgae chlorella sp. Into 5-hydroxymethylfurfural and levulinic acid by metal sulfate catalyst. Biomass Bioenergy 148, 106053.
Jiang, Z., Ding, W., Xu, S., Remón, J., Shi, B., Hu, C., Clark, J.H., 2020. A 'Trojan horse strategy' for the development of a renewable leather tanning agent produced via an AlCl3-catalyzed cellulose depolymerization. Green Chem. 22 (2), 316–321.
Jiang, Z., Gao, M., Ding, W., Huang, C., Hu, C., Shi, B., Tsang, D.C.W., 2021a. Selective degradation and oxidation of hemicellulose in corncob to oligosaccharides: from biomass into masking agent for sustainable leather tanning. J. Hazard. Mater. 413, 125425.
Jiang, Z., Xu, S., Ding, W., Gao, M., Fan, J., Hu, C., Shi, B., Clark, J.H., 2021b. Advanced masking agent for leather tanning from stepwise degradation and oxidation of cellulose. Green Chem. 23 (11), 4044–4050.
Jiang, Z., Zhao, P., Li, J., Liu, X., Hu, C., 2018. Effect of tetrahydrofuran on the solubilization and depolymerization of cellulose in a biphasic system. ChemSusChem 11 (2), 397–405.
Jin, X., Ku, A., Ohara, B., Huang, K., Singh, S., 2021. Performance analysis of a 550MWe solid oxide fuel cell and air turbine hybrid system powered by coal-derived syngas. Energy 222, 119917.
Jing, Y., Guo, Y., Xia, Q., Liu, X., Wang, Y., 2019. Catalytic production of value-added chemicals and liquid fuels from lignocellulosic biomass. Chem 5 (10), 2520–2546.
Jones, S.B., Zhu, Y., Anderson, D.B., Hallen, R.T., Elliott, D.C., Schmidt, A.J., Albrecht, K.O., Hart, T.R., Butcher, M.G., Drennan, C., 2014. Process Design and Economics for the Conversion of Algal Biomass to Hydrocarbons: Whole Algae Hydrothermal Liquefaction and Upgrading. Pacific Northwest National Lab.(PNNL), Richland, WA (United States).
Kang, J., He, S., Zhou, W., Shen, Z., Li, Y., Chen, M., Zhang, Q., Wang, Y., 2020. Single-pass transformation of syngas into ethanol with high selectivity by triple tandem catalysis. Nat. Commun. 11 (1), 827.
Karthikeyan, S., Periyasamy, M., Mahendran, G., 2020. Assessment of engine performance using syngas. Mater. Today: Proc. 33, 4142–4144.
Kim, Y., Kim, M., Jeong, H., Kim, Y., Choi, S.H., Ham, H.C., Lee, S.W., Kim, J.Y., Song, K.H., Yoon, C.W., Jo, Y.S., Sohn, H., 2020. High purity hydrogen production via aqueous phase reforming of xylose over small pt nanoparticles on a γ-Al2O3 support. Int. J. Hydrog. Energy 45 (27), 13848–13861.

Kohansal, K., Sharma, K., Haider, M.S., Toor, S.S., Castello, D., Rosendahl, L.A., Zimmermann, J., Pedersen, T.H., 2022. Hydrotreating of bio-crude obtained from hydrothermal liquefaction of biopulp: effects of aqueous phase recirculation on the hydrotreated oil. Sustainable Energy Fuels 6 (11), 2805–2822.

Kohansal, K., Toor, S., Sharma, K., Chand, R., Rosendahl, L., Pedersen, T.H., 2021. Hydrothermal liquefaction of pre-treated municipal solid waste (biopulp) with recirculation of concentrated aqueous phase. Biomass Bioenergy 148, 106032.

Kumar, M., Olajire Oyedun, A., Kumar, A., 2018. A review on the current status of various hydrothermal technologies on biomass feedstock. Renew. Sust. Energ. Rev. 81, 1742–1770.

Kumar, S., R, M.D., M, A.V., Ramanathan, A., 2021. Bio-Ethanol production from syngas-derived biomass: a review. Mater. Today: Proc. 46, 9989–9993.

Lang, L., Zhu, H.-Y., Ding, Y.-N., Yin, X.-L., Wu, C.-Z., Yu, X., Bridgwater, A.V., 2021. Mini-review on hot gas filtration in biomass gasification: focusing on ceramic filter candles. Energy Fuel 35 (15), 11800–11819.

Lang, Q., Guo, Y., Zheng, Q., Liu, Z., Gai, C., 2018. Co-hydrothermal carbonization of lignocellulosic biomass and swine manure: hydrochar properties and heavy metal transformation behavior. Bioresour. Technol. 266, 242–248.

Lee, J., Hong, J., Jang, D., Park, K.Y., 2019. Hydrothermal carbonization of waste from leather processing and feasibility of produced hydrochar as an alternative solid fuel. J. Environ. Manag. 247, 115–120.

Leng, L., Yang, L., Chen, J., Hu, Y., Li, H., Li, H., Jiang, S., Peng, H., Yuan, X., Huang, H., 2021a. Valorization of the aqueous phase produced from wet and dry thermochemical processing biomass: a review. J. Clean. Prod. 294, 126238.

Leng, L., Yang, L., Leng, S., Zhang, W., Zhou, Y., Peng, H., Li, H., Hu, Y., Jiang, S., Li, H., 2021b. A review on nitrogen transformation in hydrochar during hydrothermal carbonization of biomass containing nitrogen. Sci. Total Environ. 756, 143679.

Leng, S., Leng, L., Chen, L., Chen, J., Chen, J., Zhou, W., 2020. The effect of aqueous phase recirculation on hydrothermal liquefaction/carbonization of biomass: a review. Bioresour. Technol. 318, 124081.

Li, B., Guo, J.Z., Liu, J.L., Fang, L., Lv, J.Q., Lv, K., 2020a. Removal of aqueous-phase lead ions by dithiocarbamate-modified hydrochar. Sci. Total Environ. 714, 136897.

Li, D., Cui, H., Cheng, Y., Xue, L., Wang, B., He, H., Hua, Y., Chu, Q., Feng, Y., Yang, L., 2021. Chemical aging of hydrochar improves the Cd(2+) adsorption capacity from aqueous solution. Environ. Pollut. 287, 117562.

Li, N., Jiao, F., Pan, X., Chen, Y., Feng, J., Li, G., Bao, X., 2019. High-quality gasoline directly from syngas by dual metal oxide-zeolite (OX-ZEO) catalysis. Angew. Chem. Int. Ed. 58 (22), 7400–7404.

Li, N., Jiao, F., Pan, X., Ding, Y., Feng, J., Bao, X., 2018. Size effects of ZnO nanoparticles in bifunctional catalysts for selective syngas conversion. ACS Catal. 9 (2), 960–966.

Li, T., Remón, J., Shuttleworth, P.S., Jiang, Z., Fan, J., Clark, J.H., Budarin, V.L., 2017a. Controllable production of liquid and solid biofuels by doping-free, microwave-assisted, pressurised pyrolysis of hemicellulose. Energy Convers. Manag. 144, 104–113.

Li, X., Henson, M.A., 2019. Metabolic modeling of bacterial co-culture systems predicts enhanced carbon monoxide-to-butyrate conversion compared to monoculture systems. Biochem. Eng. J. 151, 107338.

Li, Y., Gao, W., Peng, M., Zhang, J., Sun, J., Xu, Y., Hong, S., Liu, X., Liu, X., Wei, M., Zhang, B., Ma, D., 2020b. Interfacial Fe5C2-cu catalysts toward low-pressure syngas conversion to long-chain alcohols. Nat. Commun. 11 (1), 61.

Li, Y., Leow, S., Fedders, A.C., Sharma, B.K., Guest, J.S., Strathmann, T.J., 2017b. Quantitative multiphase model for hydrothermal liquefaction of algal biomass. Green Chem. 19 (4), 1163–1174.

Li, Z., Huang, Y., Chi, X., Li, D., Zhong, L., Li, X., Liu, C., Peng, X., 2022. Biomass-based N doped carbon as metal-free catalyst for selective oxidation of d-xylose into d-xylonic acid. Green Energy Environ. 7 (6), 1310–1317.

Liao, G., Liu, L., E, J., Zhang, F., Chen, J., Deng, Y., Zhu, H., 2019. Effects of technical progress on performance and application of supercritical carbon dioxide power cycle: a review. Energy Convers. Manag. 199, 111986.

Lin, C., Zhao, P., Ding, Y., Cui, X., Liu, F., Wang, C., Guo, Q., 2021. Hydrogen-rich gas production from hydrochar derived from hydrothermal carbonization of PVC and alkali coal. Fuel Process. Technol. 222, 106959.

Lin, H., Zhang, L., Zhang, S., Li, Q., Hu, X., 2022. Hydrothermal carbonization of cellulose in aqueous phase of bio-oil: the significant impacts on properties of hydrochar. Fuel 315, 123132.

Lin, T., Qi, X., Wang, X., Xia, L., Wang, C., Yu, F., Wang, H., Li, S., Zhong, L., Sun, Y., 2019. Direct production of higher oxygenates by syngas conversion over a multifunctional catalyst. Angew. Chem. Int. Ed. 58 (14), 4627–4631.

Liu, B., Rajagopal, D., 2019. Life-cycle energy and climate benefits of energy recovery from wastes and biomass residues in the United States. Nat. Energy 4 (8), 700–708.

Liu, C., Luo, G., Wang, W., He, Y., Zhang, R., Liu, G., 2018a. The effects of pH and temperature on the acetate production and microbial community compositions by syngas fermentation. Fuel 224, 537–544.

Liu, G., Du, H., Sailikebuli, X., Meng, Y., Liu, Y., Wang, H., Zhang, J., Wang, B., Saad, M.G., Li, J., Wang, W., 2021a. Evaluation of storage stability for biocrude derived from hydrothermal liquefaction of microalgae. Energy Fuel 35 (13), 10623–10629.

Liu, H., Tang, X., Hao, W., Zeng, X., Sun, Y., Lei, T., Lin, L., 2018b. One-pot tandem conversion of fructose into biofuel components with in-situ generated catalyst system. J. Energy Chem. 27 (2), 375–380.

Liu, J., Yang, L., Shuang, E., Jin, C., Gong, C., Sheng, K., Zhang, X., 2022a. Facile one-pot synthesis of functional hydrochar catalyst for biomass valorization. Fuel 315, 123172.

Liu, J., Zhang, S., Jin, C., E, S., Sheng, K., Zhang, X., 2019. Effect of swelling pretreatment on properties of cellulose-based hydrochar. ACS Sustain. Chem. Eng. 7 (12), 10821–10829.

Liu, J., Zhang, X., Yang, L., Danhassan, U.A., Zhang, S., Yang, M., Sheng, K., Zhang, X., 2021b. Glucose isomerization catalyzed by swollen cellulose derived aluminum-hydrochar. Sci. Total Environ. 777, 146037.

Liu, X., Guo, Y., Dasgupta, A., He, H., Xu, D., Guan, Q., 2022b. Algal bio-oil refinery: a review of heterogeneously catalyzed denitrogenation and demetallization reactions for renewable process. Renew. Energy 183, 627–650.

Long, C., Li, X., Guo, J., Shi, Y., Liu, S., Tang, Z., 2018. Electrochemical reduction of CO_2 over heterogeneous catalysts in aqueous solution: recent progress and perspectives. Small Methods 3, 1–20.

López Barreiro, D., Bauer, M., Hornung, U., Posten, C., Kruse, A., Prins, W., 2015. Cultivation of microalgae with recovered nutrients after hydrothermal liquefaction. Algal Res. 9, 99–106.

López, J.C., Arnáiz, E., Merchán, L., Lebrero, R., Muñoz, R., 2018. Biogas-based polyhydroxyalkanoates production by methylocystis hirsuta: a step further in anaerobic digestion biorefineries. Chem. Eng. J. 333, 529–536.

Luo, G., Jing, Y., Lin, Y., Zhang, S., An, D., 2018a. A novel concept for syngas biomethanation by two-stage process: focusing on the selective conversion of syngas to acetate. Sci. Total Environ. 645, 1194–1200.

Luo, Y., Li, D., Li, R., Li, Z., Hu, C., Liu, X., 2020. Roles of water and aluminum sulfate for selective dissolution and utilization of hemicellulose to develop sustainable corn Stover-based biorefinery. Renew. Sust. Energ. Rev. 122, 109724.

Luo, Y., Li, Z., Li, X., Liu, X., Fan, J., Clark, J.H., Hu, C., 2019. The production of furfural directly from hemicellulose in lignocellulosic biomass: a review. Catal. Today 319, 14–24.

Luo, Y., Li, Z., Zuo, Y., Su, Z., Hu, C., 2018b. Effects of gamma-Valerolactone/H2O solvent on the degradation of pubescens for its fullest utilization. J. Agric. Food Chem. 66 (24), 6094–6103.

Lv, B.W., Xu, H., Guo, J.Z., Bai, L.Q., Li, B., 2022. Efficient adsorption of methylene blue on carboxylate-rich hydrochar prepared by one-step hydrothermal carbonization of bamboo and acrylic acid with ammonium persulphate. J. Hazard. Mater. 421, 126741.

Lv, S., Yuan, J., Peng, X., Borges Cabrera, M., Guo, S., Luo, X., Gao, J., 2020. Performance and optimization of bio-oil/Buton rock asphalt composite modified asphalt. Constr. Build. Mater. 264.

Lyu, X., Li, H., Xiang, H., Mu, Y., Ji, N., Lu, X., Fan, X., Gao, X., 2022. Energy efficient production of 5-hydroxymethylfurfural (5-HMF) over surface functionalized carbon superstructures under microwave irradiation. Chem. Eng. J. 428, 131143.

Ma, J., Li, Y., Jin, D., Yang, X., Jiao, G., Liu, K., Sun, S., Zhou, J., Sun, R., 2021a. Reasonable regulation of carbon/nitride ratio in carbon nitride for efficient photocatalytic reforming of biomass-derived feedstocks to lactic acid. Appl. Catal. B Environ. 299, 120698.

Ma, R., Fakudze, S., Shang, Q., Wei, Y., Chen, J., Liu, C., Han, J., Chu, Q., 2021b. Catalytic hydrothermal carbonization of pomelo peel for enhanced combustibility of coal/hydrochar blends and reduced CO2 emission. Fuel 304, 121422.

Maddi, B., Panisko, E., Wietsma, T., Lemmon, T., Swita, M., Albrecht, K., Howe, D., 2017. Quantitative characterization of aqueous byproducts from hydrothermal liquefaction of municipal wastes, food industry wastes, and biomass grown on waste. ACS Sustain. Chem. Eng. 5 (3), 2205–2214.

Maddi, B., Panisko, E., Wietsma, T., Lemmon, T., Swita, M., Albrecht, K., Howe, D., 2016. Quantitative characterization of the aqueous fraction from hydrothermal liquefaction of algae. Biomass Bioenergy 93, 122–130.

Madduluri, V.R., Mandari, K.K., Velpula, V., Varkolu, M., Kamaraju, S.R.R., Kang, M., 2020. Rice husk-derived carbon-silica supported ni catalysts for selective hydrogenation of biomass-derived furfural and levulinic acid. Fuel 261, 116339.

Madsen, R.B., Biller, P., Jensen, M.M., Becker, J., Iversen, B.B., Glasius, M., 2016. Predicting the chemical composition of aqueous phase from hydrothermal liquefaction of model compounds and biomasses. Energy Fuel 30 (12), 10470–10483.

Malool, M.E., Keshavarz Moraveji, M., Shayegan, J., 2021. Optimized production, Pb(II) adsorption and characterization of alkali modified hydrochar from sugarcane bagasse. Sci. Rep. 11 (1), 22328.

Manjare, S.D., Dhingra, K., 2019. Supercritical fluids in separation and purification: a review. Mater. Sci. Energy Technol. 2 (3), 463–484.

Mankar, A.R., Pandey, A., Modak, A., Pant, K.K., 2021. Pretreatment of lignocellulosic biomass: a review on recent advances. Bioresour. Technol. 334, 125235.

Marangon, B.B., Castro, J.S., Assemany, P.P., Couto, E.A., Calijuri, M.L., 2022. Environmental performance of microalgae hydrothermal liquefaction: life cycle assessment and improvement insights for a sustainable renewable diesel. Renew. Sust. Energ. Rev. 155, 111910.

Marrakchi, F., Sohail Toor, S., Haaning Nielsen, A., Helmer Pedersen, T., Aistrup Rosendahl, L., 2023. Bio-crude oils production from wheat stem under subcritical water conditions and batch adsorption of post-hydrothermal liquefaction aqueous phase onto activated hydrochars. Chem. Eng. J. 452, 139293.

Masoumi, S., Dalai, A.K., 2021a. NiMo carbide supported on algal derived activated carbon for hydrodeoxygenation of algal biocrude oil. Energy Convers. Manag. 231, 113834.

Masoumi, S., Dalai, A.K., 2021b. Techno-economic and life cycle analysis of biofuel production via hydrothermal liquefaction of microalgae in a methanol-water system and catalytic hydrotreatment using hydrochar as a catalyst support. Biomass Bioenergy 151, 106168.

Matayeva, A., Biller, P., 2021. Hydrothermal liquefaction aqueous phase treatment and hydrogen production using electro-oxidation. Energy Convers. Manag. 244, 114462.

Miao, D., Ding, Y., Yu, T., Li, J., Pan, X., Bao, X., 2020. Selective synthesis of benzene, toluene, and xylenes from syngas. ACS Catal. 10 (13), 7389–7397.

Mondal, P., Dang, G.S., Garg, M.O., 2011. Syngas production through gasification and cleanup for downstream applications — recent developments. Fuel Process. Technol. 92 (8), 1395–1410.

Monir, M.U., Aziz, A.A., Khatun, F., Yousuf, A., 2020. Bioethanol production through syngas fermentation in a tar free bioreactor using clostridium butyricum. Renew. Energy 157, 1116–1123.

Monteiro, C.R.M., Avila, P.F., Pereira, M.A.F., Pereira, G.N., Bordignon, S.E., Zanella, E., Stambuk, B.U., de Oliveira, D., Goldbeck, R., Poletto, P., 2021. Hydrothermal treatment on depolymerization of hemicellulose of mango seed shell for the production of xylooligosaccharides. Carbohydr. Polym. 253, 117274.

Montesantos, N., Pedersen, T.H., Nielsen, R.P., Rosendahl, L., Maschietti, M., 2019. Supercritical carbon dioxide fractionation of bio-crude produced by hydrothermal liquefaction of pinewood. J. Supercrit. Fluids 149, 97–109.
Motagamwala, A.H., Won, W., Sener, C., Alonso, D.M., Maravelias, C.T., Dumesic, J.A., 2018. Toward biomass-derived renewable plastics: production of 2,5-furandicarboxylic acid from fructose. Sci. Adv. 4 (1), eaap9722.
Musci, J.J., Montaña, M., Rodríguez-Castellón, E., Lick, I.D., Casella, M.L., 2020. Selective aqueous-phase hydrogenation of glucose and xylose over ruthenium-based catalysts: influence of the support. Mol. Catal. 495, 111150.
Nagappan, S., Bhosale, R.R., Nguyen, D.D., Chi, N.T.L., Ponnusamy, V.K., Woong, C.S., Kumar, G., 2021. Catalytic hydrothermal liquefaction of biomass into bio-oils and other value-added products – a review. Fuel 285, 119053.
Nanda, S., Okolie, J.A., Patel, R., Pattnaik, F., Fang, Z., Dalai, A.K., Kozinski, J.A., Naik, S., 2022. Catalytic hydrothermal co-gasification of canola meal and low-density polyethylene using mixed metal oxides for hydrogen production. Int. J. Hydrog. Energy 42084–42098.
Nguyen, S.T., Le, T.M., Nguyen, H.V., 2021. Iron-catalyzed fast hydrothermal liquefaction of Cladophora socialis macroalgae into high quality fuel precursor. Bioresour. Technol. 337, 125445.
Ni, Y., Liu, Y., Chen, Z., Yang, M., Liu, H., He, Y., Fu, Y., Zhu, W., Liu, Z., 2018. Realizing and recognizing syngas-to-olefins reaction via a dual-bed catalyst. ACS Catal. 9 (2), 1026–1032.
Nie, S.Q., Chen, M.Q., Li, Q.H., 2022. Evaluation on hydrothermal gasification of waste tires based on chemical equilibrium analysis. Int. J. Hydrog. Energy 47 (3), 1435–1448.
Oasmaa, A., Sundqvist, T., Kuoppala, E., Garcia-Perez, M., Solantausta, Y., Lindfors, C., Paasikallio, V., 2015. Controlling the phase stability of biomass fast pyrolysis bio-oils. Energy Fuel 29 (7), 4373–4381.
Obeid, F., Van, T.C., Horchler, E.J., Guo, Y., Verma, P., Miljevic, B., Brown, R.J., Ristovski, Z., Bodisco, T.A., Rainey, T., 2020. Engine performance and emissions of high nitrogen-containing fuels. Fuel 264, 116805.
Okolie, J.A., Mukherjee, A., Nanda, S., Dalai, A.K., Kozinski, J.A., 2021. Catalytic supercritical water gasification of soybean straw: effects of catalyst supports and promoters. Ind. Eng. Chem. Res. 60 (16), 5770–5782.
Okolie, J.A., Nanda, S., Dalai, A.K., Berruti, F., Kozinski, J.A., 2020a. A review on subcritical and supercritical water gasification of biogenic, polymeric and petroleum wastes to hydrogen-rich synthesis gas. Renew. Sust. Energ. Rev. 119, 109546.
Okolie, J.A., Nanda, S., Dalai, A.K., Kozinski, J.A., 2020b. Hydrothermal gasification of soybean straw and flax straw for hydrogen-rich syngas production: experimental and thermodynamic modeling. Energy Convers. Manag. 208, 112545.
Oliveira, A.S., Aho, A., Baeza, J.A., Calvo, L., Simakova, I.L., Gilarranz, M.A., Murzin, D.Y., 2021. Enhanced H2 production in the aqueous-phase reforming of maltose by feedstock pre-hydrogenation. Appl. Catal. B Environ. 281, 119469.
Oliveira, A.S., Baeza, J.A., Saenz de Miera, B., Calvo, L., Rodriguez, J.J., Gilarranz, M.A., 2020. Aqueous phase reforming coupled to catalytic wet air oxidation for the removal and valorisation of phenolic compounds in wastewater. J. Environ. Manag. 274, 111199.
Onwudili, J.A., Lea-Langton, A.R., Ross, A.B., Williams, P.T., 2013. Catalytic hydrothermal gasification of algae for hydrogen production: composition of reaction products and potential for nutrient recycling. Bioresour. Technol. 127, 72–80.
Opia, A.C., Hamid, M.K.B.A., Syahrullail, S., Rahim, A.B.A., Johnson, C.A.N., 2021. Biomass as a potential source of sustainable fuel, chemical and tribological materials – overview. Mater. Today: Proc. 39, 922–928.
Ou, H., Ning, S., Zhu, P., Chen, S., Han, A., Kang, Q., Hu, Z., Ye, J., Wang, D., Li, Y., 2022. Carbon nitride photocatalysts with integrated oxidation and reduction atomic active centers for improved CO2 conversion. Angew. Chem. Int. Ed. 61 (34), e202206579.
Ozsel, B.K., Ozturk, D., Nis, B., 2019. One-pot hydrothermal conversion of different residues to value-added chemicals using new acidic carbonaceous catalyst. Bioresour. Technol. 289, 121627.
Paida, V.R., Kersten, S.R.A., van der Ham, A.G.J., Brilman, D.W.F., 2019. A two-step approach to the hydrothermal gasification of carbohydrate-rich wastes: process design and economic evaluation. Int. J. Hydrog. Energy 44 (47), 25524–25541.
Park, H., Lee, J., Jamsran, N., Oh, S., Kim, C., Lee, Y., Kang, K., 2021. Comparative assessment of stoichiometric and lean combustion modes in boosted spark-ignition engine fueled with syngas. Energy Convers. Manag. 239, 114224.
Parra-Marfil, A., Ocampo-Perez, R., Collins-Martinez, V.H., Flores-Velez, L.M., Gonzalez-Garcia, R., Medellin-Castillo, N.A., Labrada-Delgado, G.J., 2020. Synthesis and characterization of hydrochar from industrial Capsicum annuum seeds and its application for the adsorptive removal of methylene blue from water. Environ. Res. 184, 109334.
Pauletto, P.S., Moreno-Perez, J., Hernandez-Hernandez, L.E., Bonilla-Petriciolet, A., Dotto, G.L., Salau, N.P.G., 2021. Novel biochar and hydrochar for the adsorption of 2-nitrophenol from aqueous solutions: an approach using the PVSDM model. Chemosphere 269, 128748.
Peng, X., Ma, X., Lin, Y., Wang, J., Wei, X., Chen, X., 2017. Combustion performance of biocrude oil from solvolysis liquefaction of Chlorella pyrenoidosa by thermogravimetry-fourier transform infrared spectroscopy. Bioresour. Technol. 238, 510–518.
Perez, R.F., Borges, L.E.P., Fraga, M.A., 2021. Catalytic upgrading of xylose to furfuryl alcohol over zr-SBA-15. Ind. Eng. Chem. Res. 60 (51), 18739–18749.
Pinheiro Pires, A.P., Arauzo, J., Fonts, I., Domine, M.E., Fernández Arroyo, A., Garcia-Perez, M.E., Montoya, J., Chejne, F., Pfromm, P., Garcia-Perez, M., 2019. Challenges and opportunities for bio-oil refining: a review. Energy Fuel 33 (6), 4683–4720.
Pipitone, G., Tosches, D., Bensaid, S., Galia, A., Pirone, R., 2018. Valorization of alginate for the production of hydrogen via catalytic aqueous phase reforming. Catal. Today 304, 153–164.
Pipitone, G., Zoppi, G., Bocchini, S., Rizzo, A.M., Chiaramonti, D., Pirone, R., Bensaid, S., 2020. Aqueous phase reforming of the residual waters derived from lignin-rich hydrothermal liquefaction: investigation of representative organic compounds and actual biorefinery streams. Catal. Today 345, 237–250.
Pongsiriyakul, K., Kiatkittipong, W., Adhikari, S., Lim, J.W., Lam, S.S., Kiatkittipong, K., Dankeaw, A., Reubroycharoen, P., Laosiripojana, N., Faungnawakij, K., Assabumrungrat, S., 2021. Effective Cu/Re promoted ni-supported γ-Al2O3 catalyst for upgrading algae biocrude oil produced by hydrothermal liquefaction. Fuel Process. Technol. 216, 106670.
Qu, L., Jiang, X., Zhang, Z., Zhang, X.-G., Song, G.-Y., Wang, H.-L., Yuan, Y.-P., Chang, Y.-L., 2021. A review of hydrodeoxygenation of bio-oil: model compounds, catalysts, and equipment. Green Chem. 23 (23), 9348–9376.
Radenahmad, N., Azad, A.T., Saghir, M., Taweekun, J., Bakar, M.S.A., Reza, M.S., Azad, A.K., 2020. A review on biomass derived syngas for SOFC based combined heat and power application. Renew. Sust. Energ. Rev. 119, 109560.
Rahimi, K., Riahi, S., Abbasi, M., Fakhroueian, Z., 2019. Modification of multi-walled carbon nanotubes by 1,3-diaminopropane to increase CO(2) adsorption capacity. J. Environ. Manag. 242, 81–89.
Ramachandra, T.V., Hebbale, D., 2020. Bioethanol from macroalgae: prospects and challenges. Renew. Sust. Energ. Rev. 117, 109479.
Rathsack, P., Wollmerstaedt, H., Kuchling, T., Kureti, S., 2019. Analysis of hydrogenation products of biocrude obtained from hydrothermally liquefied algal biomass by comprehensive gas chromatography mass spectrometry (GC×GC-MS). Fuel 248, 178–188.
Rehman, A., Nazir, G., Rhee, K.Y., Park, S.J., 2022. Valorization of orange peel waste to tunable heteroatom-doped hydrochar-derived microporous carbons for selective CO(2) adsorption and separation. Sci. Total Environ. 849, 157805.
Remón, J., Danby, S.H., Clark, J.H., Matharu, A.S., 2020. A new step forward nonseasonal 5G biorefineries: microwave-assisted, synergistic, co-depolymerization of wheat straw (2G Biomass) and Laminaria saccharina (3G Biomass). ACS Sustain. Chem. Eng. 8 (33), 12493–12510.
Remón, J., García, L., Arauzo, J., 2016a. Cheese whey management by catalytic steam reforming and aqueous phase reforming. Fuel Process. Technol. 154, 66–81.
Remón, J., Latorre-Viu, J., Matharu, A.S., Pinilla, J.L., Suelves, I., 2021a. Analysis and optimisation of a novel 'almond-refinery' concept: simultaneous production of biofuels and value-added chemicals by hydrothermal treatment of almond hulls. Sci. Total Environ. 765, 142671.
Remón, J., Matharu, A.S., Clark, J.H., 2018. Simultaneous production of lignin and polysaccharide rich aqueous solutions by microwave-assisted hydrothermal treatment of rapeseed meal. Energy Convers. Manag. 165, 634–648.
Remón, J., Ravaglio-Pasquini, F., Pedraza-Segura, L., Arcelus-Arrillaga, P., Suelves, I., Pinilla, J.L., 2021b. Caffeinating the biofuels market: effect of the processing conditions during the production of biofuels and high-value chemicals by hydrothermal treatment of residual coffee pulp. J. Clean. Prod. 302, 127008.
Remón, J., Ruiz, J., Oliva, M., García, L., Arauzo, J., 2016b. Cheese whey valorisation: production of valuable gaseous and liquid chemicals from lactose by aqueous phase reforming. Energy Convers. Manag. 124, 453–469.
Remón, J., Zapata, G., Oriol, L., Pinilla, J.L., Suelves, I., 2022. A novel 'sea-thermal', synergistic co-valorisation approach for biofuels production from unavoidable food waste (almond hulls) and plastic residues (disposable face masks). Chem. Eng. J. 449, 137810.
Roy, P., Dutta, A., Gallant, J., 2020. Evaluation of the life cycle of hydrothermally carbonized biomass for energy and horticulture application. Renew. Sust. Energ. Rev. 132, 110046.
Sahena, F., Zaidul, I.S.M., Jinap, S., Karim, A.A., Abbas, K.A., Norulaini, N.A.N., Omar, A.K.M., 2009. Application of supercritical CO2 in lipid extraction – a review. J. Food Eng. 95 (2), 240–253.
Saleem, F., Harris, J., Zhang, K., Harvey, A., 2020. Non-thermal plasma as a promising route for the removal of tar from the product gas of biomass gasification – a critical review. Chem. Eng. J. 382, 122761.
Samiee-Zafarghandi, R., Karimi-Sabet, J., Abdoli, M.A., Karbassi, A., 2018. Increasing microalgal carbohydrate content for hydrothermal gasification purposes. Renew. Energy 116, 710–719.
Santos, R.G.D., Alencar, A.C., 2020. Biomass-derived syngas production via gasification process and its catalytic conversion into fuels by Fischer Tropsch synthesis: a review. Int. J. Hydrog. Energy 45 (36), 18114–18132.
Saquic, B.E.B., Irmak, S., Wilkins, M., 2022. Enhancement of catalytic performance of graphene supported pt catalysts by ni and W for hydrogen gas production by hydrothermal gasification of biomass-derived compounds. Fuel 308, 122079.
Sarker, T.R., Pattnaik, F., Nanda, S., Dalai, A.K., Meda, V., Naik, S., 2021. Hydrothermal pretreatment technologies for lignocellulosic biomass: a review of steam explosion and subcritical water hydrolysis. Chemosphere 284, 131372.
Scarsella, M., de Caprariis, B., Damizia, M., De Filippis, P., 2020. Heterogeneous catalysts for hydrothermal liquefaction of lignocellulosic biomass: a review. Biomass Bioenergy 140, 105662.
Semieniuk, G., Holden, P.B., Mercure, J.-F., Salas, P., Pollitt, H., Jobson, K., Vercoulen, P., Chewpreecha, U., Edwards, N.R., Viñuales, J.E., 2022. Stranded fossil-fuel assets translate to major losses for investors in advanced economies. Nat. Clim. Chang. 12 (6), 532–538.
Sevilla, M., Ferrero, G.A., Fuertes, A.B., 2017. Beyond KOH activation for the synthesis of superactivated carbons from hydrochar. Carbon 114, 50–58.
Shahabuddin, M., Alam, M.T., Krishna, B.B., Bhaskar, T., Perkins, G., 2020. A review on the production of renewable aviation fuels from the gasification of biomass and residual wastes. Bioresour. Technol. 312, 123596.
Shahbeik, H., Peng, W., Kazemi Shariat Panahi, H., Dehhaghi, M., Guillemin, G.J., Fallahi, A., Amiri, H., Rehan, M., Raikwar, D., Latine, H., Pandalone, B., Khoshnevisan, B., Sonne, C., Vaccaro, L., Nizami, A.-S., Gupta, V.K., Lam, S.S., Pan, J., Luque, R., Sels, B., Tabatabaei, M., Aghbashlo, M., 2022. Synthesis of liquid biofuels from biomass by hydrothermal gasification: a critical review. Renew. Sustain. Energy Rev. 167, 112833.
Shan Ahamed, T., Anto, S., Mathimani, T., Brindhadevi, K., Pugazhendhi, A., 2021. Upgrading of bio-oil from thermochemical conversion of various biomass – mechanism, challenges and opportunities. Fuel 287, 119329.
Shanmugam, S.R., Adhikari, S., Shakya, R., 2017. Nutrient removal and energy production from aqueous phase of bio-oil generated via hydrothermal liquefaction of algae. Bioresour. Technol. 230, 43–48.

Shao, Y., Long, Y., Zhou, Y., Jin, Z., Zhou, D., Shen, D., 2019. 5-hydroxymethylfurfural production from watermelon peel by microwave hydrothermal liquefaction. Energy 174, 198–205.

Sharma, I., Rackemann, D., Ramirez, J., Cronin, D.J., Moghaddam, L., Beltramini, J.N., Te'o, J., Li, K., Shi, C., Doherty, W.O.S., 2022. Exploring the potential for biomethane production by the hybrid anaerobic digestion and hydrothermal gasification process: a review. J. Clean. Prod. 362, 132507.

Shen, N., Dai, K., Xia, X.-Y., Zeng, R.J., Zhang, F., 2018a. Conversion of syngas (CO and H2) to biochemicals by mixed culture fermentation in mesophilic and thermophilic hollow-fiber membrane biofilm reactors. J. Clean. Prod. 202, 536–542.

Shen, R., Jiang, Y., Ge, Z., Lu, J., Zhang, Y., Liu, Z., Ren, Z.J., 2018b. Microbial electrolysis treatment of post-hydrothermal liquefaction wastewater with hydrogen generation. Appl. Energy 212, 509–515.

Shen, R., Lu, J., Yao, Z., Zhao, L., Wu, Y., 2021. The hydrochar activation and biocrude upgrading from hydrothermal treatment of lignocellulosic biomass. Bioresour. Technol. 342, 125914.

Shi, J., Cui, H., Xu, J., Yan, N., 2022. Carbon spheres synthesized from KHCO3 activation of glucose derived hydrochar with excellent CO2 capture capabilities at both low and high pressures. Sep. Purif. Technol. 294, 121193.

Si, B., Watson, J., Aierzhati, A., Yang, L., Liu, Z., Zhang, Y., 2019a. Biohythane production of post-hydrothermal liquefaction wastewater: a comparison of two-stage fermentation and catalytic hydrothermal gasification. Bioresour. Technol. 274, 335–342.

Si, B., Yang, L., Zhou, X., Watson, J., Tommaso, G., Chen, W.-T., Liao, Q., Duan, N., Liu, Z., Zhang, Y., 2019b. Anaerobic conversion of the hydrothermal liquefaction aqueous phase: fate of organics and intensification with granule activated carbon/ozone pretreatment. Green Chem. 21 (6), 1305–1318.

Sladkovskiy, D.A., Godina, L.I., Semikin, K.V., Sladkovskaya, E.V., Smirnova, D.A., Murzin, D.Y., 2018. Process design and techno-economical analysis of hydrogen production by aqueous phase reforming of sorbitol. Chem. Eng. Res. Des. 134, 104–116.

Solangi, N.H., Anjum, A., Tanjung, F.A., Mazari, S.A., Mubarak, N.M., 2021. A review of recent trends and emerging perspectives of ionic liquid membranes for CO2 separation. J. Environ. Chem. Eng. 9 (5), 105860.

Son Le, H., Chen, W.H., Forruque Ahmed, S., Said, Z., Rafa, N., Tuan Le, A., Agbulut, U., Veza, I., Phuong Nguyen, X., Quang Duong, X., Huang, Z., Hoang, A.T., 2022. Hydrothermal carbonization of food waste as sustainable energy conversion path. Bioresour. Technol. 363, 127958.

Song, Y.-Q., Nanda, S., Cong, W.-J., Sun, J., Dong, G.-H., Magdziarz, A., Fang, Z., Dalai, A.K., Kozinski, J.A., 2022. Hydrogen production from cotton stalk over ni-La catalysts supported on spent bleaching clay via hydrothermal gasification. Ind. Crop. Prod. 186, 115228.

Staples, M.D., Malina, R., Barrett, S.R.H., 2017. The limits of bioenergy for mitigating global life-cycle greenhouse gas emissions from fossil fuels. Nat. Energy 2 (2), 16202.

Sultana, A.I., Reza, M.T., 2022. Investigation of hydrothermal carbonization and chemical activation process conditions on hydrogen storage in loblolly pine-derived superactivated hydrochars. Int. J. Hydrog. Energy 47 (62), 26422–26434.

Sultana, A.I., Saha, N., Reza, M.T., 2021. Upcycling simulated food wastes into superactivated hydrochar for remarkable hydrogen storage. J. Anal. Appl. Pyrolysis 159, 105322.

Sun, X., Atiyeh, H.K., Huhnke, R.L., Tanner, R.S., 2019. Syngas fermentation process development for production of biofuels and chemicals: a review. Bioresour. Technol. Rep. 7, 100279.

Sun, X., Atiyeh, H.K., Kumar, A., Zhang, H., Tanner, R.S., 2018. Biochar enhanced ethanol and butanol production by clostridium carboxidivorans from syngas. Bioresour. Technol. 265, 128–138.

Sun, X., Thunuguntla, R., Zhang, H., Atiyeh, H., 2022. Biochar amended microbial conversion of C1 gases to ethanol and butanol: effects of biochar feedstock type and processing temperature. Bioresour. Technol. 360, 127573.

Susanti, R.F., Wiratmadja, R.G.R., Kristianto, H., Arie, A.A., Nugroho, A., 2022. Synthesis of high surface area activated carbon derived from cocoa pods husk by hydrothermal carbonization and chemical activation using zinc chloride as activating agent. Mater. Today: Proc. 63, S55–S60.

Sztancs, G., Juhasz, L., Nagy, B.J., Nemeth, A., Selim, A., Andre, A., Toth, A.J., Mizsey, P., Fozer, D., 2020. Co-hydrothermal gasification of Chlorella vulgaris and hydrochar: the effects of waste-to-solid biofuel production and blending concentration on biogas generation. Bioresour. Technol. 302, 122793.

Taghipour, A., Hornung, U., Ramirez, J.A., Brown, R.J., Rainey, T.J., 2021. Aqueous phase recycling in catalytic hydrothermal liquefaction for algal biomass and the effect on elemental accumulation and energy efficiency. J. Clean. Prod. 289, 125582.

Tan, L., Wang, F., Zhang, P., Suzuki, Y., Wu, Y., Chen, J., Yang, G., Tsubaki, N., 2020. Design of a core-shell catalyst: an effective strategy for suppressing side reactions in syngas for direct selective conversion to light olefins. Chem. Sci. 11 (16), 4097–4105.

Tasca, A.L., Puccini, M., Gori, R., Corsi, I., Galletti, A.M.R., Vitolo, S., 2019. Hydrothermal carbonization of sewage sludge: a critical analysis of process severity, hydrochar properties and environmental implications. Waste Manag. 93, 1–13.

Thananatthanachon, T., Rauchfuss, T.B., 2010. Efficient production of the liquid fuel 2,5-dimethylfuran from fructose using formic acid as a reagent. Angew. Chem. 122 (37), 6766–6768.

Tommaso, G., Chen, W.T., Li, P., Schideman, L., Zhang, Y., 2015. Chemical characterization and anaerobic biodegradability of hydrothermal liquefaction aqueous products from mixed-culture wastewater algae. Bioresour. Technol. 178, 139–146.

Tong, S., Shen, J., Jiang, X., Li, J., Sun, X., Xu, Z., Chen, D., 2021. Recycle of Fenton sludge through one-step synthesis of aminated magnetic hydrochar for Pb(2+) removal from wastewater. J. Hazard. Mater. 406, 124581.

Torres-Mayanga, P.C., Lachos-Perez, D., Mudhoo, A., Kumar, S., Brown, A.B., Tyufekchiev, M., Dragone, G., Mussatto, S.I., Rostagno, M.A., Timko, M., Forster-Carneiro, T., 2019. Production of biofuel precursors and value-added chemicals from hydrolysates resulting from hydrothermal processing of biomass: a review. Biomass Bioenergy 130, 105397.

Triyono, B., Prawisudha, P., Aziz, M., Mardiyati, Pasek, A.D., Yoshikawa, K., 2019. Utilization of mixed organic-plastic municipal solid waste as renewable solid fuel employing wet torrefaction. Waste Manag. 95, 1–9.

Tushar, M.S.H.K., Dutta, A., Xu, C., 2016. Catalytic supercritical gasification of biocrude from hydrothermal liquefaction of cattle manure. Appl. Catal. B Environ. 189, 119–132.

Usman, M., Chen, H., Chen, K., Ren, S., Clark, J.H., Fan, J., Luo, G., Zhang, S., 2019. Characterization and utilization of aqueous products from hydrothermal conversion of biomass for bio-oil and hydro-char production: a review. Green Chem. 21 (7), 1553–1572.

Usman, M., Ren, S., Ji, M., O-Thong, S., Qian, Y., Luo, G., Zhang, S., 2020. Characterization and biogas production potentials of aqueous phase produced from hydrothermal carbonization of biomass – major components and their binary mixtures. Chem. Eng. J. 388, 124201.

van Santen, R.A., Markvoort, A.J., Filot, I.A., Ghouri, M.M., Hensen, E.J., 2013. Mechanism and microkinetics of the fischer-tropsch reaction. Phys. Chem. Chem. Phys. 15 (40), 17038–17063.

Vitasari, C.R., Meindersma, G.W., de Haan, A.B., 2011. Water extraction of pyrolysis oil: the first step for the recovery of renewable chemicals. Bioresour. Technol. 102 (14), 7204–7210.

Wagner, D.S., Cazzaniga, C., Steidl, M., Dechesne, A., Valverde-Perez, B., Plosz, B.G., 2021. Optimal influent N-to-P ratio for stable microalgal cultivation in water treatment and nutrient recovery. Chemosphere 262, 127939.

Wainaina, S., Horvath, I.S., Taherzadeh, M.J., 2018. Biochemicals from food waste and recalcitrant biomass via syngas fermentation: a review. Bioresour. Technol. 248 (Pt A), 113–121.

Walsh, J.J., Jiang, C., Tang, J., Cowan, A.J., 2016. Photochemical CO2 reduction using structurally controlled g-C3N4. Phys. Chem. Chem. Phys. 18 (36), 24825–24829.

Wang, H.J., Dai, K., Wang, Y.Q., Wang, H.F., Zhang, F., Zeng, R.J., 2018a. Mixed culture fermentation of synthesis gas in the microfiltration and ultrafiltration hollow-fiber membrane biofilm reactors. Bioresour. Technol. 267, 650–656.

Wang, Q., Santos, S., Urbina-Blanco, C.A., Zhou, W., Yang, Y., Marinova, M., Heyte, S., Joelle, T.-R., Ersen, O., Baaziz, W., Safonova, O.V., Saeys, M., Ordomsky, V.V., 2022a. Ru(III) single site solid micellar catalyst for selective aqueous phase hydrogenation of carbonyl groups in biomass-derived compounds. Appl. Catal. B Environ. 300, 120730.

Wang, T., Si, B., Gong, Z., Zhai, Y., Cao, M., Peng, C., 2020a. Co-hydrothermal carbonization of food waste-woody sawdust blend: interaction effects on the hydrochar properties and nutrients characteristics. Bioresour. Technol. 316, 123900.

Wang, T., Zhai, Y., Zhu, Y., Li, C., Zeng, G., 2018b. A review of the hydrothermal carbonization of biomass waste for hydrochar formation: process conditions, fundamentals, and physicochemical properties. Renew. Sust. Energ. Rev. 90, 223–247.

Wang, X., Cao, L., Lewis, R., Hreid, T., Zhang, Z., Wang, H., 2020b. Biorefining of sugarcane bagasse to fermentable sugars and surface oxygen group-rich hierarchical porous carbon for supercapacitors. Renew. Energy 162, 2306–2317.

Wang, Y., Chen, E., Tang, J., 2022b. Insight on reaction pathways of photocatalytic CO2 conversion. ACS Catal. 12 (12), 7300–7316.

Wang, Y., Liu, X., Kraslawski, A., Gao, J., Cui, P., 2019. A novel process design for CO2 capture and H2S removal from the syngas using ionic liquid. J. Clean. Prod. 213, 480–490.

Wang, Y., Zhang, Y., Yoshikawa, K., Li, H., Liu, Z., 2021a. Effect of biomass origins and composition on stability of hydrothermal biocrude oil. Fuel 302, 121138.

Wang, Z., Liu, Z., Yuan, C., Zhao, X., Zhang, Y., Liu, Z., 2022c. Construction of a novel closed-loop livestock waste valorization paradigm: bridging manure and ammonia gas via phosphate-doped hydrochar. ACS ES&T Eng. 2 (9), 1732–1744.

Wang, Z., Watson, J., Wang, T., Yi, S., Si, B., Zhang, Y., 2021b. Enhancing energy recovery via two stage co-fermentation of hydrothermal liquefaction aqueous phase and crude glycerol. Energy Convers. Manag. 231, 113855.

Watson, J., Si, B., Li, H., Liu, Z., Zhang, Y., 2017. Influence of catalysts on hydrogen production from wastewater generated from the HTL of human feces via catalytic hydrothermal gasification. Int. J. Hydrog. Energy 42 (32), 20503–20511.

Wei, Y., Fakudze, S., Zhang, Y., Ma, R., Shang, Q., Chen, J., Liu, C., Chu, Q., 2022. Co-hydrothermal carbonization of pomelo peel and PVC for production of hydrochar pellets with enhanced fuel properties and dechlorination. Energy 239, 122350.

Wen, J., Liu, Z., Xi, H., Huang, B., 2023. Synthesis of hierarchical porous carbon with high surface area by chemical activation of (NH4)2C2O4 modified hydrochar for chlorobenzene adsorption. J. Environ. Sci. 126, 123–137.

Werpy, T., Petersen, G., 2004. Top Value Added Chemicals From Biomass: Volume I–Results of Screening for Potential Candidates From Sugars and Synthesis Gas. National Renewable Energy Lab, Golden, CO (US).

White, M.T., Bianchi, G., Chai, L., Tassou, S.A., Sayma, A.I., 2021. Review of supercritical CO2 technologies and systems for power generation. Appl. Therm. Eng. 185, 116447.

Wibowo, H., Susanto, H., Grisdanurak, N., Hantoko, D., Yoshikawa, K., Qun, H., Yan, M., 2021. Recent developments of deep eutectic solvent as absorbent for CO2 removal from syngas produced from gasification: current status, challenges, and further research. J. Environ. Chem. Eng. 9 (4), 105439.

Woolcock, P.J., Brown, R.C., 2013. A review of cleaning technologies for biomass-derived syngas. Biomass Bioenergy 52, 54–84.

Wu, X.-F., Zhang, J.-J., Li, M.-F., Bian, J., Peng, F., 2019. Catalytic hydrothermal liquefaction of eucalyptus to prepare bio-oils and product properties. Energy Convers. Manag. 199, 111955.

Wu, Z., Zhao, C., Zeng, W., Wang, X., Liu, C., Yu, Z., Zhang, J., Qiu, Z., 2022. Ultra-high selective removal of CR and Cr(VI) from aqueous solutions using polyethyleneimine functionalized magnetic hydrochar: application strategy and mechanisms insight. Chem. Eng. J. 448, 137464.

Xia, J., Han, L., Zhang, C., Guo, H., Rong, N., Baloch, H.A., Wu, P., Xu, G., Ma, K., 2022. Hydrothermal co-liquefaction of rice straw and nannochloropsis: the interaction effect on mechanism, product distribution and composition. J. Anal. Appl. Pyrolysis 161, 105368.

Xia, Y., Yang, T., Zhu, N., Li, D., Chen, Z., Lang, Q., Liu, Z., Jiao, W., 2019. Enhanced adsorption of Pb(II) onto modified hydrochar: modeling and mechanism analysis. Bioresour. Technol. 288, 121593.

Xiang, Y., Luo, H., Liu, G., Zhang, R., 2022. Improvement of organic acid production with sulfate addition during syngas fermentation using mixed cultures. Water Cycle 3, 26–34.
Xiao, K., Liu, H., Li, Y., Yang, G., Wang, Y., Yao, H., 2020. Excellent performance of porous carbon from urea-assisted hydrochar of orange peel for toluene and iodine adsorption. Chem. Eng. J. 382, 122997.
Xiao, K., Liu, H., Li, Y., Yi, L., Zhang, X., Hu, H., Yao, H., 2018. Correlations between hydrochar properties and chemical constitution of orange peel waste during hydrothermal carbonization. Bioresour. Technol. 265, 432–436.
Xiong, J.-B., Pan, Z.-Q., Xiao, X.-F., Huang, H.-J., Lai, F.-Y., Wang, J.-X., Chen, S.-W., 2019. Study on the hydrothermal carbonization of swine manure: the effect of process parameters on the yield/properties of hydrochar and process water. J. Anal. Appl. Pyrolysis 144, 104692.
Xiong, S., Guan, Y., Luo, C., Zhu, L., Wang, S., 2021. Critical review on the preparation of platform compounds from biomass or saccharides via hydrothermal conversion over carbon-based solid acid catalysts. Energy Fuel 35 (18), 14462–14483.
Xu, D., Lin, G., Guo, S., Wang, S., Guo, Y., Jing, Z., 2018a. Catalytic hydrothermal liquefaction of algae and upgrading of biocrude: a critical review. Renew. Sust. Energ. Rev. 97, 103–118.
Xu, D., Lin, G., Liu, L., Wang, Y., Jing, Z., Wang, S., 2018b. Comprehensive evaluation on product characteristics of fast hydrothermal liquefaction of sewage sludge at different temperatures. Energy 159, 686–695.
Xu, S., He, T., Li, J., Huang, Z., Hu, C., 2021a. Enantioselective synthesis of D-lactic acid via chemocatalysis using MgO: experimental and molecular-based rationalization of the triose's reactivity and preliminary insights with raw biomass. Appl. Catal. B Environ. 292, 120145.
Xu, S., Wu, Y., Li, J., He, T., Xiao, Y., Zhou, C., Hu, C., 2020. Directing the simultaneous conversion of hemicellulose and cellulose in raw biomass to lactic acid. ACS Sustain. Chem. Eng. 8 (10), 4244–4255.
Xu, Z., Qi, R., Zhang, D., Gao, Y., Xiong, M., Chen, W., 2021b. Co-hydrothermal carbonization of cotton textile waste and polyvinyl chloride waste for the production of solid fuel: interaction mechanisms and combustion behaviors. J. Clean. Prod. 316, 128306.
Yan, P., Mensah, J., Drewery, M., Kennedy, E., Maschmeyer, T., Stockenhuber, M., 2021. Role of metal support during ru-catalysed hydrodeoxygenation of biocrude oil. Appl. Catal. B Environ. 281, 119470.
Yang, C., Wang, S., Jiang, Z., Li, J., He, C., Xu, T., Xu, D., 2022a. Catalytic hydrotreatment upgrading of biocrude oil derived from hydrothermal liquefaction of animal carcass. Fuel 317, 123528.
Yang, C., Wang, S., Yang, J., Xu, D., Li, Y., Li, J., Zhang, Y., 2020. Hydrothermal liquefaction and gasification of biomass and model compounds: a review. Green Chem. 22 (23), 8210–8232.
Yang, L., Shuang, E., Liu, J., Sheng, K., Zhang, X., 2022b. Endogenous calcium enriched hydrochar catalyst derived from water hyacinth for glucose isomerization. Sci. Total Environ. 807 (Pt 2), 150660.
Yang, Y., Tilman, D., Lehman, C., Trost, J.J., 2018. Sustainable intensification of high-diversity biomass production for optimal biofuel benefits. Nat. Sustain. 1 (11), 686–692.
Ye, Z., Zhang, L., Huang, Q., Tan, Z., 2019. Development of a carbon-based slow release fertilizer treated by bio-oil coating and study on its feedback effect on farmland application. J. Clean. Prod. 239.
Yin, Z., Palmore, G.T.R., Sun, S., 2019. Electrochemical reduction of CO2 catalyzed by metal nanocatalysts. Trends Chem. 1 (8), 739–750.
Ying, W., Zhou, K., Hou, Q., Chen, D., Guo, Y., Zhang, J., Yan, Y., Xu, Z., Peng, X., 2019. Selectively tuning gas transport through ionic liquid filled graphene oxide nanoslits using an electric field. J. Mater. Chem. A 7 (25), 15062–15067.
Yoon, J., Oh, M.K., 2022. Strategies for biosynthesis of C1 gas-derived polyhydroxyalkanoates: a review. Bioresour. Technol. 344 (Pt B), 126307.
Yu, J., Tang, T., Cheng, F., Huang, D., Martin, J.L., Brewer, C.E., Grimm, R.L., Zhou, M., Luo, H., 2021. Exploring spent biomass-derived adsorbents as anodes for lithium ion batteries. Mater. Today Energy 19, 100580.
Yu, X., Liu, S., Lin, G., Yang, Y., Zhang, S., Zhao, H., Zheng, C., Gao, X., 2019. Promotion effect of KOH surface etching on sucrose-based hydrochar for acetone adsorption. Appl. Surf. Sci. 496, 143617.
Yu, Y., Wang, H., Wang, Y.-N., Zhou, J., Shi, B., 2022. Chrome-free synergistic tanning system based on biomass-derived hydroxycarboxylic acid–zirconium complexes. J. Clean. Prod. 336, 130428.
Zhang, C., Tang, X., Sheng, L., Yang, X., 2016. Enhancing the performance of co-hydrothermal liquefaction for mixed algae strains by the maillard reaction. Green Chem. 18 (8), 2542–2553.
Zhang, C., Zheng, C., Ma, X., Zhou, Y., Wu, J., 2021a. Co-hydrothermal carbonization of sewage sludge and banana stalk: fuel properties of hydrochar and environmental risks of heavy metals. J. Environ. Chem. Eng. 9 (5), 106051.
Zhang, J., Yan, W., An, Z., Song, H., He, J., 2018a. Interface-promoted dehydrogenation and water-gas shift toward high-efficient H2 production from aqueous phase reforming of cellulose. ACS Sustain. Chem. Eng. 6 (6), 7313–7324.
Zhang, M., Hu, Y., Wang, H., Li, H., Han, X., Zeng, Y., Xu, C.C., 2021b. A review of bio-oil upgrading by catalytic hydrotreatment: advances, challenges, and prospects. Mol. Catal. 504, 111438.
Zhang, R., Chen, Y., Zhou, Y., Tong, D., Hu, C., 2019a. Selective conversion of hemicellulose in macroalgae Enteromorpha prolifera to rhamnose. ACS Omega 4 (4), 7023–7028.
Zhang, X., Xiang, W., Wang, B., Fang, J., Zou, W., He, F., Li, Y., Tsang, D.C.W., Ok, Y.S., Gao, B., 2020. Adsorption of acetone and cyclohexane onto CO(2) activated hydrochars. Chemosphere 245, 125664.
Zhang, X.-P., Zhang, C., Li, X., Yu, S.-H., Tan, P., Fang, Q.-Y., Chen, G., 2018b. A two-step process for sewage sludge treatment: hydrothermal treatment of sludge and catalytic hydrothermal gasification of its derived liquid. Fuel Process. Technol. 180, 67–74.
Zhang, X.S., Yang, G.X., Jiang, H., Liu, W.J., Ding, H.S., 2013. Mass production of chemicals from biomass-derived oil by directly atmospheric distillation coupled with co-pyrolysis. Sci. Rep. 3, 1120.
Zhang, Y., Jiang, Q., Xie, W., Wang, Y., Kang, J., 2019b. Effects of temperature, time and acidity of hydrothermal carbonization on the hydrochar properties and nitrogen recovery from corn Stover. Biomass Bioenergy 122, 175–182.
Zhang, Y., Qu, J., Yuan, Y., Song, H., Liu, Y., Wang, S., Tao, Y., Zhao, Y., Li, Z., 2022. Simultaneous scavenging of Cd(II) and Pb(II) from water by sulfide-modified magnetic pinecone-derived hydrochar. J. Clean. Prod. 341, 130758.
Zhang, Z., Macquarrie, D.J., De Bruyn, M., Budarin, V.L., Hunt, A.J., Gronnow, M.J., Fan, J., Shuttleworth, P.S., Clark, J.H., Matharu, A.S., 2015. Low-temperature microwave-assisted pyrolysis of waste office paper and the application of bio-oil as an Al adhesive. Green Chem. 17 (1), 260–270.
Zhang, Z., Zhu, Z., Shen, B., Liu, L., 2019c. Insights into biochar and hydrochar production and applications: a review. Energy 171, 581–598.
Zhao, B., Yang, Q., Qin, L., Shan, W., Zhang, Q., Chen, W., Han, J., 2021. Nanoscale ni enveloped in hydrochar prepared by one-step hydrothermal method for dry reforming of CH4 with CO2. Mol. Catal. 514, 111869.
Zhong, H., Ma, L., Zhu, Y., Jin, B., Wang, T., Wang, Y., Jin, F., 2020. Hydrothermal conversion of microalgae and its waste residue after biofuel extraction to acetic acid with CuO as solid oxidant. J. Supercrit. Fluids 157, 104717.
Zhou, W., Cheng, K., Kang, J., Zhou, C., Subramanian, V., Zhang, Q., Wang, Y., 2019. New horizon in C1 chemistry: breaking the selectivity limitation in transformation of syngas and hydrogenation of CO2 into hydrocarbon chemicals and fuels. Chem. Soc. Rev. 48 (12), 3193–3228.
Zhou, Y., Hu, C., 2020. Catalytic thermochemical conversion of algae and upgrading of algal oil for the production of high-grade liquid fuel: a review. Catalysts 10 (2), 145.
Zhou, Y., Li, M., Chen, Y., Hu, C., 2021. Conversion of polysaccharides in Ulva prolifera to valuable chemicals in the presence of formic acid. J. Appl. Phycol. 33 (1), 101–110.
Zhou, Y., Liu, L., Li, M., Hu, C., 2022a. Algal biomass valorisation to high-value chemicals and bioproducts: recent advances, opportunities and challenges. Bioresour. Technol. 344, 126371.
Zhou, Y., Remón, J., Gracia, J., Jiang, Z., Pinilla, J.L., Hu, C., Suelves, I., 2022b. Toward developing more sustainable marine biorefineries: a novel 'sea-thermal' process for biofuels production from microalgae. Energy Convers. Manag. 270, 116201.
Zhou, Y., Remón, J., Jiang, Z., Matharu, A.S., Hu, C., 2022c. Tuning the selectivity of natural oils and fatty acids/esters deoxygenation to biofuels and fatty alcohols: a review. Green Energy Environ. https://doi.org/10.1016/j.gee.2022.03.001.
Zhu, Z., Liu, Z., Zhang, Y., Li, B., Lu, H., Duan, N., Si, B., Shen, R., Lu, J., 2016. Recovery of reducing sugars and volatile fatty acids from cornstalk at different hydrothermal treatment severity. Bioresour. Technol. 199, 220–227.
Zhu, Z., Ma, C., Yu, K., Lu, Z., Liu, Z., Huo, P., Tang, X., Yan, Y., 2020. Synthesis ce-doped biomass carbon-based g-C3N4 via plant growing guide and temperature-programmed technique for degrading 2-mercaptobenzothiazole. Appl. Catal. B Environ. 268, 118432.
Zhuang, X., Liu, J., Ma, L., 2022a. Facile synthesis of hydrochar-supported catalysts from glucose and its catalytic activity towards the production of functional amines. Green Energy Environ. https://doi.org/10.1016/j.gee.2022.01.012.
Zhuang, X., Liu, J., Wang, C., Zhang, Q., Ma, L., 2022b. A review on the stepwise processes of hydrothermal liquefaction (HTL): recovery of nitrogen sources and upgrading of biocrude. Fuel 313, 122671.
Zhuang, X., Song, Y., Zhan, H., Yin, X., Wu, C., 2020. Gasification performance of biowaste-derived hydrochar: the properties of products and the conversion processes. Fuel 260, 116320.
Zoppi, G., Pipitone, G., Galletti, C., Rizzo, A.M., Chiaramonti, D., Pirone, R., Bensaid, S., 2021. Aqueous phase reforming of lignin-rich hydrothermal liquefaction by-products: a study on catalyst deactivation. Catal. Today 365, 206–213.